中山醫學大學生化暨生物科技研究所博士論文

Ph.D. Thesis, Institute of Biochemistry and Biotechnology,

Chung Shan Medical University

高血壓性肥大心臟中細胞色素C氧化酶表現模式及類胰島素生長因子-I訊息路徑活性之探討

Cytochrome c oxidase (COX) gene expression profile and IGF-I signaling in hypertensive cardiac hypertrophy

指導老師：朱嘉一 教授 (Chia-Yih Chu)

研究生：郭薇雯 (Wei-Wen Kuo)

中華民國九十四年六月

June, 2005

目　錄

圖 目 錄

表 目 錄

第一章 文獻回顧

I.高血壓與心臟

A. 血壓的調節

人體內針對血管內血壓有一套複雜的系統來調節，大約可分為短效性及長效性兩種：

1.短效性－壓力受納器反射(Baroreceptor)：是由週邊接受體與中央神經系統共同完成作用。壓力受納器存在於主動脈弧即主動脈血管彎曲之處及頸動脈竇，即頸動脈分叉處，這些區域皆是屬於最容易感受到血壓變化的地方，並可進而發生反射的調節，當動脈壓太高時，由接受器感應後，從竇神經及主動脈弧神經分別傳到延髓之血管運動中樞之前部與後部，藉由交感神經的作用，使血管擴大，心跳速率減少，使血壓降低，反之則反[1]。

2.長效性：Renin angiotensin系統：是由週邊組織及中央內分泌系統共同完成之作用。當動脈壓下降時，腎臟受到刺激，由Juxtaglomerular cell分泌腎高壓蛋白酶(renin)，乃是一種蛋白質分解酶使血漿內之Angiotensinogen (由肝臟合成)水解成Angiotensin I，經肺臟時，由肺臟分泌之converting enzyme把Angiotensin I轉變為具有活性之

Angiotensin II，作用於(1)血管內皮細胞，使血管收縮，血壓上升。(2)腎臟，使Adrenal cortex分泌Aldosterone，增加鈉離子與水分子的回收，而改變了血液總體積，使血壓上升，反之則反。以嚴重出血，而引起之低血壓為例，即藉由Renin-Angiotensin系統引起血壓上升的作用。又如結紮老鼠左、右腎動脈之間腹部動脈，即可產生持續性高血壓，乃因結紮後引起腎臟低血壓缺血，使renin分泌提高，產生一連串的反應後，Angiotensin II引起血管收縮，使血壓急速上升，即應用此一原理。此外，一些降血壓藥物，即利用Converting enzyme抑制劑，亦即抑制此一連串反應，而達到降血壓的效果[1]。

B. 高血壓之定義及種類

高血壓定義為血壓不正常之上升，而影響血壓的原因包括心輸出量，週邊血管阻力，動脈血管彈性，及血流之體積及濃稠度。而所謂的收縮壓指的是當心臟收縮把血液打到血管所測得的血壓。根據世界衛生組織的定義，高血壓是當靜止的狀態下，(1)收縮壓超過 140 毫米汞柱。(2) 舒張壓超過 90 毫米汞柱，即可稱為高血壓[1,2]，高血壓又可分為原發性及續發性高血壓，前者佔臨床總數之 80-90%，詳細病理原因還不太清楚，可能與環境或遺傳有關。後者佔臨床總數 10-20%，可能是由其它疾病所引起，如腎臟病或內分泌失調，如先

天性主動脈狹窄或不正常的甲狀腺素、胰島素、腎上腺皮質素(Adrenal steroids)，如aldosterone，glucocorticoid及腎上腺素等[2]。若是長期高血壓控制不良，易造成心臟肥大、心肌梗塞、以及腦中風的情況；腎臟方面，會造成腎臟衰竭。

C. 血壓對心臟之影響：

當renin-angiotensin使血壓上升時，即造成Preload之上升，而增加心臟收縮頻率，長期以來，亦會影響到Afterload之上升，對心跳影響更形增加，無形當中，而增加了心臟的工作負擔。為了應付外來增加之工作量，在心臟細胞維持不變的條件下，心臟細胞則以增加實體，即細胞大小的方式來應付[3,4]，而preload及afterload之定義分別如下：

1.Preload：所謂preload為靜脈迴流至心室血液之體積，亦即舒張結束流回左心室之血流體積。而舒張壓往往即是preload之指標，Volume-overload高血壓即可造成preload之升高[5]。

2.Afterload：即血液自左心室打出後所受到之阻力。此阻力來自週邊血管的阻抗及動脈之血壓所造成，而動脈血管收縮壓即是afterload之指標，Pressure-overload高血壓即動脈血管收縮之上升，亦即afterload已上升[5]。

D.引起高血壓之動物模式

1.先天性高血壓大白鼠(Spontaneously hypertensive rats, SHR)

先天性高血壓大白鼠，可代表人類原發性高血壓的實驗動物模式，是 1963 年由Okamote及Aoki所培育出來[6,7]。他們藉著由選擇性地自Wistar大白鼠培育出先天性高血壓大白鼠，其與正常壓大白鼠(Wistar-kyoto)血壓 125 毫米汞柱比較起來，不需任何實驗外力之作用，即可自然產生高血壓之先天性高血壓大白鼠。在一個月大時，血壓即開始逐漸上升，而後在 12 個月大時，達 200 毫米汞柱，並持續到整個生命期，而平均壽命 1.5 年，推測大多是由於心肌組織necrosis及心肌細胞凋亡引起死亡[8]。

2.中風傾向先天性高血壓大白鼠 (Stroke prone spontaneously hypertensive rats, SPSHR)

大約十年後，同一批研究者更進一步培育出SHR另一亞種，顯現出更快速血壓上升，引發大腦血管病變的中風傾向先天性高血壓大白鼠，牠們是以先天性高血壓大白鼠餵以 1%鹽水培育而來，展示出更高比例之中風罹患率之表現型，其在 15 週大時，血壓即可上升到 240 毫米汞柱，其平均壽命僅有 33-41 週[6]。

3.腹動脈結紮

許多動物以動脈部分結紮來探討血壓與心臟之關係[9]，但若進一步以Sprague-Dawley 大白鼠，應用其與生俱有良好側支循環特性，施行左、右腎動脈之間腹動脈完全結紮(Fig 1-1)， 使左腎缺氧，分泌 renin，進入循環系統進行反應，則可使血壓快速上升[10]，在吾人實驗結果 1 至 7 天，無論左心室重或心肌細胞大小都顯著上升，若與控制組的血壓 143 毫米汞柱比較，其血壓都維持在 173 毫米汞柱左右，並且在已肥大心肌組織中，IGF-I蛋質白及mRNA之含量皆顯著上升[11]。

II、心臟肥大

人類自青春期後，心肌細胞即維持一定數目並不再分裂，一旦心肌細胞受損，則可造成心臟不可回復之傷害。所以，為了因應外來的物理及機械性刺激（例如高血壓），心肌細胞則以生理代償性肥大的方式來因應外在環境的改變。但是，若外在環境持續發生，則生理性肥大易轉變成病理性肥大。就臨床上而言，心肌肥大患者，其心血管疾病的死亡率為正常人之兩倍。另一方面，不論是正常成長或由外力造成的心臟肥大，皆是透過細胞增大，增加心臟肌肉實體 (muscle mass)來達成，而不是透過細胞數目增加所造成的結果[12]。

心臟肥大分為生理性及病理性肥大兩種，就心臟細胞的構形而

言，心臟肥大可分為下列數種 (Fig 1-2, 1-3)：

A.同心性病理肥大(concentric hypertrophy)：亦即心臟細胞以橫向延長，可形成心室壁增厚的肥厚型心肌症(hypertrophic cardiomyopathy)屬之。

B.延長性病理肥大(eccentric hypertrophy)：心臟細胞以縱向延長擴大，可形成心臟腔室擴張之擴張性心肌症屬之(dilated cardiomyopathy)。

C.生理性肥大(physiological hypertrophy)：就正常的生理成長，或由運動所引起心臟細胞之長及寬等比例擴大，即同心性及延長性擴大同時發生，二者平衡進行，運動員之心臟肥大屬之。

其中，後二者均屬病理性肥大，此時若以心肌組織橫向截面(cross section area,CSA)來計算心肌細胞面積，則可觀察到後二者CSA顯著上升，若以H.E.染色(Fig 1-4)，則可見肥厚型心肌症顯示細胞間隙纖維化 (interstitial fibrosis) 及細胞走向改變 (disarray)，而擴張性心肌症亦顯示細胞走向改變，未見細胞間隙纖維化的現象[12]。二者同時可啟動心臟細胞胚胎基因(embryonic genes)如：atrial natriuretic peptide (ANP)，以及胎兒收縮蛋白，如β-myocin heavy chain (β-MHC) 之表達。在所有哺乳類動物心臟中，這些基因表達的上升是心臟肥大的一個表徵，並且是臨床判斷肥大程度的一個指標[12]。當心臟肥大嚴重時

可進一步造成心肌細胞凋亡，引發心臟衰竭。

III 細胞色素 C 氧化酶(Cytochrome *c* oxidase, COX)---粒腺體製造能量活性的指標酵素

A. 氧化磷酸化(oxidative phosphrylation, OXPHOS)

有關oxidative phosphrylation (OXPHOS) 疾病首先在 1962 年，在一位年輕女性病患身上發現，其具代謝不平衡、不正常粒腺體結構以及不正常OXPHOS功能等症狀，此病症即為今日所稱之Luft's disease[13]，為一種OXPHOS依賴型肌肉纖維化症(a degeneration of the OXPHOS-dependent type I skeletal muscle fibers)而異常的OXPHOS酵素活性即為典型發病原因之一[14]。所謂OXPHOS包括了 5 種位在粒腺體內膜上之酵素複合體，其中包括複合體I (NADH：ubiquinone oxidoreductase, EC 1.6.5.3)、複合體II (Succinate: ubiquinone oxidoreductase, EC 1.3.5.1)、複合體III (ubiquinol: ferrocytochrome c oxidoreductase, EC 1.10.2.2)、複合體IV(cytochrome *c* oxidase, EC 1.9.3.1) 以及複合體V (ATP synthase，EC 3.6.1.34)。複合體I和II接收來自醣類,脂肪及蛋白質代謝的電子,並傳遞予ubiquinone (Co enzyme Q 10)，接著依序移往複合體III，細胞色素C和複合體IV。最後與O_2分子反應成水，複合體I、III、IV在傳遞電子的同時，將氫離子自matrix

打入內外膜間質，而造成一氫離子濃度梯度，而複合體V利用此濃度梯度的能量，將ADP與磷酸根合成為ATP，(Fig 1-5) [15]，而其中複合體IV，即為Cytochrome *c* oxidase (COX)，是整個電子傳遞鍊中的最終步驟，使氧氣成為最終的電子接收者，並轉變成水。為整個氧化磷酸化過程的關鍵步驟。所以當COX活性少量的改變，則整個粒腺體製造能量的效率，即受到很大的影響，目前更有許多文獻發現由於合成COX之基因發生突變，而導致粒腺體功能失調，造成嚴重疾病之發生[16-18]。

B. 細胞色素 C 氧化酶(COX)

COX是電子傳遞鏈中重要酵素，其主要的作用是將正二價還原態細胞色素C，所攜帶電子交予氧氣，形成水之同時，將細胞色素C轉變成正三價之氧化態，故稱細胞色素C氧化酶，其反應如下[19]：

$$2\ \text{Cyt}\ c^{2+} + \ 2H^{+} + \tfrac{1}{2}\ O_2 \longrightarrow 2\text{Cyt}\ c^{3+} + H_2O$$

(Reduced) (Oxidized)

在哺乳類動物，COX酵素由 13 個次單元所組成，其中三個最大次單元(I、II和III)是由粒腺體DNA所製造合成，執行催化及將氫離子

自Matrix打出內外膜間質的功用。其餘的 10 個較小次單元(IV、Va、Vb、VIa、VIb，VIc、VIIa、VIIb、VIIc和VIII [20]，則是由細胞核DNA所控制，在細胞質合成，過程中還需要其他細胞質DNA合成之蛋白的輔助，以製造完整功能之COX[21]。由於控制COX完整蛋白組合，不僅來自細胞核DNA，也來自粒腺體DNA的控制，所以粒腺體基因的特性，也同時影響COX蛋白的合成完整與否。

C. 粒腺體基因

粒腺體是細胞內主要製造ATP的胞器，其擁有自己來自母系遺傳的DNA[22]。 粒腺體DAN是一雙股環形分子，(Fig 1-6)帶有 16569 對鹼基，其中guanine高含量的區域稱heavy(H) strain，而cytosine高含量的區域稱之light (L) strain。而其中一個包含 1122 對鹼基專門執行粒腺體DNA的複製(replication)及轉錄(transcription)，被稱為D-loop。整個粒腺體基因，可表達 37 種基因；其中包括 2 個核糖體rRNA，22 個傳送之tRNA，及其餘 13 個屬於電子傳遞鍊上的反應蛋白，7 個複合體I的次單元，1 個複合體III的次單元，其中複合體IV的I、II、III次單元分別位於第 5904-7444，3586-8262，及 9203-9990 對鹼基的位置 [15]。

由於粒腺體DNA缺乏histone的保護，並且其本身並無自己的DNA修復系統，在粒腺體中高氧含量的環境下，其DNA非常容易受到氧

化傷害，故隨著年齡的增加，粒腺體DNA發生突變的機率也隨之增加[15]。

Ⅳ、類胰島素生長因子-I 與心臟

A. 細胞凋亡(Apoptosis)

細胞之凋亡在胚胎發育及成年組織中皆扮演重要角色，相對於意外傷害所造成之細胞死亡，細胞凋亡是一連串形態上特殊改變的過程，其中包括DNA斷裂 (DNA fragmentation)，最後由細胞膜內縮成凋亡小體 (apoptotic body)，為巨噬細胞 (macrophages) 所吞噬。故由細胞凋亡所引起死亡之細胞，會自組織中消失，不同於因意外傷害引起之死亡細胞(necrosis)，凋亡細胞內之成份未釋放到細胞間液，故不會引起發炎之反應[23]。

粒腺體細胞色素C (COX)是引起細胞凋亡的重要訊息因子（Fig 1-7)，當細胞受到外來引發凋亡之刺激時，粒腺體內膜上的，細胞素C會被釋放出來，而引發Apaf-1 與不活化caspase 9 的結合，活化caspase 9。此一屬上游之執行caspase，將活化另一下游執行者caspase 3，進而造成細胞凋亡。其作用包括了切割 40 多種細胞重要蛋白，如DNase的抑制者，而造成DNA斷裂，以及細胞骨架蛋白，造成細胞的瓦解等等。然而細胞中另有一群BCl_2家族，其中BCl_2依附於粒腺體膜上，

可調節粒腺體外膜之通透性，抑制細胞色素C的釋放，同時抑制caspases之活化，進而抑制細胞凋亡。相對的，其他BCl_2家族成員，亦包括有促進細胞凋亡作用的蛋白，如Bad，反而增加粒腺體外膜通透性，促進細胞色素C的釋放，而達到促進細胞凋亡的作用[23]。

對心臟細胞而言，細胞凋亡具有特殊的意義，由於心臟細胞數目固定，當細胞凋亡發生時，整個心臟組織可產生收縮功能的細胞數目將減少，達一定程度時，即造成心臟衰竭，使得整個心肌組織壞死，所以能夠維持並促進心肌細胞中抗細胞凋亡作用之 IGF-I 訊息路徑，則為大家期待的焦點之一。

B. 心臟細胞中 IGF-I 的來源

IGFs在哺乳類生物之生長及分化過程中，伴演著重要角色[24,25]，其中，包括了胚胎心臟發育[26]。透過循環系統中與攜帶蛋白質（IGF-I binding protein, IGFB的P-3)緊密結合的IGF-Ⅰ，以endocrine的方式，送達標的器官與細胞表面之IGF-I接受體(IGF-IR)結合，執行其功用[24,25]。心臟細胞，亦可製造IGF-I，雖然胚胎期心臟中IGFI之mRNA含量極低，但會隨胚胎成長而逐漸上升[27]。目前研究也顯示，許多細胞合成的IGF-I也可以autocrine 或paracrine的方式作用在分泌細胞本身

或鄰近的細胞，且文獻上認為這些由組織本身所分泌之IGF-I，對組織之生長與分化的作用，較endocrine來得重要[25]。

C. IGF-I 與心臟肥大

已有不少文獻報導多種引起大白鼠心臟肥大的動物模式，包括由生長激素(Growth hormone)[28] 高甲狀腺素 (hyperthyroidism)[29]所誘導、長期缺氧[30]、動脈結紮[31,32]、Volume-overload 之心臟[33] 等，皆可觀察到動物心肌中IGF-I mRNA上升。在細胞培養的實驗中，進一步證實IGF-I可以刺激新生大白鼠心肌細胞肥大[34]，IGF-I可促進成鼠心肌細胞肌纖維發育與蛋白之合成[35]。在以腹動脈完全結紮誘發心臟肥大的模式中，我們亦發現術後第一天IGF-I mRNA即已上升，由於此一現象，發生於心臟肥大之前，顯示IGF-I可能為誘發心臟肥大之起始因子[11]。

D、心臟細胞中 IGF-I 訊息路徑之促進細胞存活作用

在生長激素當中，以IGF-I最具代表性，因其在多種細胞中皆可促進生長與分化。存在心臟細胞的IGF-I及IGF-IR以autocrine或paracrine的方式作用，執行功用。IGF-IR是一個$\alpha_2\beta_2$ 4 個蛋白之結合體[36]，與

IGF-I結合後，細胞內β次單元發生自我磷酸化(autophosphorylation)，而活化了接受體的tyrosine kinase活性[37,38]，進一步磷酸化其主要之受質-胰島素接受體受質(IRS)，IRS可與具SH_2 domain 之PI_3K蛋白結合[39,40]，而引發存活訊息路徑。帶有活性的PI_3K，將PIP_2磷酸化成PIP_3，PIP_3則將Serine/threonine kinase Akt 吸引到細胞膜上，使其被PDK所磷酸化，而後磷酸化之Akt再以磷酸化的方式引發下游與細胞存活有關之訊息蛋白的活性，比如Akt可磷酸化Bad蛋白，使其失去活性而自粒腺體表面移除，因而抑制了細胞色素C自粒腺體之釋放游離；Akt也可藉磷酸化之作用直接抑制Caspase 9之活性；除此之外，Akt也可磷酸化其他促細胞存活的蛋白、或調節細胞代謝與蛋白合成有關之酵素，如GSK-3（Fig 1-8）[23]。

細胞的存活不只受到PI_3K/Akt訊息路徑所調控，IGF-I另可活化下游之Ras/Raf/MAPK途徑（Fig 1-9），且其多作用在心肌組織中的非心肌細胞，而Ras/Raf/MAPK抑制細胞凋亡並促進非心肌細胞增生，是透過ERK磷酸化RSK，與Akt類似的是RSK亦可將Bad磷酸化，達到促進細胞存活的效果[41]。

V. 研究動機

已知心臟細胞具有兩大特點：(1) 不再具有細胞分裂(Cell differantiation)之能力，(2) 心臟細胞絕對依賴有氧呼吸。且就單位組織能量之耗氧量來計算，心臟在人體器官名列第一，其次是腎臟、腦、肝等[15]。足見氧氣之供應，能量之製造對心臟之重要性。由於不具分裂能力和高能量需求的特性，維持心臟細胞之存活，及維持粒腺體中消耗氧氣產生能量之氧化磷酸化之系統完整，顯得格外重要。而在一般的生理狀態下，對心臟而言，最直接影響心臟之工作負擔的，即為血壓的上升。所以在工作量超過正常時，在細胞數目不變之狀況下，心臟細胞被迫選擇以增加質量即心臟肥大(cardiac hypertrophy)的方式來因應。此時，細胞存活能力之維持，及能量之充足供應即顯得更形重要。所以在本研究報告第二章中，我們將探討，以腹動脈完全結紮快速誘發高血壓之動物模式，在 1-20 天中，觀察從心臟肥大的起始，維持，到心臟衰竭的過程中，以負責心肌細胞有氧呼吸能量來源的粒線體酵素COX為指標，探討在整個心肌肥大過程中COX之基因及活性的表現模式。而第三章中，我們將同時以先天性高血壓大白鼠為模式，探討與心肌細胞存活息息相關的IGF-I訊息路徑活性是否在幼年期大白鼠心肌中，即已有功能之不足，來確認此IGF-I路徑，確實在整個生命週期中，均扮演心肌細胞生存、生長之主要角色。

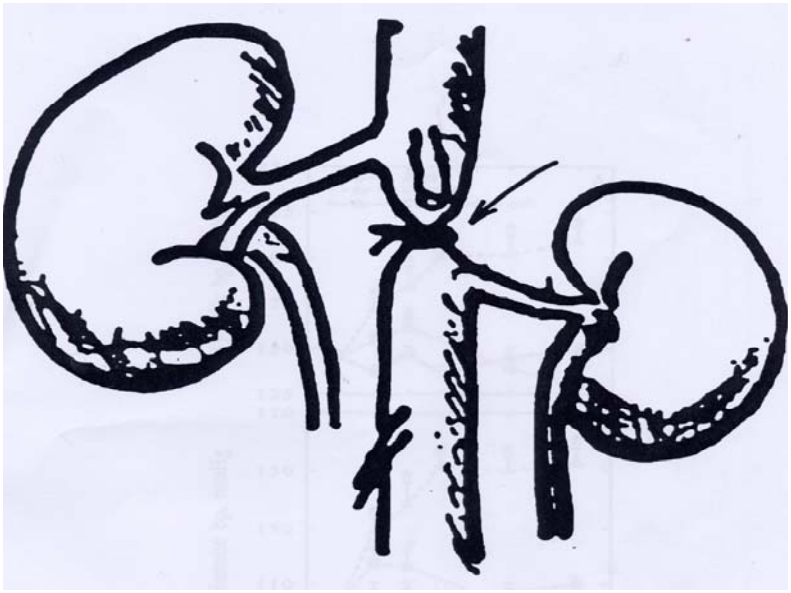

Fig. 1-1. 腹動脈結紮

以 Sprague-Dawley 大白鼠施行左、右腎動脈之間腹動脈結紮。

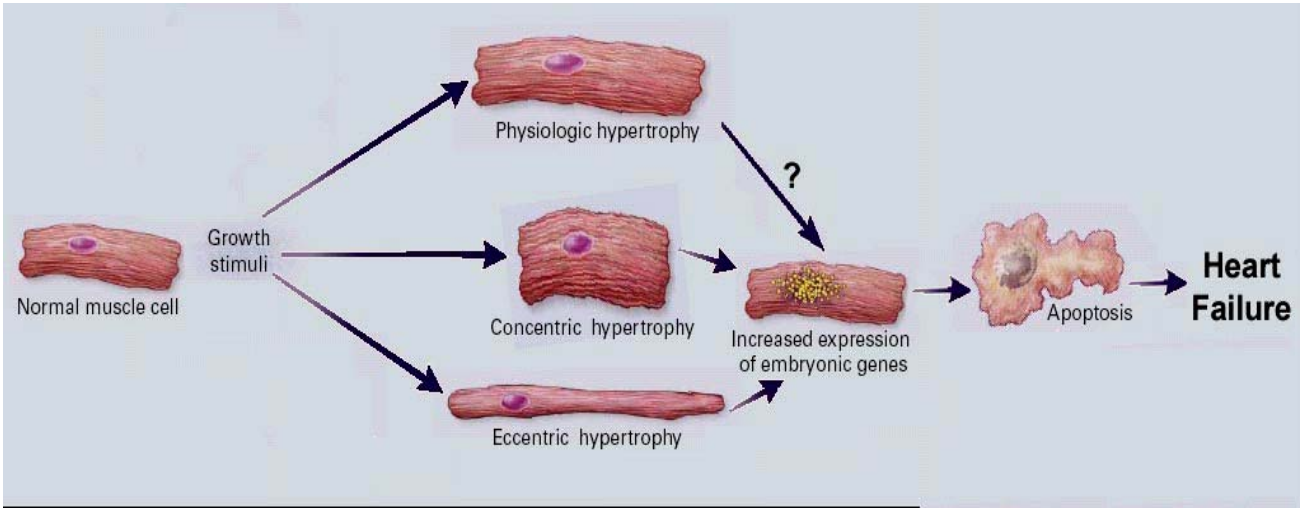

Fig. 1-2. 心臟肥大之種類[12]

就心臟細胞的構形而言，心臟肥大可分為：同心性病理肥大(concentric hypertrophy) 和延長性病理肥大(eccentric hypertrophy）。前者心臟細胞以橫向延長，肥厚型心肌症(hypertrophic cardiomyopathy)屬之。後者心臟細胞以縱向擴大，擴張性心肌症屬之(dilated cardiomyopathy）。而生理性肥大(Physiological hypertrophy)，亦即心臟細胞之長及寬等比例擴大，運動員之心臟肥大屬之。

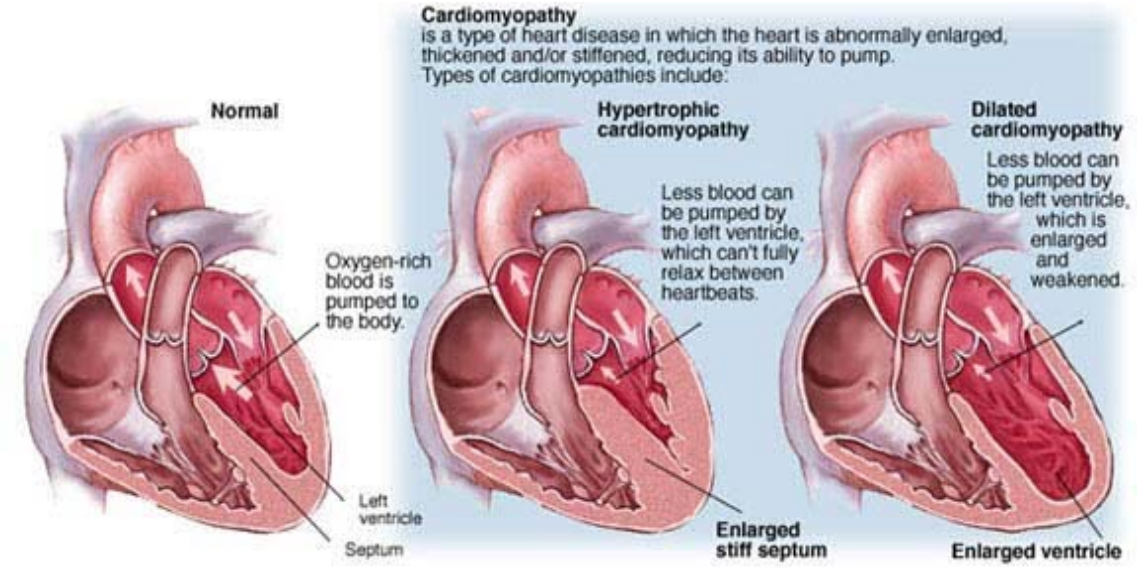

Fig. 1-3. 病理性心臟肥大[12]

可分為肥厚型心肌症(hypertrophic cardiomyopathy) 和擴張性心肌症屬之(dilated cardiomyopathy)兩種。

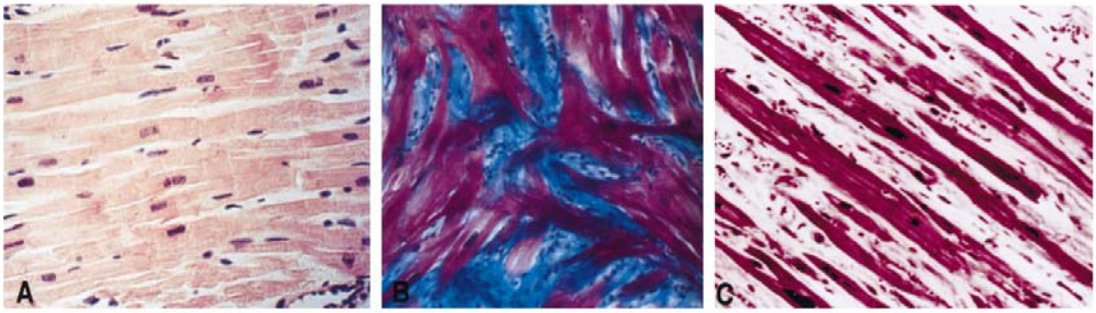

Fig. 1-4. 心臟肥大病理切片圖[12]

以 H.E.染色，與正常心臟切片(左)比較起來，則可見肥厚型心肌症(中)顯示細胞間隙纖維化 (interstitial fibrosis) 及細胞走向改變 (disarray)，而擴張性心肌症 (右)未顯示細胞走向改變，而可見細胞間隙纖維化的現象。

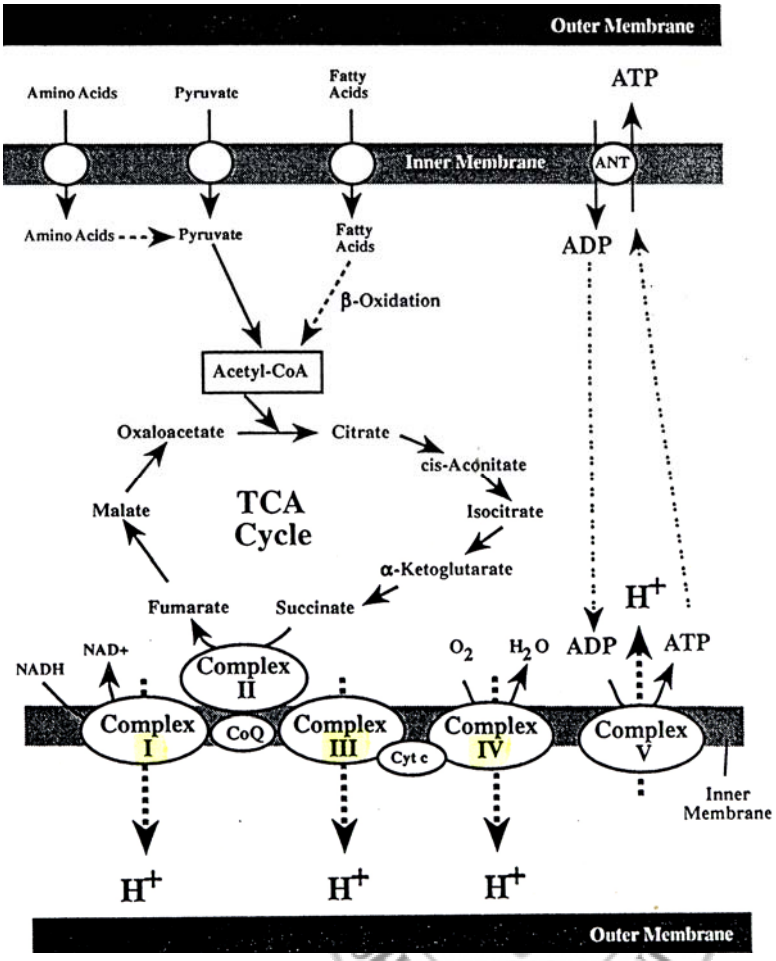

Fig. 1-5. 粒腺體內膜上之氧化磷酸化(oxidative phosphrylation, OXPHOS)反應[15]

在氧化磷酸化(oxidative phosphrylation, OXPHOS)的過程中，複合體I和II接收來自醣類，脂肪及蛋白質代謝的電子，並傳遞予ubiquinone (Co enzyme Q 10)，接著依序移往複合體III，細胞色素C和複合體IV。最後與O_2分子反應成水，複合體I、III、IV在傳遞電子的同時，將氫離子自matrix打入內外膜間質，而造成一氫離子濃度梯度，而複合體V利用此濃度梯度的能量，將ADP與磷酸根合成為ATP。

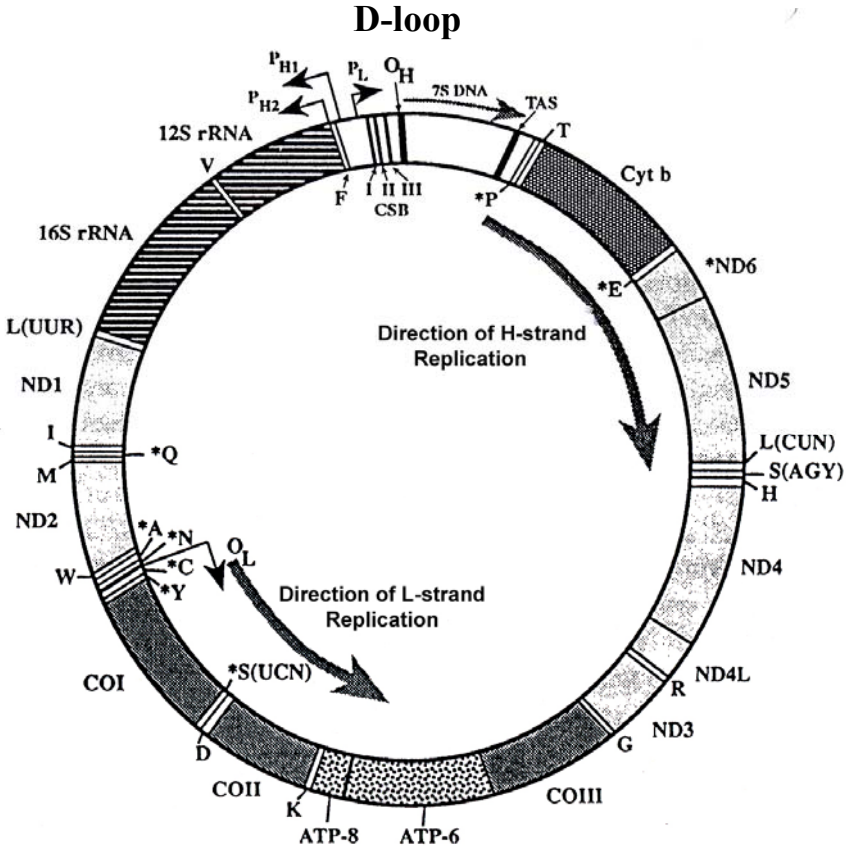

Fig. 1-6. 粒腺體DAN[15]

是一雙股環形分子，帶有 16569 對鹼基，其中 guanine 高含量的區域稱 heavy(H) strain，而 cytosine 高含量的區域稱之 light(L) strain。而其中一個包含 1122 對鹼基專門執行粒腺體 DNA 的複製及記錄，被稱為 D-loop。整個粒腺體基因，可表達到 37 種基因；其中包括 2 個核糖體 rRNA，22 個傳送之 tRNA，及其餘 13 個屬於電子傳遞鍊上的反應蛋白，7 個複合體 I 的次單元，1 個複合體 III 的次單元，其中複合體 IV 的 I、II、III 次單元分別位於第 5904-7444，3586-8262，及 9203-9990 對鹼基的位置。

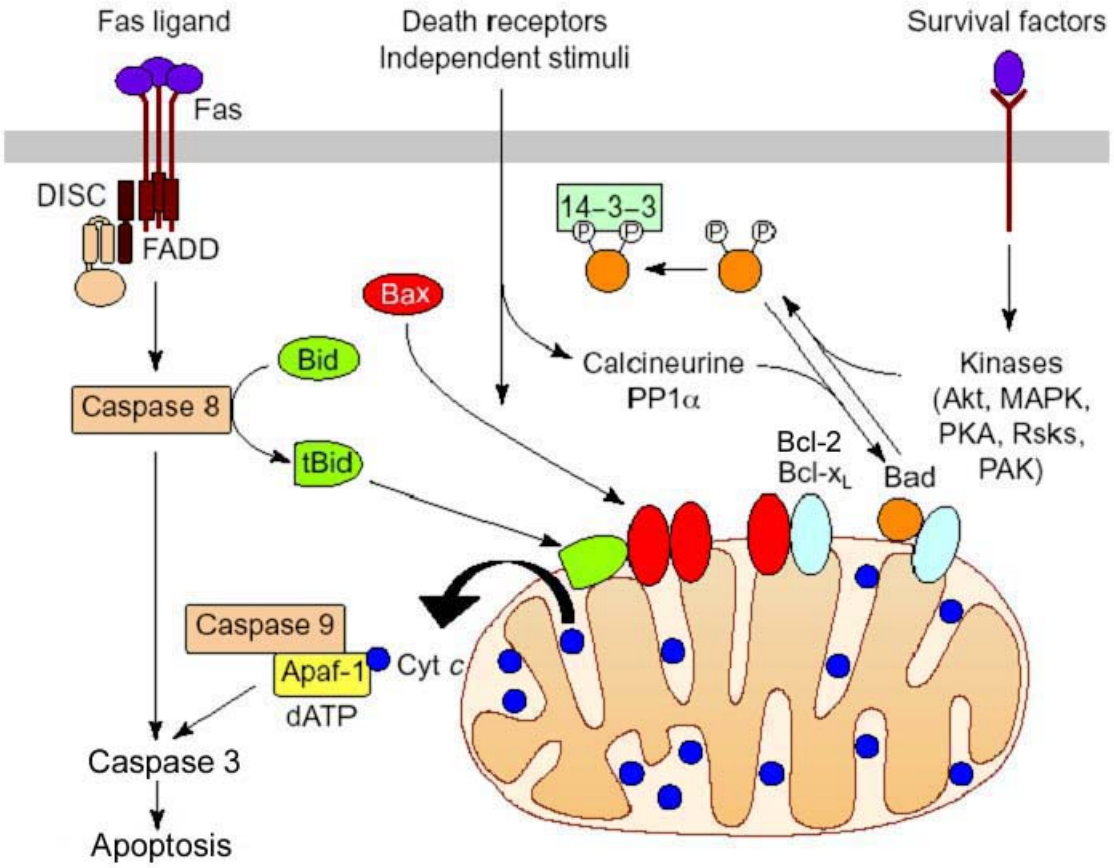

Fig. 1-7. 細胞凋亡之路徑[23]

當細胞受到外來引發凋亡之刺激時，粒腺體內膜上的，細胞素C會被釋放出來，而引發Apaf-1 與不活化caspase 9 的結合，而誘發具活性之caspase 9。此一屬上游之執行caspase，將活化另一下游執行者caspase 3，進而造成細胞凋亡。細胞中另有一群BCl_2家族，其中BCl_2依附於粒腺體膜上，可調節粒腺體外膜之通透性，並抑制細胞色素C的釋放，同時抑制caspases之活化，進而抑制細胞凋亡作用。相對的，BCl_2家族成員中，亦包括促進細胞凋亡作用的蛋白如Bad，反而增加粒腺體外膜通透性，促進細胞色素C的釋放，而達到促進細胞凋亡的作用。

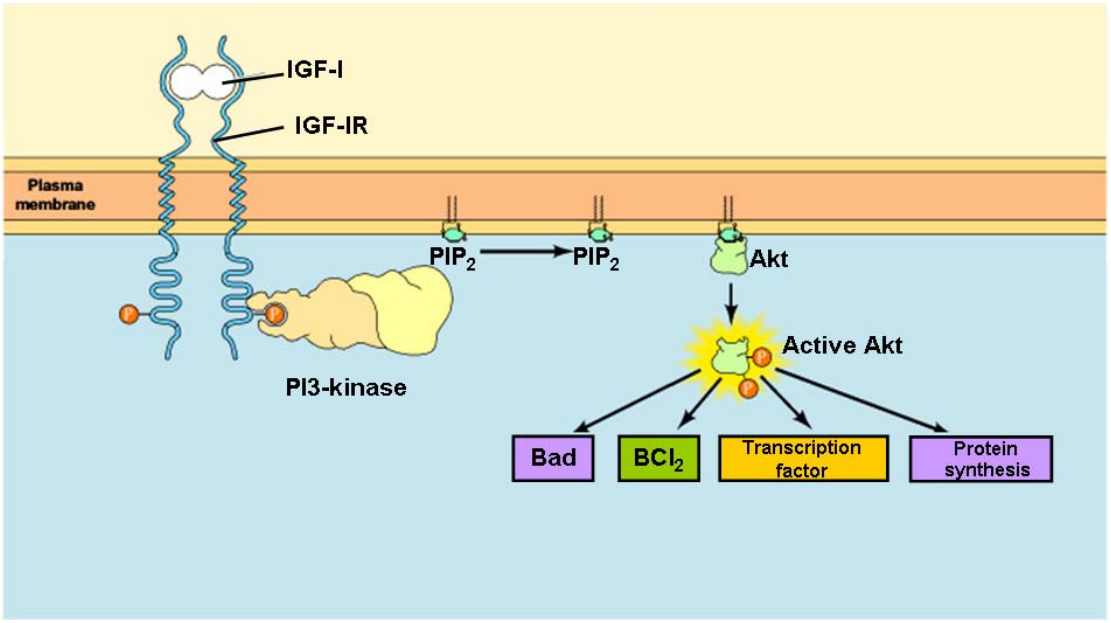

Fig. 1-8. IGF-I訊息路徑之促進細胞存活作用[23]

IGF-IR與IGF-I結合後活化下游的PI_3K，其將PIP_2磷酸化成PIP_3，PIP_3則將Serine/threonine kinase Akt 吸引到細胞膜上，使其被PDK所磷酸化，而後磷酸化之Akt則以磷酸化的方式引發下游與細胞存活有關之訊息蛋白的活性，並可抑制BCl_2家族中之Bad蛋白，Akt可將其磷酸化，使其失去活性而自粒腺體表面移除，因而抑制了細胞色素C自粒腺體之釋放游離。Akt並可藉磷酸化之作用直接抑制了Caspase 9 之活性。Akt也磷酸化其他促細胞存活的蛋白，與調節細胞代謝與蛋白合成有關之酵素如GSK-3。

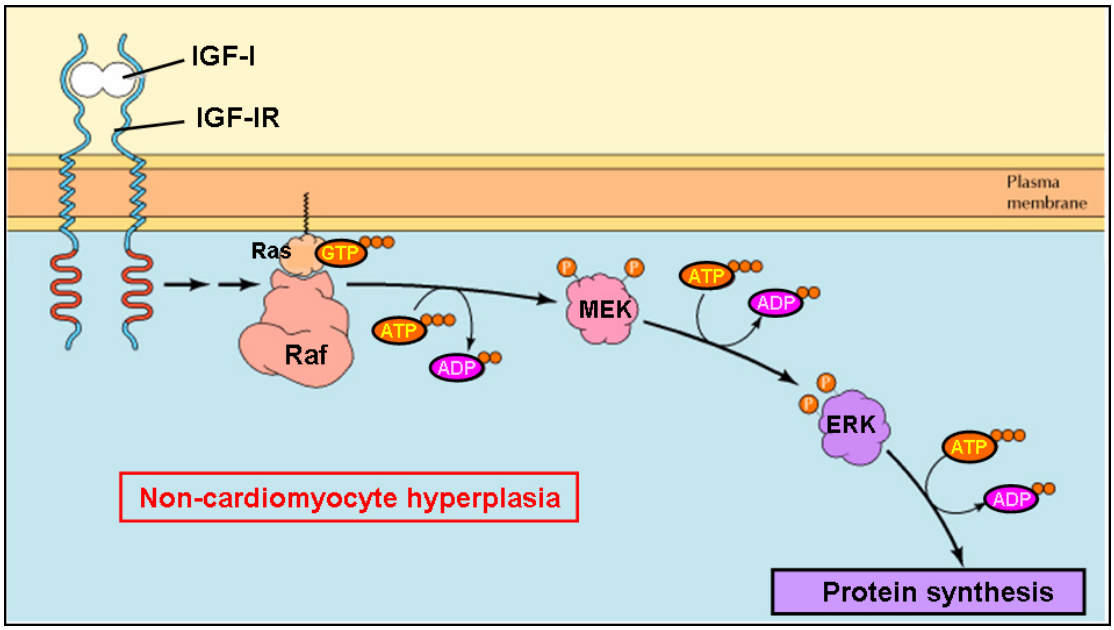

Fig. 1-9. IGF-I另一下游之Ras/Raf/MAPK途徑[41]

其多作用在心肌組織中的非心肌細胞，而 Ras/Raf/MAPK 抑制細胞凋亡並促進非心肌細胞增生，是透過 ERK 磷酸化 RSK，與 Akt 類似的是 RSK 亦可將 Bad 磷酸化，達到促進細胞存活的效果。

第二章

藉大白鼠腹動脈完全結紮誘發心肌肥大模式，探討心肌 cytochrome *c* oxidase (COX)基因表現及蛋白活性變化

中文摘要

眾所周知，過度血壓上升可導致心臟的肥大。但發生在心臟細胞中生理、生化及分子之肥大機制，則還不太清楚。再則心臟細胞中，粒腺體是提供心臟能量的關鍵，但其如何應付心臟過度負擔之需求，亦不得而知。在本實驗中,我們應用大白鼠腹動脈完全結紮模式，誘發心臟肥大，我們除了觀察到血壓上升外，並發現心臟肥大在手術之後的 1 到 2 天即發生，並持續至實驗結束(第 20 天)。同時心臟粒腺體中 COX-Vb 蛋白質量及 COX-Vb 酵素活性，亦隨著心臟的肥大而上升，且在第 5-7 天達到最高值，但第 10 天開始下降，手術後第 20 天則下降得比基礎值低。藉由 *in situ* hybridization 及 dot blotting 測量，心臟細胞色素 *c* 氧化酶(cytochrome *c* oxidase-Vb, COX-Vb) mRNA，亦在結紮第一天快速上升，且持續增加，在第 5-7 天達到最高值，並在第 20 天降低，與基礎值差不多。此外,採 Wistar(WKY)正常鼠與先天性高血壓大白鼠(SHR & SPSHR)作比較，發現 SHR 及 SPSHR 心臟中，COX-Vb 蛋白質量在生長初期之 12 週齡內，即比正常血壓(WKY)大白鼠低。綜觀而論，1.COX 之基因表現及蛋白活性可能在心肌肥大的過程中，伴演一適應之角色。2.不論是長效性腹動脈完全結紮大白鼠(第 20 天)或先天性高血壓大白鼠的模式，在肥大之心臟細胞中，低效率粒腺體活性，可能或至少部分是造成心肌衰竭

的原因。3.腹動脈完全結紮造成心臟快速肥大的模式中，COX 之活性上升，可能是用來供應心臟在過度負擔時所需之額外能量。

關鍵字：細胞色素 *c* 氧化酶; 腹動脈完全結紮； 心臟肥大; 先天性高血壓大白鼠(SHR)和中風傾向先天性高血壓大白鼠(SPSHR)

英文摘要

It is well known that pressure overload leads to cardiac hypertrophy. The physiological, biochemical, or molecular mechanisms, that underlie the myocyte enlargement occurring during cardiac hypertrophy are not completely understood. The contribution of the mitochondrial components, the main source of energy for the hypertrophic growth of the heart, is not well understood. In the present study, using a model system, complete coarctation of the rat abdominal aorta was used to study the rapid development of cardiac hypertrophy. One to two days after surgery, we observed significantly higher blood pressure and cardiac hypertrophy, which remained constantly high afterwards. We found that mitochondrial COX protein level and enzyme activity increased as the heart enlarged and, however, dropped even lower than baseline 20 days following surgery. We also found an early increased level of cytochrome *c* oxidase (COX) mRNA determined by *in situ* hybridization and dot blotting assays in the hypertrophied hearts, though the increased level had dropped to the baseline 20 days after surgery. In addition, the COX protein was significantly lower in natural hypertension-induced hypertrophic hearts in spontaneously hypertensive rats (SHR) and stroke-prone SHR (SPSHR) than in normotensive rats (WKY) throughout the whole period of 12 weeks. Taken together, the lower efficiency of mitochondrial activity in the enlarged hearts of rats with long-term complete coarctation or SHR and SPSHR could be, at least partially, the cause of hypertensive cardiac disease in these two models. Additionally, the rapid cardiac hypertrophy induced by experimental complete coarctation was accompanied by a disproportionate increase in COX activity, which was suggested to maintain the cardiac energy-producing capacity in overloaded hearts.

Key words: cytochrome *c* oxidase (COX); complete coarctation; cardiac hypertrophy; spontaneously hypertensive rats (SHR) and stroke-prone SHR (SPSHR)

前 言

心臟藉著實體之增加(即心臟肥大)來應付額外增加的工作負荷,例如高血壓。而在實驗動物模式中，所引起之高血壓又可分為病理性(自然性)或實驗性兩種[4]。為了應付額外的負擔，心肌收縮增加,更多的能量製造是必須的。心臟細胞百分之百藉粒腺體的有氧呼吸提供能量來源，而調控能量產生的則是心臟細胞中粒腺體的氧化磷酸化(oxidative phosphorylation，OXPHOS)過程。不過,在文獻上有關粒腺體能量產生的結果與心臟肥大關係的報告則大多是不一致的[42]。再者，有關粒腺體之生合成與功能和心臟肥大之研究是很少的。尤其，特別值得注意的是心臟衰竭末期，肥大的心肌和COX關係密切，且與產生能量有關的氧化磷酸化活性，往往都有不足的現象[43,44]。

COX 蛋白位於粒腺體的內膜,屬於呼吸鏈的四個複合體中的最後一個。這種由COX催化的反應，是提供心肌能量氧化磷酸化(phosphorylation，OXPHOS) 反應的關鍵步驟。所以COX在正常心臟功能的維持伴演著重要角色[45,46]。在哺乳動物裡，COX包含 13 個不同的亞單元。其中，三個較大的亞單元 (I,II 和III) 是在粒腺體內合成，並由粒腺體 DNA (mtDNA)基因所控制。其餘 10 個較小的亞單元(IV，Va，Vb，VIc,VIb，VIc，VIIa，VIIb，VIIc 和VIII)是在細胞

質裡合成，由核DNA (nDNA) 基因所主宰[46]。由於COX 控制著氧化磷酸化(phosphorylation，OXPHOS)反應步驟，所以，在正常生理情況下，只要COX功能些許改變，則可影響整個氧化磷酸化(phosphorylation，OXPHOS) 反應速率。所以，若COX功能稍有缺失，即很可能造成心肌細胞中粒腺體病變[47,48]，而引起心臟衰竭。實際上，由COX各亞單元基因突變所導致之心臟病變，已逐漸被發現[16-18]。

在很多研究中，採用主動脈結紮來引發心臟的肥大。而我們先前的實驗，顯示腹動脈完全結紮實驗動物模式，除快速造成血壓上升外，更在手術後 1-2 天內，即可觀察到心臟肥大之現象[11,42,49]。因此，在本實驗中，我們進一步以此模式來探討在心臟肥大過程中，心臟細胞內粒腺體的組成成分，如何來因應心臟因過度負擔所需之額外能量。我們將以COX-Vb 為對象，來探討其基因及蛋白活性變化之模式。在腹動脈完全結紮 1-20 天所造成之心臟快速肥大過程中，我們除了測定COX-Vb酵素活性及蛋白質量，並同時測量COX-Vb mRNA來評估COX-Vb之基因表現模型。另外，實驗並比較早期(4-12 週齡)先天性高血壓大白鼠(SHR)和中風傾向先天性高血壓大白鼠(SPSHR)之肥大心臟中，COX蛋白質量之變化。

材料與方法

腹動脈結紮 Coarctation

本實驗中， 體重 240 和 300 克之間的Sprague-Dawley雄性大白鼠(購自國科會動物中心，台北，台灣) 藉由左右腎動脈之間的腹動脈完全結紮(Coarctation)引起心臟的肥大[10]。 經過注射pentobarbital (45.5 毫克/千克)使麻醉之後, 將其身體側躺，以膠帶固定四肢，左邊腹部去毛後,再髖股往上三指處下刀。切開表皮及腹部肌肉組織層後，使內臟暴露, 以棉花棒游離脂肪，找出腹主動脈，並在兩腎之間的腹主動脈，以棉線打結，接著將傷口縫合。並且使用傷口夾子使表皮重新結合。然後，以含l% 碘酒的 70% 的酒精溶液用來清潔傷口。老鼠返回動物籠(每籠一隻)並且使其恢復。全部動物飲用水添加tetracycline (22 毫克/ 千克體重)以避免感染。假手術老鼠接受相同的步驟處理，但是沒有結紮腹動脈。接著依結紮天數 1、2、3、5、7、10 和 20 天，測完股動脈壓力後，大白鼠施以斷頭處理，並快速取出心臟以二次水清洗，並分離出左心室以為實驗的檢體。

股動脈壓力測量

在結紮手術l，2，3，5，7，10 和 20 天後，我們測量腹動脈結紮和

假手術老鼠的股動脈血壓。 未處理手術之動物血壓測量為 0 日之控制組。 當大白鼠股動脈插管完成後，大白鼠血壓之測定是透過導管與血壓偵測感應器(Recorder 2200S, GOULD, U. S. A.)之連接後，測量並且連續記錄收縮和舒張的壓力[50]。

心臟分離

一旦大白鼠股動脈血壓測量完成後，進行斷頭犧牲。 打開胸腔，取出心臟。 在除去脂肪和連接組織之後，去除血液並稱重。計算出總心重量和體重的比率。稱重完之心臟在冰溫(0-4 ℃)之SNTE緩沖液(0.20 M 蔗糖，0.13 NaCl，l Li Tns。 HCl，pH值 7.4 [45],以Tri調整pH值 7.4 之lmM EGTA)中沖洗後，取下整個左心室，分成 4 個部分，除心尖部份用來in situ hybridization分析外，其餘冷凍於-70℃冰箱待進一步分析。

粒腺體的製備

第一個部分的左心室以剪刀剪碎，與SNTE緩沖液(每克組織 1.5 ml)混和，在冰溫下，每一個樣品以均質機(PT l0/35 Polytron, Brinkmann Instrument, Westburg,NY,USA)以每一個循環l0 秒兩次的方式磨碎。磨好之均質液第一轉以離心機(Backman J20.1) 500 X g之速率離心 15 分鐘。 然後，上清液更進一步以 8000 X g之速率離心 15 分鐘分離。 取

下沉澱以SNTE緩沖液回溶。此即粒腺體液。測量蛋白質[51]後,為COX活性分析作準備。

Cytochrome *c* oxidase 活性測定

Cytochrome *c* (取自馬之心臟, Sigma Chemical Co. no. C-7752, TypeⅢ,USA) 在緩沖液(50 nM 磷酸鹽(K_2HPO_4-KH_2PO_4)，pH值7.0)中以dithionite 還原[52,53]。還原態之 Cytochrome *c* 必需在每個實驗前新鮮配製，並保持在冰溫狀態下，加入心臟粒腺體液樣品後，COX活性以分光光度計在波長550nm下測量還原態Cytochrome *c*氧化產物之量，整個過程在磷酸鹽緩沖液(50 mM，0.5% Tween 80 pH 7.0) [54]環境下進行。反應速率以"μmol cytochrome *c* oxidized per min per mg mitochondrial protein"表示。

蛋白質萃取和西方的墨點分析

第二個部分的左心室同樣以剪刀剪碎，用lysis緩沖液(50 mM Tris (pH 7.5), 0.5M NaCl, 1.0 mM EDTA (pH 7.5), 10% glycerol, 1mM BME, 1% IGEPAL-630 and proteinase 抑制劑 (Roche)) 以均質機(PT l0/35 Polytron，Brinkmann Instrument, Westburg,NY,USA)磨碎，以離心機1200rpm之速率離心 30 分鐘。 然後，取上清液測量蛋白質後[51], 取

20μg，加入PBS buffer至體積為 20μl，再加入 5μl Loading dye使總體積為 25μl，將其混合均勻。接著將樣品置於 99℃10 分鐘後，進行SDS-PAGE電泳分析，以 140 伏特進行電泳分析約三個半小時。待電泳結束即可進行轉漬(transfer)，於轉漬緩沖液(25 mM Tris-HCl, pH8.3, 192 mM glycine and 20% (v/v)甲醇) 4℃下進行 100 伏特電轉漬(Transfer) 14 個小時，將被電泳分離的蛋白質轉漬到NC paper(Amersham, Hybond-C Extra Supported, 0.45 Micro)。轉漬成功之NC paper加入Blocking buffer (100 mM Tris-HCl, pH7.5, 0.9% (w/v) NaCl, 0.1% (v/v) fetal bovine serum.)於室溫下搖動 2 小時後，加入以緩沖液(100 mM Tris-HCl, pH7.5, 0.9%(w/v) NaCl, 0.1%(v/v) Tween-20 and 1%(v/v) fetal bovine serum)稀釋之COX 1 級抗體(Santa Cruz Biotechnology)，於室溫下反應 3.5 小時。之後以 1× TBS buffer清洗。而後加入 2 級抗體(alkaline phosphatase goat anti-rabbit IgG (Promega))，反應 1 小時，再以 1× TBS清洗 10 分鐘。最後分別加入Substrate buffer (7 mg nitro blue tetrazolium, 5 mg 5-bromo-4-chloro-3-indolyl-phosphate, 100 mM NaCl and 5 mM $MgCl_2$ in 100 mM Tris-HCl, pH9.5)、37% H_2O_2及(4~5μl) DAB進行呈色反應即可。同一樣品中，以電泳分離的蛋白質，以α-tubulin為抗體，根據相同之步驟所偵測之值為internal control。

心臟 RNA 的萃取

第三個部分的左心室用來萃取RNA。使用Ultraspec RNA 萃取液(Biotecx Laboratories, lnc.)根據製造商提供的步驟，每個樣品與萃取液混合後(1ml Ultraspec reagent 與每 100 mg 樣品)，以均質機(PT l0/35 Polytron，Brinkmann Instrument, Westburg,NY,USA)充分磨碎，並於冰溫放置 5 分鐘，再加入 200μl氯仿(Chloroform)並充分混合均勻後，於冰溫放置 5 分鐘，接著以 12000 rpm，冰溫下離心 15 分鐘。離心後取出上層液加入等體積之phenol-chloroform，充分混合後再以 12000 rpm，冰溫下離心 10 分鐘。離心後取出上層液加入等體積之 Isopropanol，充分混合後，於冰溫放置 10 分鐘，以 12000 rpm，冰溫下離心 10 分鐘，接著將isopropanol移除，所得之白色小片沈澱用 70%的酒精溫和的vortexing 後，每次皆以 12000 rpm，離心 5 分鐘。最後去除酒精之白色小片沈澱於空氣中乾燥後，加入 50μl之滅菌 0.1% DEPC-H_2O回溶沈澱物，並於 55℃水浴槽 10 分鐘。最後測其吸光值(OD_{260})以換算所萃取之RNA濃度。

RNA濃度(μg/ml)＝稀釋倍數 × OD_{260} × 40 (μg/ml)

COX 探針之製備

來自大白鼠 COX-Vb基因(帶有 500 對鹼基之模版)之質體 pGEM-7Zf(+)(promega)，經過直線化 (linearized)，及根據以 digoxigenin (DIG)標定UTP 之kit (Roche) 轉譯成“anti-sense” COX mRNA探針[55]。以 2% agarose gel確認此探針長度無誤。以同樣步驟製備“sense” COX mRNA。

Dot blotting

Dot blotting 之步驟是根據 Huang et al 等之快速偵測法(見附錄一) 。以上製備之 DIG 標定 “anti-sense” COX mRNA 探針以 1μg/ml 濃度於雜交緩沖液(hybridization buffer)與每點 80 ng 左心室 total RNA 做雜交(hybridization)。以 18 SrRNA 之偵測當作 internal control。以帶有鹼性磷酸酶(alkaline phosphostase,AP)標定之 anti-DIG 抗體作用後，加入 CDP-star 受質反應後，產生冷光，在暗房壓片後，以 Image-analysis 定量每一樣品所含 COX mRNA 之圓點信號，被偵測到 COX mRNA 之量，以 18SrRNA 標準化後，製作成長條圖。

In situ hybridization 和量化

第四部分的左心室用來以in situ hybridization 方法[11]，偵測心臟組織內之COX mRNA量。冷凍後之左心室切成 4μm 薄片，平放於載

玻片上，並且與上述“anti-sense”COX-Vb mRNA 探針雜交。雜交過之組織切片，並以帶有鹼性磷酸酶(alkaline phosphostase,AP) 之anti-DIG 抗體 (稀釋 3:500) 偵測探針。以DIG 標定之”sense” mRNA探針，或無探針之使用作為控制實驗。所偵測組織切片中COX-Vb mRNA，在顯微鏡下觀察並照相。在每一組大白鼠左心室認意挑選三個切片，各三個 100μm^2 區塊，計算點數，作成量化長條圖。

統計分析

本實驗以單變項變異數分析(ANOVA)來分析統計差異。當處理組數大於 2 時，則以 Fisher's Least Significant Difference test 來決定各處理間之差異性。本研究各項試驗所設定之統計顯著水準以 $P<0.05$ 為標準。所有數據以平均值(mean) ± 標準誤差(SE)表示。

結 果

壓力過度負荷大白鼠的高血壓性心臟肥大

腹動脈完全結紮大白鼠血壓之測定，清楚的顯示動脈結紮所造成之高血壓的效應(Fig 2-1)。控制組大白鼠動脈收縮的血壓，在術後 1，7 和 20 天，分別是 l37 ± 5, 148 ± 3 and 152 ± 6 mm Hg，但結紮組大白鼠為 172 ± 6, 220 ± 10 and 200 ± 10 mm Hg。與此類似，控制組大白鼠動脈舒張的血壓為 l00 ± 5, 110 ± 5 and 115 ± 5 mm Hg，而結紮組大白鼠為 128 ± 5, 154 ± 6 and 148 ± 9mmHg。

腹動脈完全結紮所造成之心臟肥大的結果說明在 Table 2-1。控制組大白鼠心臟全重在整個實驗過程維持不變。相反的，結紮組大白鼠在術後 2 天前，心臟全重即顯著上升，直到實驗結束。與 0 日控制組大白鼠比較起來，結紮組大白鼠在術後 2 到 20 天，心重量對體重的比率顯著增加。這比率在控制組大白鼠在整個實驗過程維持不變。

COX-Vb 蛋白及酵素活性之變化

COX 酵素活性與 Vb 次單元蛋白量分別以酵素動力法及西方的墨點分析來測定。術後 1 天即有增加趨勢，術後 2 天，結紮組大白鼠心臟 COX 酵素活性即顯著增加，除了第 20 天明顯低於控制組外，其餘時間點之活性值(每 mg 心臟粒腺體蛋白)，皆顯著高於控制組(Table

2-2)。與 0 日之控制組(未處理手術)之大白鼠比較起來，結紮組大白鼠心臟 COX-Vb 蛋白量亦在術後第 2，3，5 和 7 天即有顯著意義之上升。相反的，在術後第 20 天，COX-Vb 蛋白量，低於 0 日之控制組(Fig 2-2)。

COX-Vb 基因表現

本研究以 *in situ* hybridization (Fig **2-3**) dot blotting (Fig 2-4) 之實驗所測定大白鼠心臟中 mRNA 之量來當做 COX-Vb 基因表現之指標。而二者都是以 Dig 標定之 antisense COX-Vb mRNA 為探針所測定。無論 dot blotting 結果或結紮組大白鼠心臟切片所雜交到之 COX-Vb mRNA，在術後第 1 天即顯著增加，並在術後第 5 天達到最高值。而後持續下降，在術後第 20 天達到和控制組大白鼠一樣之基礎值(Fig 2-3A, 2-3C)。而控制組大白鼠心臟中 mRNA 之量，在整個 20 天當中並無改變(Fig 2-3C)。在 Fig 2-3B 中為所攝得第 7 天 *in situ* hybridization 的結果。在以 sense mRNA 為探針或缺少探針之控制實驗中，並未偵測出 COX-Vb mRNA，顯示整個實驗系統條件控制良好，且無非專一性雜交現象發生。而 dot blotting 偵測 COX-Vb mRNA 的結果整理於 Fig 2-4A。以 GAPDH mRNA 當做 internal control。每一 COX-Vb mRNA 之量，是經過 GAPDH mRNA 標準化(除以相對

GAPDH mRNA 值)而得。Fig 2-4B 為量化之結果。其中顯示在每一時間點之測定，腹動脈完全結紮大白鼠心臟中 COX-Vb mRNA 之量，顯著高於控制組，並在術後第 20 天下降至基礎值。

早期遺傳性高血壓老鼠心臟 COX-Vb 蛋白的缺損

相對於腹動脈結紮所造成心臟過度負擔之大白鼠模式，本研究亦測量了早期 12 週齡內之先天性高血壓大白鼠(spontaneously hypertensive rats (SHR) and stroke-prone SHR (SPSHR))心臟中 COX 蛋白質量。以 Wistar 大白鼠為控制組，所得之結果整理於 Fig 2-5。以 β-actin 為 internal control，但無論年齡是 4，6 或 12 週大，高血壓大白鼠心臟 COX-Vb 蛋白質量皆低於 Wistar 大白鼠。這意味著先天性高血壓大白鼠心臟 COX-Vb 蛋白可能在早期即有缺損的現象。

討　論

在本實驗中，以完全結紮於大白鼠左右腎動脈間腹動脈之模式，快速造成血壓上升，增加心臟之負荷(loading)，而引發心臟肥大。此動物模型中，術後 1 天即可觀察到血壓上升。到第 3 天達最高值(200 mmHg)，並持續至 20 天實驗結束。而控制組大白鼠在整個實驗過程中血壓都維持在 140 mmHg左右。而結紮組大白鼠，術後 2 天即出現顯著心臟肥大現象，此一現象說明了本研究中，腹動脈完全結紮模式，確能快速的造成高血壓性心臟肥大。比其他模式如，非完全性(partial)動脈結紮[42,49]，或高劑量甲狀腺素處理等均來的快速[49]。

在心臟肥大期間，為保持正常的心臟組織功能，因應額外的工作量，心臟細胞的擴大必伴隨著胞器及肌節組成分的增加。而為了提供增加能量需要，粒腺體製造能量之機器增加也是必然的。在本實驗中，以 *in situ* hybridization 和 dot blotting 所測定大白鼠心臟中 COX-Vb mRNA，開始於術後 1 天增加，第 5 到 7 天達到最高值，而後持續下降，在術後第 20 天達到和控制組大白鼠一樣之基礎值。在 COX-Vb 蛋白量及酵素活性之變化，亦呈現類似之趨勢。唯第 2 天才有達顯著增加，然而，在第 20 天，降至比基礎值低。事實上，由此時(第 20 天)時腹動脈完全結紮大白鼠死亡率已達 50%的結果看來，

COX 是高血壓性心臟肥大早期過程中，一個重要的調適因子。並且，由術後 10 天後之結果 COX 之逐漸減少的現象看來，腹動脈完全結紮已對心臟造成不可回復之傷害。致使結紮之大白鼠瀕臨死亡。

不過，相關的文獻[42]顯示, 關於粒腺體內成分的作用，無論是在心臟肥大的前期或發展期間，即使所使用刺激心臟肥大的方法相同，都有不同的說法。雖曾有研究發現，以不完全腹動脈結紮所造成心臟肥大，顯示粒腺體內含物增加,即 ”mitochondrial biogenesis”。但此一發現並不與其他研究發現[42]一致。同時，針對神經血管性引起之高血壓心臟的肥大，粒腺體呈現出之變化量也並不一致。有兩份報告指出，腹動脈不完全結紮之肥大心臟COX酵素活性與mRNA之量，若以每mg總心臟蛋白計算，仍維持不變。其作者認為，在術後第 7 天[49]或者甚至多達 28 天[42]，”mitochondrial biogenesis”(粒腺體內含物增加)應與心臟重量增加成平衡發展。

另一方面，在本實驗中，快速心臟肥大的模式裡，在第 7 天前，COX酵素活性上升 30-47%。此一結果與Legato 等[56]報告相符合，其報告中指出，在心臟肥大的同時，粒腺體DNA在心臟組織中的含量隨之增加，並且粒腺體變得更小和被皺折(cristae)和內膜(inner membrane)包裹得更濃密。與此類似，在本研究中，COX酵素活性是以每毫克粒腺體蛋白質計算，故此增加的活性應是來自於于粒腺體內

成份之上升，而非粒腺體數量之上升。本實驗中，相較於其他實驗，使用了更嚴格之完全結紮，可能因此導致粒腺體增加了更多之酵素活性來因應。此外，所觀察到的來自細胞核mRNA轉譯出COX Vb亞單元蛋白之上升，亦符合在心臟肥大的同時，COX-Vb活性亦上升達到最高值。故我們認為COX-Vb之調節應屬於轉譯層次上的。我們推論，COX其他亞單元蛋白應也會有類似的調控情形[49]。由COX-Vb mRNA及蛋白之快速上升現象看來，COX-Vb應被考慮為在心臟肥大的適應期間一個很重要的調適因子。而在術後第 20 天，經過長時間的結紮後，大白鼠心臟COX的mRNA及酵素活性大大的下降，顯示COX之上升與心臟肥大平行發展的現象已不存在了。相信此時心臟衰竭的情形已開始發生。

另在 12 週齡內之早期遺傳性高血壓大白鼠 (SHR & SPSHR)模式，我們已發現有心臟肥大情形，且即使大白鼠只有 4 週齡而已，COX蛋白質量已呈現顯著降低。有趣的是Tokoro等人[57]之實驗曾發現，SPSHR大白鼠心臟中抗氧化重要酵素superoxide dismuatse (SOD)明顯較低。此外，一些來自粒腺體可轉譯成COX之基因，因缺乏鹼性蛋白(histone)的保護，在此時抗氧化能力下降的情形下，則基因更容易遭受氧化之傷害，而發生突變[58]。所以，在基因突變分析(restriction fragment length polymorphisms, RFLP) 結果中，可觀察到心臟細胞粒

腺體中發生突變之較短片段DNA[57]。這些報告或許可用於解釋COX-Vb蛋白在遺傳性高血壓大白鼠心臟中，量較少之原因。另外，Wanagat 研究[59] 認為COX-Vb蛋白可能的缺損，是隨著年齡上升才逐漸發生，與本研究發現缺失早發生在 4 週齡如此年輕之遺傳性高血壓大白鼠心臟的結果，恰好相反。我們認為SHR及 SPSHR大白鼠先天遺傳基因上缺失的可能性，亦是不能被排除的。再者，在遺傳性高血壓大白鼠 SHR & SPSHR的平均壽命分別只有一年半及八個月，與正常大白鼠的 2.5 年，著實短了許多。並且心臟COX蛋白質量在很早期(4 週齡)即有缺失的現象。因此，COX蛋白表現增加適應無法與心臟肥大平行發展，可能導致SHR及 SPSHR大白鼠心臟適應力減弱，致使早期衰竭原因之一。而間接造成較短之生命期。這就好比是腹動脈完全結紮大白鼠在第 20 天時，COX活性降至最低，無法繼續維持與肥大心臟的平行發展作用，而可能導致心臟衰竭的現象，是類似的例子。

總括言之，本實驗中首度驗證由腹動脈完全結紮造成心臟急速肥大，同時伴隨心臟中能量製造系統活性上升，此外,在諸多原因所引發心臟肥大的情形下，能量製造活性不足，往往是導致心臟衰竭的主要原因[54]。在本研究中，喪失功能的COX-Vb發生在SHR及 SPSHR大白鼠心臟中及腹動脈完全結紮大白鼠末期(第 20 天時)，顯示COX

的確是心臟肥大過程中，能量提供系統中的一個重要的因子。本實驗中，因應血壓上升心臟迅速肥大的過程，提供了能量製造活性的調適:從上升到下降使心臟瀕臨衰竭的一個完整的研究模式。未來的研究方向，將以本實驗中所建立腹動脈完全結紮模式，進一步探討COX基因上升或下降的機轉。

Table. 2-1. 腹動脈完全結紮與控制組大白鼠心臟全重及心重量對體重的比率

Day Postsurgery	H, g		H:B, mg:g	
	Sham	Coarcted	Sham	Coarcted
0	0.96±0.02 (n=8)	----------	3.63±0.08 (n=8)	----------
1	0.92±0.03 (n=4)	0.97±0.02 (n=4)	3.48±0.08 (n=4)	3.64±0.14 (n=4)
2	0.94±0.02 (n=5)	1.07±0.03* (n=5)	3.53±0.07 (n=5)	4.31±0.19* (n=5)
3	0.95±0.03 (n=7)	1.13±0.03§ (n=6)	3.47±0.07 (n=7)	4.56±0.13§ (n=6)
5	0.93±0.01 (n=3)	1.11±0.02§ (n=3)	3.51±0.08 (n=3)	4.98±0.18§ (n=3)
7	1.00±0.07 (n=4)	1.12±0.04 (n=4)	*3.44±0.08 (n=4)	4.63±0.30‡ (n=4)
10	1.04±0.05 (n=4)	1.16±0.03* (n=4)	3.42±0.09 (n=4)	4.83±0.31‡ (n=4)
20	1.10±0.04 (n=3)	1.20±0.03* (n=3)	3.40±0.12 (n=3)	4.99±0.20§ (n=3)

Data are mean ± SE. H and H:B are the heart weights (g) and heart weight to body weight ratios (mg:g), respectively, following surgery; n, number of animals. Zero day values represent baseline data from animals sacrificed on the day of surgery. * $P<0.05$, ‡ $P<0.025$, § $P<0.001$ compared to the sham animals.

Table. 2-2. **腹動脈完全結紮與控制組大白鼠，在術後 1 到 20 天期間，心臟粒腺體 COX 及酵素活性之變化**

Activity (μmol cytochrome *c* oxidized / min per mg mitochondrial protein)

	Days Postsurgery	
	CR	S
1	0.43±0.11 (n=4)	0.31±0.06 (n=4)
2	0.44±0.06 (n=4)	0.30±0.05* (n=4)
3	0.43±0.05 (n=3)	0.30±0.03* (n=3)
5	0.47±0.02 (n=3)	0.33±0.02* (n=3)
7	0.49±0.04 (n=4)	0.33±0.05* (n=3)
10	0.47±0.03 (n=3)	0.35±0.03* (n=3)
20	0.24±0.10 (n=3)	0.36±0.09§ (n=3)

Activity values are μmoles oxidized cytochrome *c* /min/mg mitochondrial protein (mean ± SE); n, number of animals. * $P < 0.05$ represents significant increase when compared to the sham animals. § $P < 0.05$ represents significant decrease when compared to the sham animals.

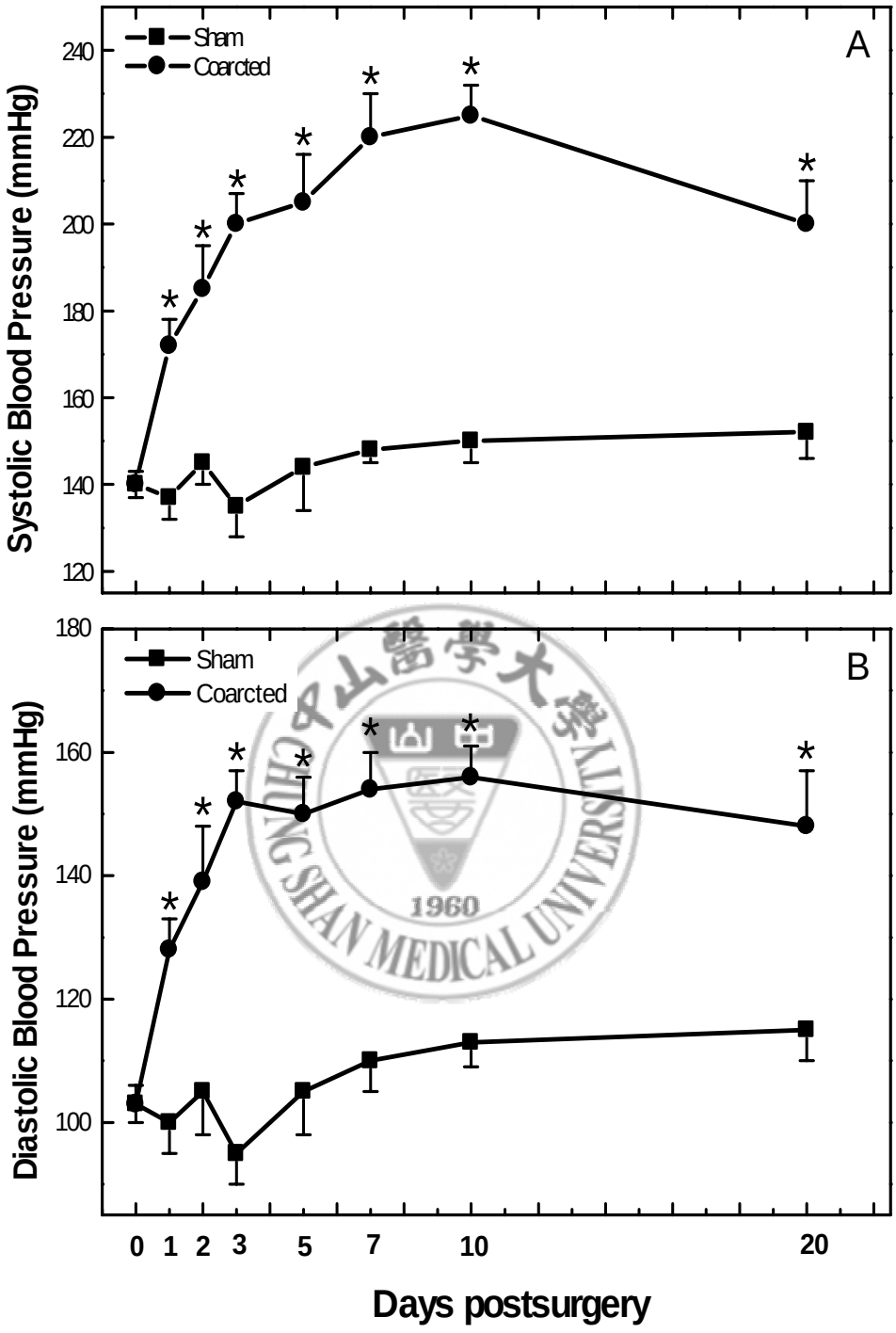

Fig 2-1. Arterial systolic and diastolic blood pressures of sham-operated and coarcted rats following surgery.

Zero day values represent baseline data from animals sacrificed on the day of surgery. Values are mean ± SE. Numbers of animals measured at each data point are given in Table 1. * $P<0.001$ represents the comparison to zero day sham animals.

(A)

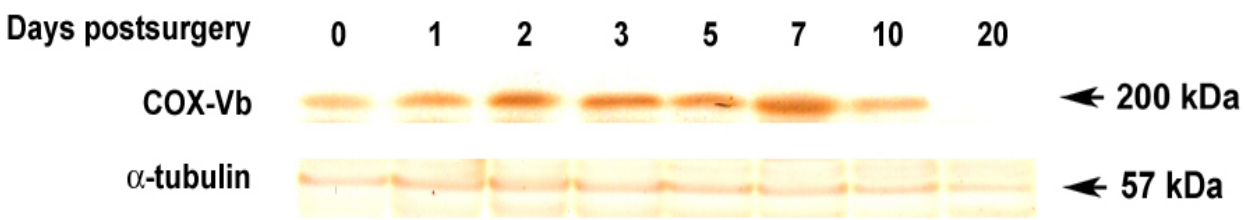

(B)

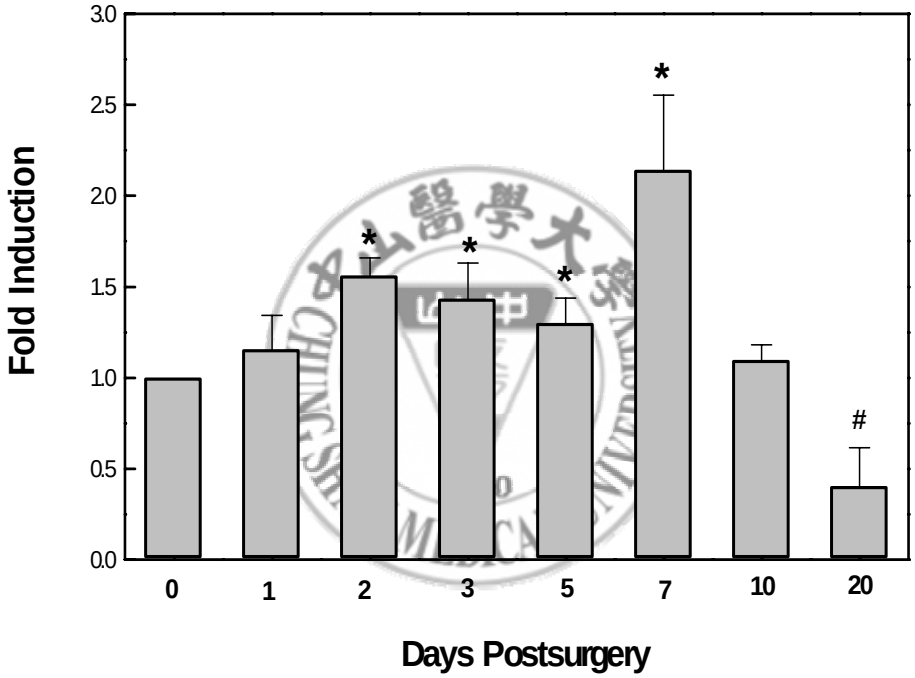

Fig 2-2. Activations of mitochondrial COX-Vb in cardiac tissues of rats.
(A) Western blotting analysis of COX-Vb proteins in LVs of sham-operated and coarcted rats at 0, 1, 2, 3, 5, 7, 10 and 20 days postsurgery. The blotting of α-tubulin was used as a loading control. (B) Signal intensity of western blotting was quantitated using a PhosphoImager. The averaged result ± SD of three independent experiments is shown. The 0-day value represents baseline data from animals sacrificed on the day of surgery. * represents a significant increase compared with the control group with $P < 0.05$. # represents a significant decrease compared with the control group with $P < 0.05$.

(A)

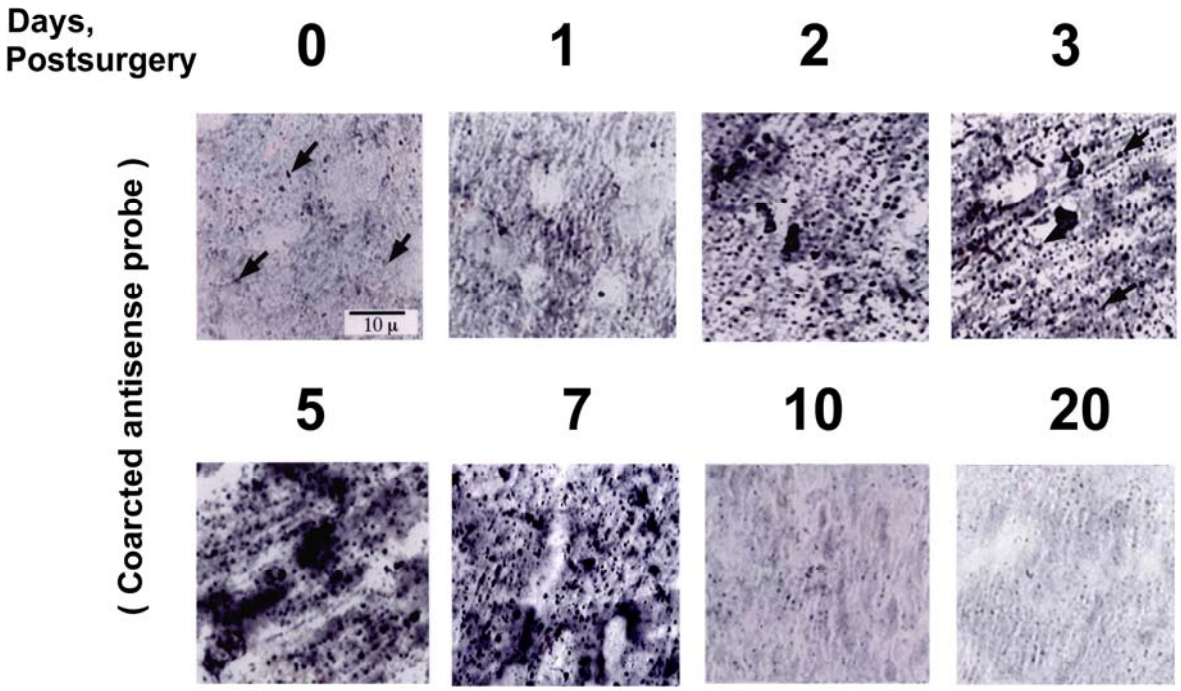
Days,
Postsurgery
0
1
2
3
(Coarcted antisense probe)
10 μ
5
7
10
20

(B)

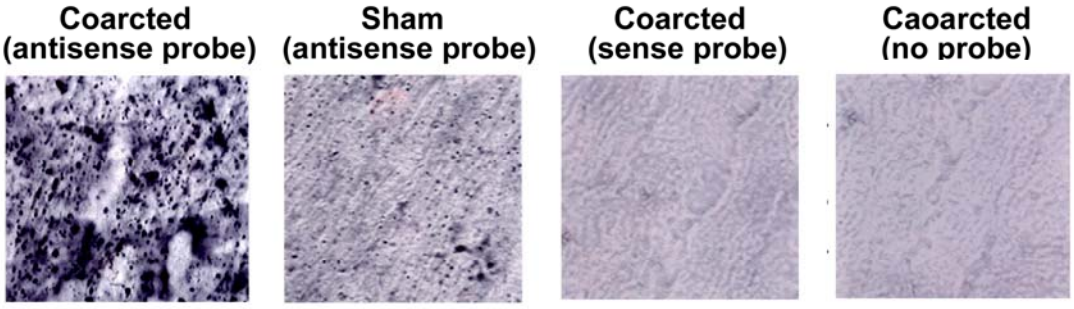
Coarcted
(antisense probe)
Sham
(antisense probe)
Coarcted
(sense probe)
Caoarcted
(no probe)

(C)

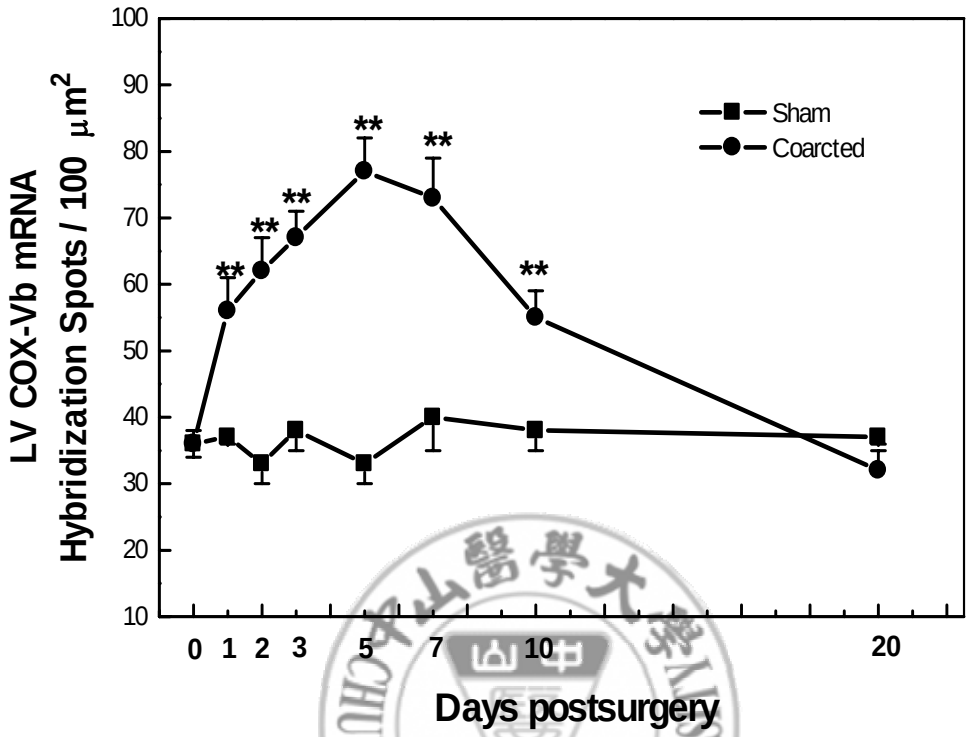

Fig 2-3. *In situ* hybridization of LV COX-Vb mRNA.

(A) Hybridization of antisense COX-Vb mRNA to LVs of sham-operated and coarcted rats at 0, 1, 2, 3, 5, 7, 10 and 20 days postsurgery. Arrows point to spots of immuno-detected hybridized antisense COX-Vb mRNA. (B) Hybridization with a digoxigenin (DIG)-labeled antisense COX-Vb mRNA probe in the LVs from sham-operated and coarcted animals at day 7 postsurgery. Control hybridizations with a sense DIG-labeled COX-Vb mRNA probe and with no probe are also shown, (essentially no hybridization is detected as expected). (C) Quantitation of *in situ* hybridization of COX-Vb mRNA in the LVs from sham-operated and coarcted rats following surgery. The 0-day value represents baseline data from animals sacrificed on the day of surgery. Hybridized spots were counted in 100μm^2 sections. Values are expressed as mea n ± SE (3 animals per value). Data were analyzed by ANOVA and significant differences between coarcted versus sham animals on each day postsurgery. ** $P< 0.01$.

(A)

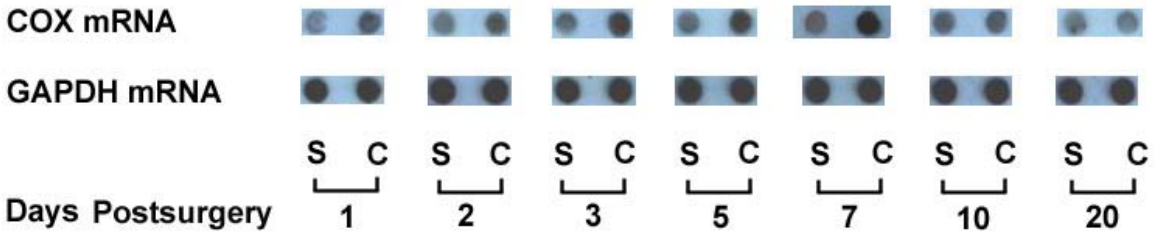

(B)

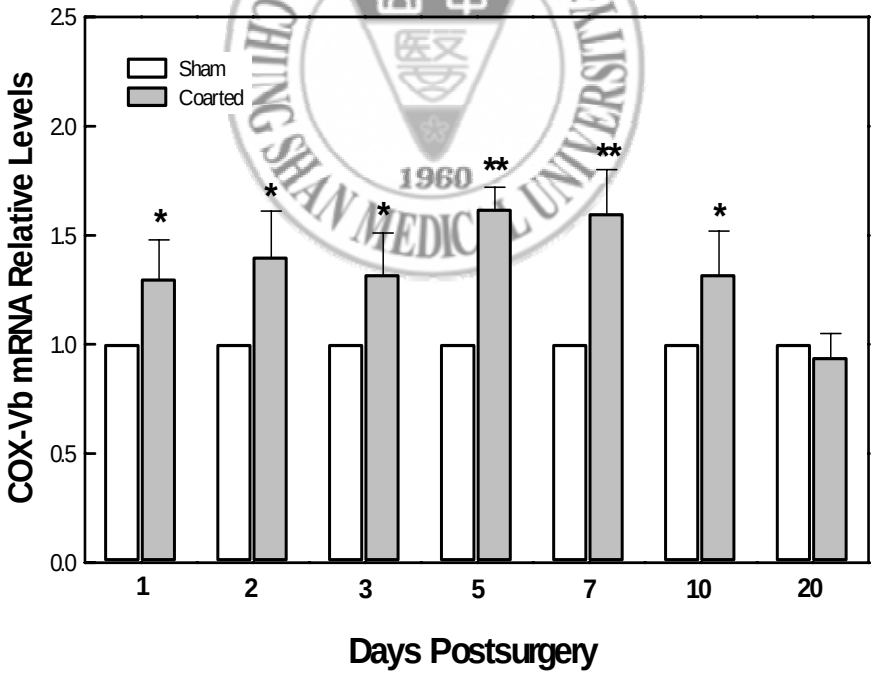

Fig.2-4. Gene expression for COX-Vb and GAPDH (loading control) mRNA in the hearts of sham-operated and coarcted rats at day 1, 2, 3, 5, 7, 10 and 20 postsurgery.

(A) COX-Vb probe labeled with DIG on UTP was hybridized to 80 ng mRNA from sham (S) and coarcted (C) animals. COX-Vb and GAPDH mRNA levels were determined from the dot blots by densitometry. No hybridization occurred with yeast tRNA which was used as a negative control (data not shown). (B) Graph showed the level of COX-Vb mRNA relative to the GAPDH mRNA level in the hearts of sham and coarcted rats at day 1 day 1, 2, 3, 5, 7, 10 and 20 postsurgery (n=3 in all cases). The level of COX-Vb mRNA in sham hearts was standardized to 1.0. *, $P<0.05$ and **, $P<0.01$ when compared to the sham rats.

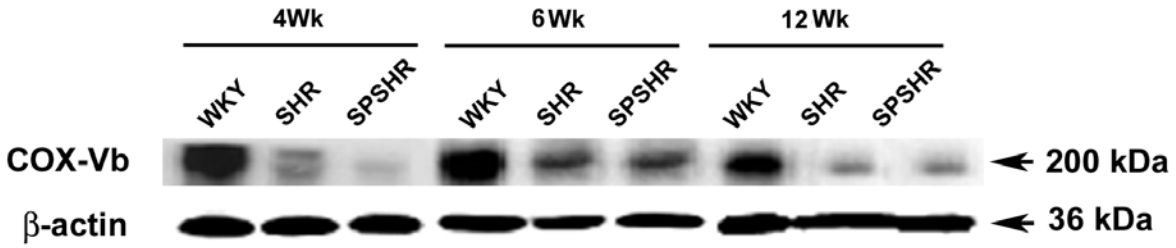

Fig 2-5. COX-Vb level in the left ventricle of hypertensive rats at different ages as determined by western blotting.

Spontaneously hypertensive rats (SHR) and stroke prone SHR (SPSHR) were sacrificed at different ages as indicated. Lysates were prepared from hearts, and equal amounts of protein were separated by SDS/PAGE and immunoblotting with anti-COX-Vb antibody. β-actin was used as a loading control. WKY, Wistar rats as a normotensive control; Wk, week.

第三章

先天性高血壓(SHR)及中風傾向(SPSHR)大白鼠肥大心肌中類胰島素生長因子Ⅰ接受體(IGF-IR)訊息路徑的缺失作用

中文摘要

報導顯示 IGF-IR 訊息途徑與血壓之調節和心臟組織存活與肥大有關係。但在高血壓大白鼠心臟組織，是否 IGF-IR 訊息途徑是否正常運作則不得而知。在本研究中, 我們以先天性高血壓(spontaneously hypertensive rats, SHR)及中風傾向(stroke-prone spontaneously hypertensive rats, SPSHR)大白鼠為實驗對象，以 Wistar-Kyoto (WKY)大白鼠為控制組，在 4、6、12 週齡之三種動物中，我們做了心臟型態及 IGF-IR 訊息途徑活性之測定。結果發現在第 12 週時，SHR 及 SPSHR 大白鼠血壓、心臟全重及左心室體重的比率均較控制組為高，但 IGF-IR 及其下游已知對心臟據有存活及維持細胞生理大小作用之蛋白濃度皆有下降趨勢，顯示 IGF-IR 訊息途徑活性有被負調控之現象。類胰島素生長因子 I (Insulin-like growth factor I,IGF-I)之 mRNA 自第 4 週起，亦較控制組為高。顯示，為因應心臟 IGF-IR 訊息途徑活性降低， IGF-IR ligan mRNA 的上升，提供了一個代償的作用。再者，另一凋亡蛋白 cytochrome-c 在 SHR 及 SPSHR 皆有升高趨式，但未達顯著水準。這些發現顯示，發生在早期(4 週齡) 心臟 IGF-IR 訊息途徑的缺損，可能導致高血壓之發生與病理性心臟肥大，而造成後來 SHR 及 SPSHR 心臟細胞凋亡之心臟衰竭。

英文摘要

Insulin-like growth factor-I (IGF-I) signaling is reported to contribute to the modulation of blood pressure and set in survival and hypertrophic responses in cardiac tissue. However, whether the IGF-I signaling normally acts in cardiac tissues of hypertensive rats is unknown. In this study, using spontaneously hypertensive rats (SHR) and stroke prone spontaneously hypertensive rats (SPSHR), both with early blood pressure increases, and Wistar-Kyoto (WKY) as controls, we measured the hypertrophic and IGF-I signaling activity changes in rat hearts at 4, 6 and 12 weeks of age. Both SHR and SPSHR were found to have significantly increased blood pressures and ratios of heart- and left ventricle- to body weight at 12 weeks of age. However, IGF-IR and its downstream signaling, including the protein levels of PI3K and phosphorylated Akt, known to maintain physiological cardiac hypertrophy and cardiomyocyte survival, were downregulated. The results of dot blotting showed that cardiac mRNA levels of IGF-I in hypertensive rats were higher than those in controls starting from the age of 4 weeks. This difference suggests the increased ligand IGF-I mRNA levels may be a compensatory response caused by the impaired IGF-I signaling. Moreover, enhanced cardiac cytosolic cytochrome-*c*, a mitochondria-dependent apoptotic pathway component, tended to occur in both hypertensive rats, although it did not reach a significant level. These findings indicate that impaired IGF-IR signaling occurs at early stages, and it may contribute, at least partially, to the development of hypertension and pathological cardiac hypertrophy and to cardiomyocyte apoptosis at later stages in SHR and SPSHR.

Keywords: insulin-like growth factor-1 signaling pathway; cardiac hypertrophy; hypertension; SHR&SPSHR

前 言

高血壓一般可引發心臟病，包括左心室肥大及心臟衰竭。就前者而言，25-50%中度高血壓病患及 90%重度高血壓病患皆有心室肥大之現象[60]。以動物模式來研究高血壓的方式最早始於 1960 年初期，然而在這些模式中，由Okamoto和Aoki [61]所發展出的spontaneously hypertensive rat (SHR)大白鼠品種被應用的最為廣泛；因其可以自然地產生高血壓的病態。另一方面，由SHR衍生而來的stroke-prone SHR (SPSHR)，是由SHR長期餵以 1% 鹽水而培育出來， 其展現出更強烈傾向之高血壓甚至中風，及心血管方面之傷害。據文獻指出[61]，這兩種完全由基因控制而形成先天性高血壓或中風的大白鼠存活之時間，前者僅有一年半，而後者為八個月。與正常大白鼠壽命 2.5 年減少許多。所以，其或由先天基因的變化或訊息傳遞途徑的改變，所造成的後天病理機轉，為人們關切的課題。而這些病理之症狀，最主要的則是因高血壓引起的心肌肥大，而導致猝死。但是，是否為訊息途徑活性的改變，而導致不可回復之心肌細胞及組織傷害，造成心臟病理肥大，不得而知。

IGF-I之上升一向與細胞之增加與心臟生理性肥大有關。在我們先前心臟細胞初代培養之實驗發現，IGF-I之處理可導致心臟肥大[62-64]，另一體內實驗顯示，腹動脈結紮大白鼠心臟中IGF-I之上升發生

於心臟肥大之前[11]。

目前為止，經過IGF-I刺激後之肥大心臟，已有數條訊息途徑被證實。透過IGF-I、IGF-IR活化PI3K-AKT/PKB為心肌細胞存活之主要途徑，並可調控心肌大小變化，可能為生理性肥大的主要機轉 [65-67]。同時，IGF-I可經IRS-1 活化訊息途徑下游另一分支Ras-Raf-MEK-ERK，活化促進心臟肥大之基因，調控非心肌細胞增生[68,69]。故，IGF-IR訊息途徑在先天性高血壓大白鼠心臟組織，可能執行著存活及肥大之效果。另一方面，先前實驗發現，以IGF-I 突變，造成小白鼠IGF-I 活性只有野生種(wild type)之 30%之的動物模式中，觀察到血壓上升[70]，及Vecchione和其同事[71]進一步證實 IGF-I使血管放鬆的特性，在 5，12，14 週齡SHR大白鼠有缺失之現象。故推測IGF-I訊息途徑之退化，可能與遺傳性高血壓之發展有關。 然而，由於心肌細胞不再分裂，所以IGF-I的存活作用，可能對於心肌細胞而言是比較迫切的。所以是否IGF-I訊息途徑之缺失亦會影響到心臟組織，是很有必要為人所了解。此外, 先天性高血壓大白鼠在年齡很輕的時候，即已出現高血壓，是否這意味IGF-I在心臟組織的特殊作用，對高血壓的發生，伴演著促進或補償之角色，亦不清楚。為了了解SHR及SPSHR在發展高血壓的階段是否心室肥大的改變，與心臟由生理性肥大轉變成病理性肥大的過程有關，在本實驗中,以WKY大白鼠為控制組，在年齡 4、6、

12 週時，測量了SHR及SPSHR心臟之肥大與IGF-IR訊息途徑活性。

材料與方法

實驗動物

WKY 及 SHR 購自動物繁殖及研究中心(台北，台灣)。SPSHR 則是來自美國 NIH 品系，由 Dr.Dennis E.Buetow 贈予。三種品系 3，5，11 週齡之大白鼠被飼養於動物中心，室內有溫度控制(24℃±1℃)，光照 12 小時(5AM-5PM)，商業配方飼料與飲水任意攝取。所有動物之照顧及控制皆依據台灣實驗動物照顧及使用須知來執行。

大白鼠尾壓之測量

測量大白鼠尾壓之血壓測定器(29SSP, IITC INC./Life Seience Instruments, U.S.A)，儀器是由主機和打氣機分開的兩部機器組合而成。將鼠隻平放在桌上，並將鼠隻尾巴放入感應器中，鼠隻尾巴基部須在感應範圍內。筆針會開始顯現出幅度較大的擺動，這便是鼠隻的最高血壓值。但是若是鼠隻在測量中途亂動，則當次的測量不適合納入紀錄中。在鼠隻亂動後須按下放氣閥，並重新再打氣測量。每隻鼠隻測量 5 次，再求 5 次平均值分析之。

心臟分離與心臟肥大的評估

一旦大白鼠尾壓測量完成後，進行斷頭犧牲。 打開胸腔，取出心臟。在除去脂肪和連接組織之後，去除血液並稱重。計算出總心重量和體重的比率。稱重完之心臟，取下整個左心室，稱重完，分成 2 個部分並冷凍於-70℃冰箱待進一步分析。

蛋白質萃取和西方的墨點分析

第一個部分的左心室以剪刀剪碎，同第二章之實驗方法。但使用 IGF-IR，PI3K，Akt，磷酸化態 Akt 和 cytochrome-*c* 1 級抗體(Santa Cruz Biotechnology)，來偵測樣品中相對蛋白之量。

心臟 RNA 的萃取

第二個部分的左心室用來萃取 RNA。使用 Ultraspec RNA 萃取液(Biotecx Laboratories, lnc.)根據製造商提供的步驟，同第二章之實驗方法。

IGF-I mRNA 探針之製備

來自大白鼠IGF-I 基因exon 3 (帶有 956 對鹼基之模版)之質體 pGEM-1，經過直線化 (linearized) [64]，及根據一組以digoxigenin (DIG) 標定UTP 之kit 轉譯成“anti-sense”IGF-I、mRNA探針[55]。以 2%

agarose gel確認此探針長度無誤。以同樣步驟製備“sense” IGF-I mRNA。

Dot blotting

心臟組織內之 IGF-I mRNA 量是以 Dot blotting 來分析。其步驟同第二章之實驗方法。

統計分析

在尾壓、左心室重/體重、全心重/體重，皆是以單變項變異數分析(ANOVA)來分析統計差異。以 Fisher’s Least Significant Difference test 來決定各處理間之差異性。本研究各項試驗所設定之統計顯著水準以 $P<0.05$ 為標準。所有數據以平均值(mean)± 標準誤差(SE)表示。

結 果

SHR 及 SPSHR 大白鼠之血壓上升和心臟肥大

Fig 3-1 顯示先天性高血壓大白鼠 (SHR & SPSHR)在整個 12 星期實驗期間，血壓明顯上升，與控制組大白鼠比較起來，SHR & SPSHR 收縮壓分別自 6 及 12 週顯著高於 Wistar 大白鼠。心臟肥大的結果說明在 Table 3-1。在第 12 週時，SHR & SPSHR 大白鼠，心臟全重及左心室重量對體重的比率顯著高於 Wistar 大白鼠。

以西方的墨點法測定之左心室 IGF-IR 及 IGF-IR 訊息途徑和 cytochrome *c* 蛋白變化量

4，6，12 週齡之大白鼠左心室 IGF-IR 蛋白變化量結果列於 Fig 3-2。SHR 大白鼠左心室 IGF-IR 蛋白自第 6 週顯著下降。SPSHR 大白鼠則下降更多。類似的結果，在同屬 IGF-IR 訊息途徑上之 PI3K 及磷酸化態 Akt 同樣被觀察到，在每個年齡組 SHR & SPSHR 之 PI3K 皆顯著低於 Wistar 大白鼠(Fig 3-3A)。但磷酸化態 Akt 顯著低於控制組，則僅見於 6 及 12 週齡 SPSHR 大白鼠(Fig 3-3B)。自粒腺體釋放出之 cyotchrome-*c* 可引發 mitochondria-dependent 細胞凋亡。偵測之結果列於 Fig 3-3C 雖然在週齡較大之 SHR & SPSHR 大白鼠與控制組差異增加，但都未達顯著水準。

以 Dot blotting 偵測大白鼠左心室 IGF-I mRNA 之變化量

大白鼠左心室 IGF-I mRNA 測定之結果列於 Fig 3-4。無論在 4，6，12 週齡之大白鼠，SHR 皆顯著高於控制組。而 SPSHR 雖然同樣上升，但都未達顯著水準。

討　論

根據文獻所知，病理性心肌肥大為心肌猝死主因，但導致病理性心肌肥大及心肌猝死的分子機轉，則還不太清楚。本研究之主要目的是以先天性高血壓或中風傾向之 SHR(Spontaneously hypertension rat) 及 SPSHR (Stroke prone SHR)大白鼠為實驗對象，以 Wistar-Kyoto (WKY) 大白鼠為控制組，在年齡 4，6 及 12 週動物，進行血壓及體重測量，並犧牲取出心臟稱重。檢測可能引起生理性肥大的 IGF-I 之訊息傳遞，主要包括 PI3K-AKT/PKB 調控心肌大小變化，且為心肌細胞存活之主要途徑。SHR 及 SPSHR 以 Wistar-Kyoto (WKY)正常鼠為控制組之動物模式中，於第 12 週時相較於控制組 WKY 大白鼠，無論在血壓、心臟全重，或左心室重量對體重的比率，SHR 及 SPSHR 組大白鼠皆顯著上升；但是在訊息傳遞之路徑探討中，Western blot 結果顯示，IGF-IR 及其下游 PI3K 蛋白質卻顯著減少，而 SHR 大白鼠心臟自第 4 週齡起 IGF-I mRNA 之量明顯上升。吾人推測，早期 IGF-I 蛋白量的減少，可能來自於較高之降解率，較短之半衰期，或轉錄後修飾 (post-translational modification)之缺陷，並且，上升的 ligand IGF-I mRNA，可能是彌補此一缺陷的代償作用。

文獻上曾指出，心臟細胞的凋亡和心臟疾病的發生有著密切的關係[72,73]。所以心臟細胞凋亡的調控，對心臟疾病之控制顯得重要。

在缺乏生長因子的狀況下，心臟細胞的BCl_2活性降低，而DNA斷裂及caspase3 之表達上升，而IGF-I之補充，則可使細胞回復到原來狀態，顯示IGF-I是透過對 caspase 3 之抑制及BCl_2之活化來達到抗凋亡的效果[74]。亦有文獻指出，IGFIR在PC2 細胞之處理，可使BCl_2 promotor之活性上升 2-3 倍[75]。臨床上證據顯示，IGF-I被用來處理急性心臟衰竭[76]。再者， IGF-I訊息途徑下游之PI3K對心肌細胞亦具體保護作用[67,77]。活化態之PI_3K已被發現可藉著磷酸化前凋亡蛋白Bad，及抑制caspase 9 活性，來達到改善心肌梗塞發作之效果[78,79]。另一研究亦顯示，在老鼠心臟表達dominant negative PI_3K，表現心臟較小之結果。 顯示PI_3K有維持心臟細胞生理大小之作用[67]。

在我們的實驗中，先天性高血壓大白鼠 IGF-I 訊息途徑活性之負調控作用，可導致心臟細胞凋亡之發生，但也可能是因為大白鼠仍在非常年輕之階段，使我們並未觀察到顯著性 cytochrome-c 之上升。可能在逐漸年長後，則顯示較嚴重之缺失，心臟細胞的凋亡較明顯。而由心臟細胞的凋亡所引發之心臟衰竭，導致這兩種大白鼠壽命減短。在本實驗中,SHR 大白鼠 IGF-I 訊息途徑活性之負調控是來自 IGF-I、PI3K 及磷酸化 Akt 蛋白之降低。這些現象在 SPSHR 大白鼠更加明顯，這與 SPSHR 大白鼠血壓上升更高，腦血管病變更嚴重之現象相符合。

所以在我們的實驗模式中，由於IGFIR 功能的缺失，導致SHR及SPSHR 心臟細胞凋亡的發生。然而，在IGF-IR可維持心臟細胞正常大小的功能降低之情況下，仍舊造成心臟肥大之現象，則必定有其他引起心臟肥大之訊息傳遞途徑參與其中。例如，1998 年，Olson首度證實病理性心肌細胞在肥大的過程中，可能經由Ca^{2+}活化calcineurin，使NFAT3 去磷酸化而進入核內，藉與GATA4 作用，而刺激了胚胎基因，如β-MHC的表現，同時提出Ca^{2+}-calcineurin所調控之$NF\text{-}AT_3$為病理性心肌肥大，甚至猝死的主因[80-82]。而鈣離子及calcineurin的活化除導致心肌病理性肥大外，更造成cytochrome-c流失、破壞，而引發心肌細胞凋亡及心肌衰竭[83]。然而在我們的測定中，SHR 及SPSHR 大白鼠心臟中NFAT及 Calcinrurin 蛋白量未有顯著上升，顯示在先天性高血壓動物模式中，引起心肌肥大之機轉，Calcineurin-NFAT之訊息傳遞途徑未參與其中。這與 Olson 後來的實驗證實[84,85]：以 Calcineurin抑制劑給予SHR大白鼠，對其心臟肥大的現象未見改善。再者，在本實驗中, 心臟中訊息途徑活性之探討亦包括IGF-I下游的另一分支ERK [86-88]。文獻指出，在先天性高血壓大白鼠心臟中ERK活性，自 5 週齡起即有下降之現象。但我們的結果顯示，在 12 週齡起即產生心臟肥大，顯示ERK可能並未參與在高血壓大白鼠心臟肥大的機轉中。所以，確實是何種因素造

成 SHR 及SPSHR大白鼠心臟肥大的機轉，有待進一步確認。

本篇文章，目的是在研究先天性高血壓導致心臟疾病之機轉，在實驗結果中證實SHR 及SPSHR 血壓的上升始於第 6 及 12 週，然而IGF-IR功能的缺失，則第４週即已出現。另一研究顯示IGF-I缺失之大白鼠血壓上升[70]，而IGF-I功能缺失發生於高血壓及心臟肥大之前。我們推測，對於高血壓所引起心臟疾病之發生，IGF-IR功能的缺失可能是一個起始者。所以，提升IGF-I之抗凋亡作用可緩和高血壓性心臟疾病的發生。期望未來之研究結果,在人類高血壓性心臟病預防藥物開發上，提供最有力之理論根據。

Table. 3-1.大白鼠心臟全重及左心室重量對體重的比率

Age (wk)	WKY	SHR	SPSHR
	(Whole heart/BW)(mg/g)		
4	4.17±0.134	4.11±0.19	4.15±0.09
6	3.34±0.07	3.51±0.13	3.53±0.07
12	2.83±0.07	3.45±0.06*	3.44±0.04*
	(LT ventricle/BW)(mg/g)		
4	3.18±0.12	3.38±0.17	3.63±0.08
6	2.67±0.04	2.81±0.11	2.85±0.07
12	2.25±0.06	2.86±0.06*	2.86±0.04*

BW indicates body weight; LT, left; WKY, Wistar-Kyoto rats as a control; SHR, spontaneously hypertensive rats; SPSHR, stroke prone spontaneously hypertensive rats. All values are expressed as mean ± S.E (n=8).

* Significant differences from the control (WKY) were determined by the Fisher PLSD test, $P < 0.05$.

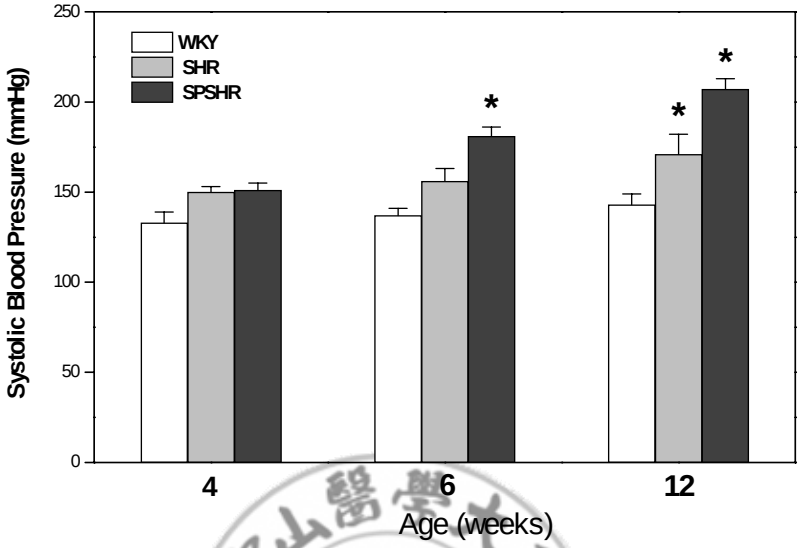

Fig. 3-1. Systolic blood pressure of WKY (white), SHR (light gray) and SPSHR (dark gray) at 4, 6 and 12 weeks of age.

Values are expressed as mean ± S.E. (n=8). Significant differences from the control (WKY) were determined using the Fisher PLSD test: * $P < 0.05$.

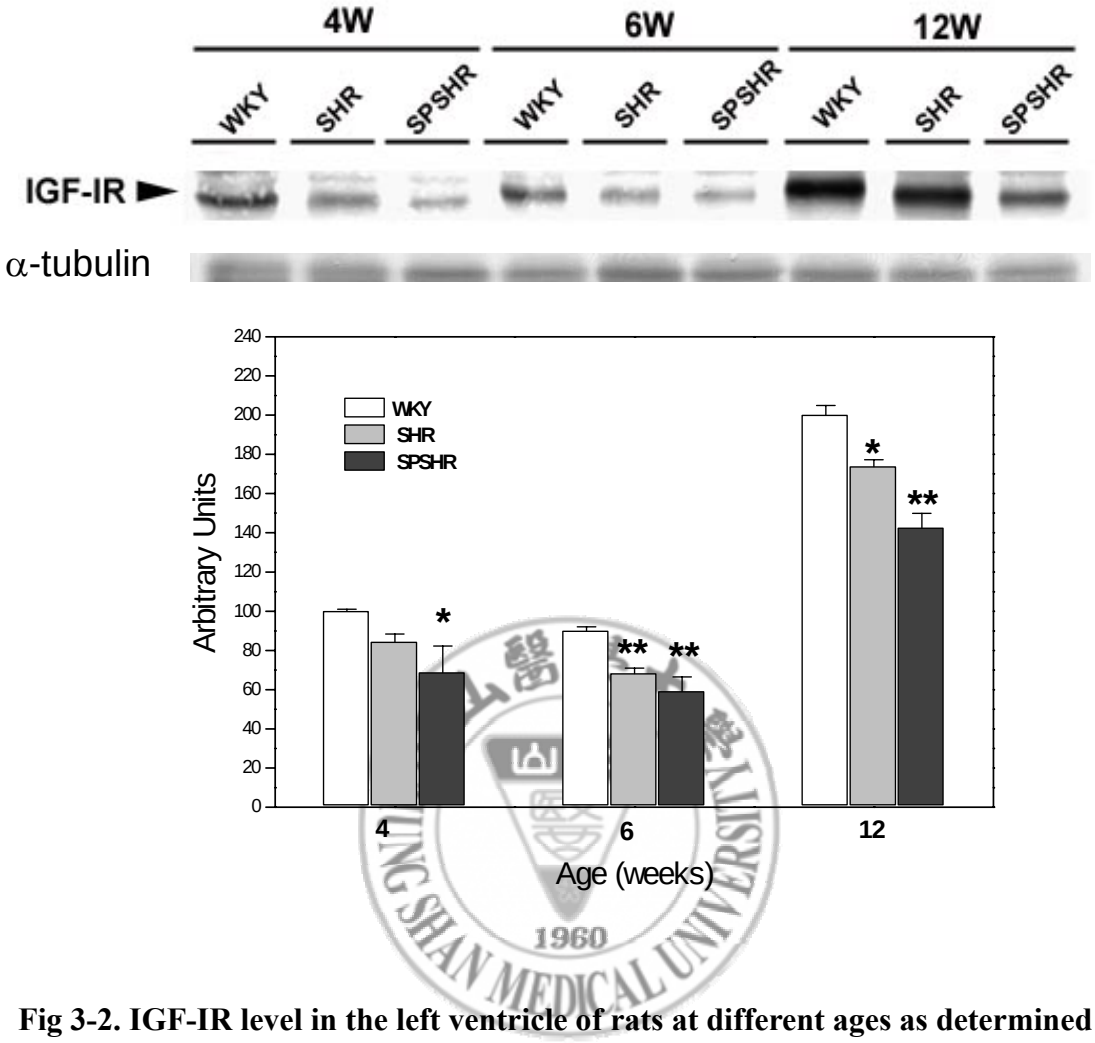

Fig 3-2. IGF-IR level in the left ventricle of rats at different ages as determined by western blotting.

Lysates were prepared from WKY (white), SHR (light gray) and SPSHR (dark gray) hearts, and equal amounts of protein were separated by SDS/PAGE and immunoblotting with anti-IGF-IR antibody. The blotting bands are shown on the top of the graph. Signal intensity was quantitated using a phosphoImager. The average percentage ± S.E. for three independent experiments is related to the control (WKY) animals in each age group. Significant differences were determined using the Fisher PLSD test from the control (WKY): $*P < 0.05$; $**P < 0.01$.

(A)

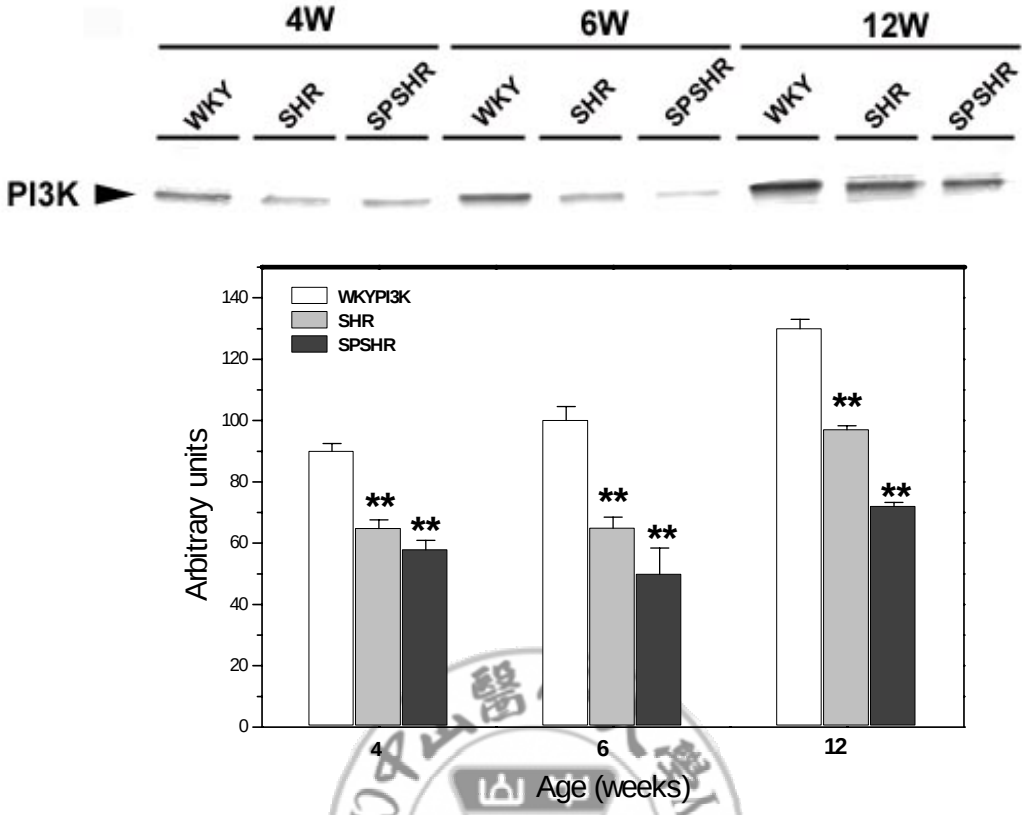
4W
6W
12W
WKY
SHR
SPSHR
PI3K
WKYPI3K
SHR
SPSHR
Arbitrary units
Age (weeks)
**

(B)

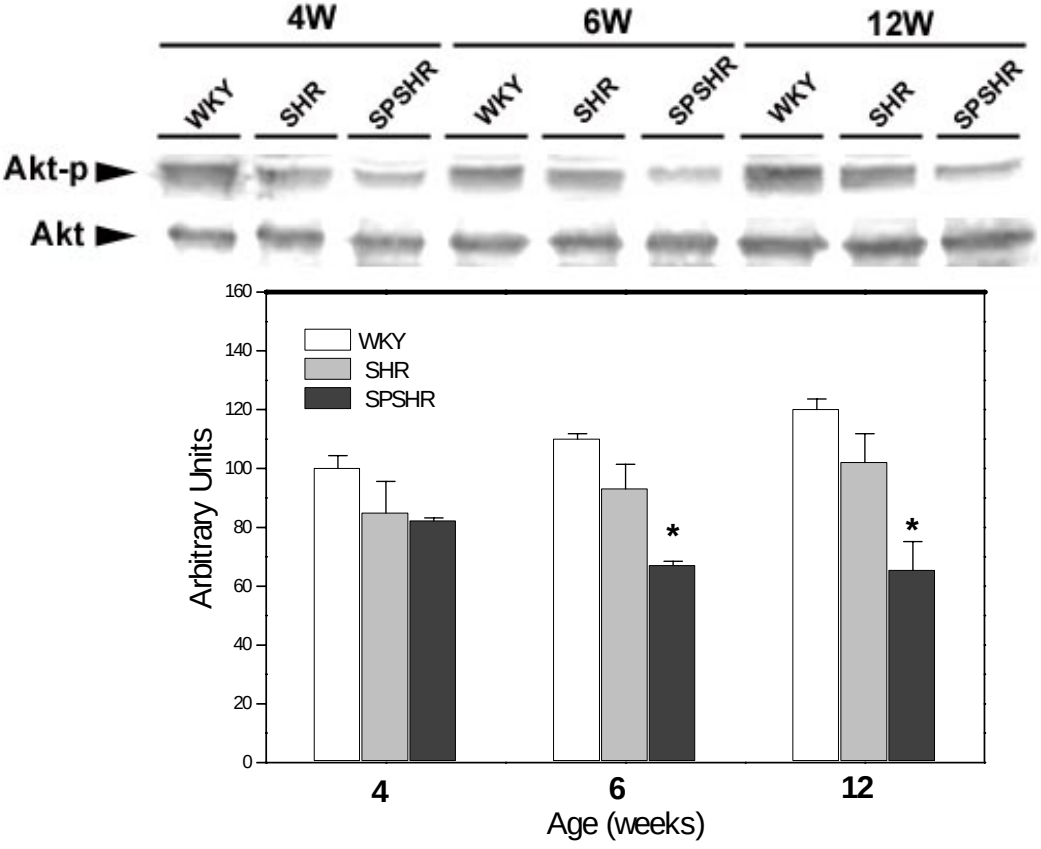
4W
6W
12W
WKY
SHR
SPSHR
Akt-p
Akt
WKY
SHR
SPSHR
Arbitrary Units
Age (weeks)
*

(C)

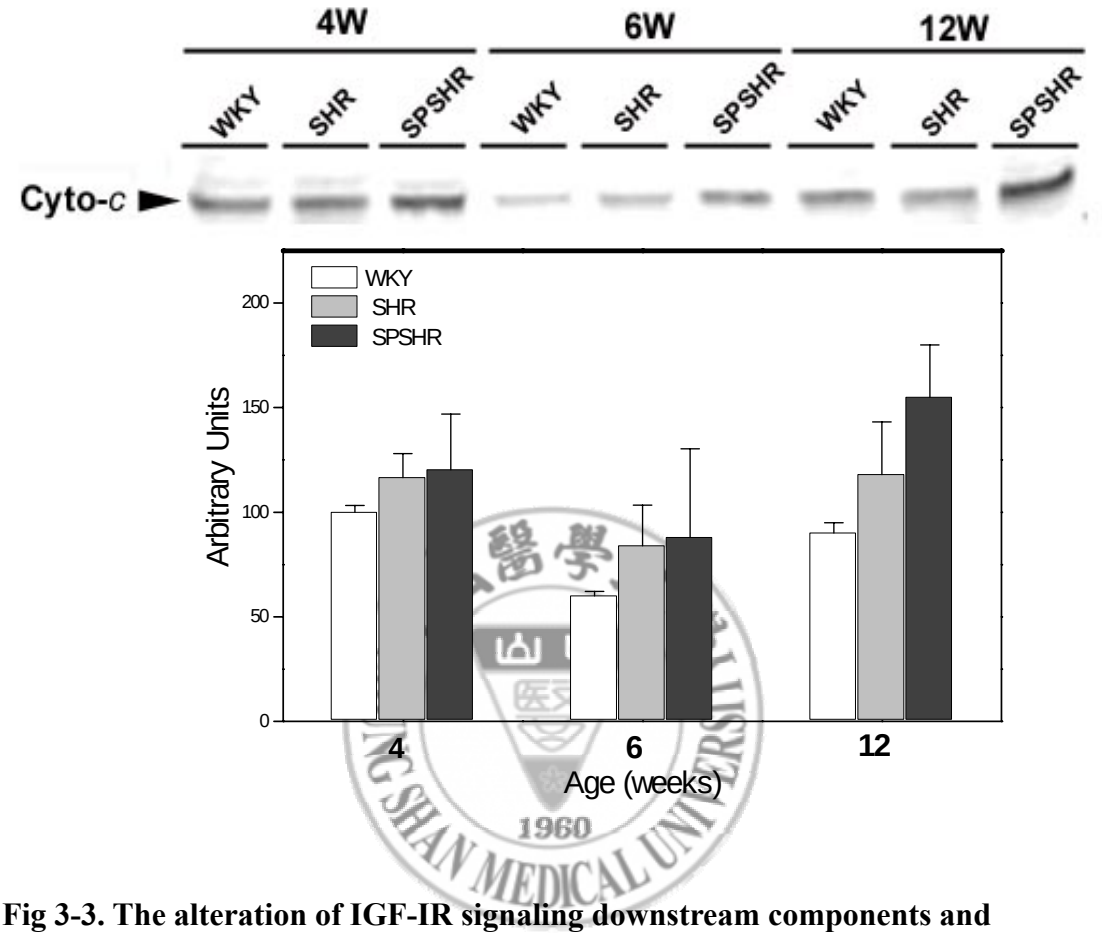

Fig 3-3. The alteration of IGF-IR signaling downstream components and cytochrome-*c* levels in the left ventricle of rats at different ages.

Lysates were prepared from WKY (white), SHR (light gray) and SPSHR (dark gray) hearts, and equal amounts of protein were separated by SDS/PAGE and immunoblotting with (A) anti-PI3K antibody, (B) anti phosphorylated Akt and Akt antibody, (C) anti-cytochrome-*c* antibody. The blotting bands are shown on the top of each graph. Signal intensity was quantitated using a phosphoImager. The average percentage ±S.E. for three independent experiments is related to the control (WKY) animals in each group. Significant differences were determined using the Fisher PLSD test from the control (WKY): $*P < 0.05$; $**P < 0.01$.

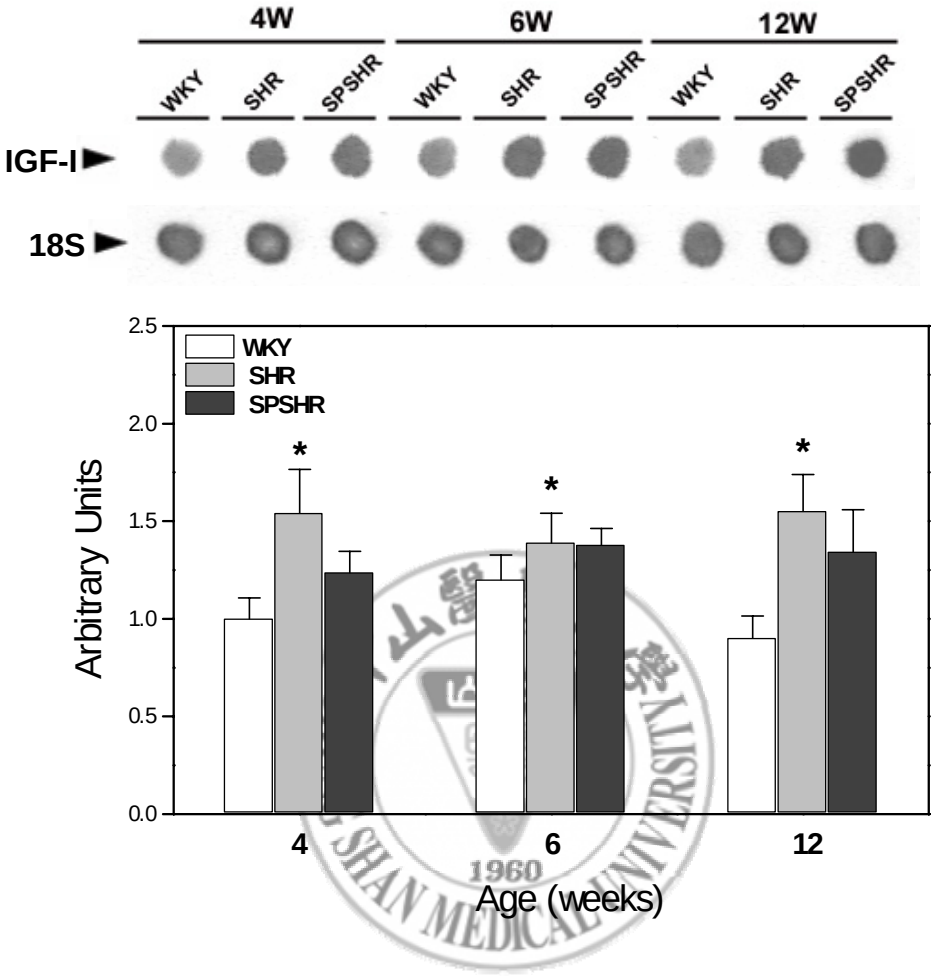

Fig 3-4. mRNA in the left ventricle of rats as determined by dot-blotting. Detection was performed with CDP-Star and the film was exposed for 10-30 sec to determine the linear range of detection for these mRNAs. Total RNA was spotted at 240 ng per dot. 18*S*-rRNA was measured as a loading control (top of graph). Quantitation of activation fold for the SHR (light gray) and SPSHR (dark gray) versus WKY (white) group is shown in the graph. Values are expressed as mean ± S.E. (n=8). Significant differences from the control (WKY) were determined using the Fisher PLSD test: **P* < 0.05.

第四章　結論

血壓之上升，可導致心臟肥大，在本篇論文中，以腹動脈完全結紮之動物模式，誘發血壓快速上升，心臟肥大，除了在先前實驗，已證實左心室 IGF-I mRNA 的量在第 3 天達最高值，而後下降。與心臟能量提供息息相關的粒腺體基因 COX，則被證實 mRNA 隨著心臟的肥大而上升，且在第 5-7 天達最高值。而後第 10 天開始下降。有趣的是，IGT-I 及 COX mRNA 之上升都發生在心臟肥大之前，而二者表達之模式皆十分類似，先上升、後降低，二者之間是否存在著一定的關連性：基因是否互相調控，值得進一步探討。此外，在此模式中，心臟肥大末期，COX 基因的負調控與心臟衰竭之因果關係，亦有待實驗進一步之釐清，如以 COX 基因直接注射心臟，觀察心臟衰竭有否改善。

而有別於侵入性手術造成血壓上升之模式，在先天性高血壓大白鼠方面，在 4 週齡起，即顯現 COX 蛋白較控制組明顯較低的情形，由 4 週齡 SHR 與 SPSHR 大白鼠血壓尚未顯著上升情形，推測先天性高血壓大白鼠心臟中 COX 蛋白之量，並不完全受到血壓之影響，在相關文獻中，觀察到心臟中抗氧化酵素，如 SOD 活性之降低，推測導致 COX 此粒腺體基因對氧化性傷害的可能性增加的情形，而影響了 COX 蛋白的穩定性。

另一方向，在心臟肥大情形下，在IGF-I訊息路徑活性由其下游PI_3K和Akt蛋白量減少看來，和COX同樣顯示出下降的現象，而IGF-I訊息路徑與心臟細胞之存活有著密切之關係，故我們推測，先天性高血壓大白鼠心臟組織中，IGF-I訊息路徑活性之降低與此模式動物心臟衰竭的發生，具有關連性，並造成動物平均壽命減少的現象，此一推測，與cytochrome-c蛋白量提高，可能造成心臟細胞凋亡之結果是一致的。

參考文獻

[1] Guyton AC. Textbook of medical physiology 7th 1986; p159.

[2] Timiras PS. Physiological basic of aging and geriatrics. 2nd chapter16, 1994; pp.199-206, CRC press.

[3] Cooper Gt. Basic determinants of myocardial hypertrophy: a review of molecular mechanisms. *Annu Rev Med* 1997; **48**: 13-23.

[4] Morgan HE, Baker KM. Cardiac hypertrophy. Mechanical, neural, and endocrine dependence. *Circulation* 1991; **83**:13-25.

[5] Berne RM, Levy MN. Physiology, 3rd ed., 1993; pp. 300, 428, 494.

[6] Okamoto K, Yamori Y, Nagaoka A. Establishment of the stroke-prone spontaneously hypertensive rat (SHR). *Circ Res* 1974: I-143-I-153.

[7] Okamoto K, Aoki K. Development of a strain of spontaneously hypertensive rats. *Jpn Circ J* 1963; **27**: 282-293.

[8] Engelmann GL, Vitullo JC, Gerrity RG. Morphometric analysis of cardiac hypertrophy during development, maturation, and senescence in spontaneously hypertensive rats. *Circ Res* 1987; **60**: 487-494.

[9] Lompre AM, Mercadier JJ, Schwartz K. Changes in gene expression during cardiac growth. *Int Rev Cytol* 1991; **124**: 137-186.

[10] White CR, Zehr JE. Spontaneous rhythmic contractile behaviour of aortic ring segments isolated from pressure loaded regions of the vasculature. *Cardiovasc Res* 1990; **24**: 953-958.

[11] Huang CY, Buchanan DL, Gordon RL, Jr., Sherman MJ, Razzaq J, White K, Buetow DE. Increased insulin-like growth factor-I gene expression precedes left ventricular cardiomyocyte hypertrophy in a rapidly-hypertrophying rat

model system. *Cell Biochem Funct* 2003; **21**: 355-361.

[12] Seidman JG, Seidman C. The genetic basis for cardiomyopathy: from mutation identification to mechanistic paradigms. *Cell* 2001; **104**: 557-567.

[13] Luft R, Ikkos D, Palmieri G, Ernster L, Afzelius B. A case of severe hypermetabolism of nonthyroid origin with a defect in the maintenance of mitochondrial respiratory control: a correlated clinical, biochemical, and morphological study. *J Clin Invest* 1962; **41**: 1776-1804.

[14] Shy GM, Gonatas NK, Perez M. Two childhood myopathies with abnormal mitochondria. I. Megaconial myopathy. II. Pleoconial myopathy. *Brain* 1966; **89**:133-158.

[15] Shoffner JM, Wallace DC. Oxidative phosphorylation diseases and mitochondrial DNA mutations: diagnosis and treatment. *Annu Rev Nutr* 1994; **14**: 535-568.

[16] Ruppert V, Nolte D, Aschenbrenner T, Pankuweit S, Funck R, Maisch B. Novel point mutations in the mitochondrial DNA detected in patients with dilated cardiomyopathy by screening the whole mitochondrial genome. *Biochem Biophys Res Commun* 2004; **318**: 535-543.

[17] Moslemi AR, Selimovic N, Bergh CH, Oldfors A. Fatal dilated cardiomyopathy associated with a mitochondrial DNA deletion. *Cardiology* 2000; **94**: 68-71.

[18] Minieri M, Zingarelli M, Shubeita H, Vecchini A, Binaglia L, Carotenuto F, Fantini C, Fiaccavento R, Masuelli L, Coletti A, Simonelli L, Modesti A, Di Nardo P. Identification of a new missense mutation in the mtDNA of hereditary hypertrophic, but not dilated cardiomyopathic hamsters. *Mol Cell Biochem* 2003; **252**: 73-81.

[19] Hatefi Y. The mitochondrial electron transport and oxidative phosphorylation

system. *Annu Rev Biochem* 1985; **54**: 1015-1069.

[20] Kadenbach B, Jarausch J, Hartmann R, Merle P. Separation of mammalian cytochrome c oxidase into 13 polypeptides by a sodium dodecyl sulfate-gel electrophoretic procedure. *Anal Biochem* 1983; **129**: 517-521.

[21] Tzagoloff A, Myers AM. Genetics of mitochondrial biogenesis. *Annu Rev Biochem* 1986; **55**: 249-285.

[22] Giles RE, Blanc H, Cann HM, Wallace DC. Maternal inheritance of human mitochondrial DNA. *Proc Natl Acad Sci U S A* 1980; **77**: 6715-6719.

[23] Cooper GM. The cell 2nd 2000; p560.

[24] Sara VR, Hall K. Insulin-like growth factors and their binding proteins. *Physiol Rev* 1990; **70**: 591-614.

[25] Cohick WS, Clemmons DR. The insulin-like growth factors. *Annu Rev Physiol* 1993; **55**: 131-153.

[26] Engelmann GL, Boehm KD, Haskell JF, Khairallah PA, Ilan J. Insulin-like growth factors and neonatal cardiomyocyte development: ventricular gene expression and membrane receptor variations in normotensive and hypertensive rats. *Mol Cell Endocrinol* 1989; **63**: 1-14.

[27] Adamo M, Lowe WL, Jr., LeRoith D, Roberts CT, Jr. Insulin-like growth factor I messenger ribonucleic acids with alternative 5'-untranslated regions are differentially expressed during development of the rat. *Endocrinology* 1989; **124**: 2737-2744.

[28] Turner JD, Rotwein P, Novakofski J, Bechtel PJ. Induction of mRNA for IGF-I and -II during growth hormone-stimulated muscle hypertrophy. *Am J Physiol* 1988; **255**: E513-E517.

[29] Thomas MR, Miell JP, Taylor AM, Ross RJ, Arnao JR, Jewitt DE, McGregor AM. Endocrine and cardiac paracrine actions of insulin-like growth factor-I

(IGF-I) during thyroid dysfunction in the rat: is IGF-I implicated in the mechanism of heart weight/body weight change during abnormal thyroid function? *J Mol Endocrinol* 1993; **10**: 313-323.

[30] Russell-Jones DL, Leach RM, Ward JP, Thomas CR. Insulin-like growth factor-I gene expression is increased in the right ventricular hypertrophy induced by chronic hypoxia in the rat. *J Mol Endocrinol* 1993; **10**: 99-102.

[31] Hanson MC, Fath KA, Alexander RW, Delafontaine P. Induction of cardiac insulin-like growth factor I gene expression in pressure overload hypertrophy. *Am J Med Sci* 1993; **306**: 69-74.

[32] Calderone A, Takahashi N, Izzo NJ, Jr., Thaik CM, Colucci WS. Pressure- and volume-induced left ventricular hypertrophies are associated with distinct myocyte phenotypes and differential induction of peptide growth factor mRNAs. *Circulation* 1995; **92**: 2385-2390.

[33] Isgaard J, Wahlander H, Adams MA, Friberg P. Increased expression of growth hormone receptor mRNA and insulin-like growth factor-I mRNA in volume-overloaded hearts. *Hypertension* 1994; **23**: 884-888.

[34] Ito H, Hirata Y, Hiroe M, Tsujino M, Adachi S, Takamoto T, Nitta M, Taniguchi K, Marumo F. Endothelin-1 induces hypertrophy with enhanced expression of muscle-specific genes in cultured neonatal rat cardiomyocytes. *Circ Res* 1991; **69**: 209-215.

[35] Fuller SJ, Mynett JR, Sugden PH. Stimulation of cardiac protein synthesis by insulin-like growth factors. *Biochem J* 1992; **282**: 85-90.

[36] LeRoith D, Werner H, Beitner-Johnson D, Roberts CT, Jr. Molecular and cellular aspects of the insulin-like growth factor I receptor. *Endocr Rev* 1995; **16**: 143-163.

[37] Kato H, Faria TN, Stannard B, Roberts CT, Jr., LeRoith D. Role of tyrosine

kinase activity in signal transduction by the insulin-like growth factor-I (IGF-I) receptor. Characterization of kinase-deficient IGF-I receptors and the action of an IGF-I-mimetic antibody (alpha IR-3). *J Biol Chem* 1993; **268**: 2655-2661.

[38] Kato H, Faria TN, Stannard B, Roberts CT, Jr., LeRoith D. Essential role of tyrosine residues 1131, 1135, and 1136 of the insulin-like growth factor-I (IGF-I) receptor in IGF-I action. *Mol Endocrinol* 1994; **8**:40-50.

[39] Myers MG, Jr., Backer JM, Sun XJ, Shoelson S, Hu P, Schlessinger J, Yoakim M, Schaffhausen B, White MF. IRS-1 activates phosphatidylinositol 3'-kinase by associating with src homology 2 domains of p85. *Proc Natl Acad Sci U S A* 1992; **89**: 10350-10354.

[40] Myers MG, Jr., Sun XJ, Cheatham B, Jachna BR, Glasheen EM, Backer JM, White MF. IRS-1 is a common element in insulin and insulin-like growth factor-I signaling to the phosphatidylinositol 3'-kinase. *Endocrinology* 1993; **132**: 1421-1430.

[41] Boguski MS, McCormick F. Proteins regulating Ras and its relatives. *Nature* 1993; **366**: 643-654.

[42] Nishio ML, Ornatsky OI, Craig EE, Hood DA. Mitochondrial biogenesis during pressure overload induced cardiac hypertrophy in adult rats. *Can J Physiol Pharmacol* 1995; **73** :630-637.

[43] Stanley WC, Hoppel CL. Mitochondrial dysfunction in heart failure: potential for therapeutic interventions? *Cardiovasc Res* 2000; **45**: 805-806.

[44] Jarreta D, Orus J, Barrientos A, Miro O, Roig E, Heras M, Moraes CT, Cardellach F, Casademont J. Mitochondrial function in heart muscle from patients with idiopathic dilated cardiomyopathy. *Cardiovasc Res* 2000; **45**: 860-865.

[45] Tanji K, Bonilla E. Neuropathologic aspects of cytochrome C oxidase

deficiency. *Brain Pathol* 2000; **10**: 422-430.

[46] Richter OM, Ludwig B. Cytochrome c oxidase--structure, function, and physiology of a redox-driven molecular machine. *Rev Physiol Biochem Pharmacol* 2003; **147**: 47-74.

[47] Kunz WS, Kudin A, Vielhaber S, Elger CE, Attardi G, Villani G. Flux control of cytochrome c oxidase in human skeletal muscle. *J Biol Chem* 2000; **275**: 27741-27745.

[48] Leary SC, Michaud D, Lyons CN, Hale TM, Bushfield TL, Adams MA, Moyes CD. Bioenergetic remodeling of heart during treatment of spontaneously hypertensive rats with enalapril. *Am J Physiol Heart Circ Physiol* 2002; **283**: H540-H548.

[49] Wiesner RJ, Aschenbrenner V, Ruegg JC, Zak R. Coordination of nuclear and mitochondrial gene expression during the development of cardiac hypertrophy in rats. *Am J Physiol* 1994; **267**: C229-C235.

[50] Bjorntorp P. Effects of physical training on blood pressure in hypertension. *Eur Heart J* 1987; **8** Suppl B:71-76.

[51] Bradford MM. A rapid and sensitive method for the quantitation of microgram quantities of protein utilizing the principle of protein-dye binding. *Anal Biochem* 1976; **72**: 248-254.

[52] Smith L. Spectrophotometric assay of cytochrome c oxidase. *Methods Biochem Anal* 1955; **2**: 427-434.

[53] Storrie B, Madden EA. Isolation of subcellular organelles. *Methods Enzymol* 1990; **182**: 203-225.

[54] Darley-Usmar VM, Kennaway NG, Buist NR, Capaldi RA. Deficiency in ubiquinone cytochrome c reductase in a patient with mitochondrial myopathy and lactic acidosis. *Proc Natl Acad Sci U S A* 1983; **80**: 5103-5106.

[55] Huang CY, Kasai M, Buetow DE. Extremely-rapid RNA detection in dot blots with digoxigenin-labeled RNA probes. *Genet Anal* 1998; **14**: 109-112.

[56] Legato MJ, Mulieri LA, Alpert NR. The ultrastructure of myocardial hypertrophy: why does the compensated heart fail? *Eur Heart J* 1984; **5** Suppl F: 251-F269.

[57] Tokoro T, Ito H, Suzuki T. Alterations in mitochondrial DNA and enzyme activities in hypertrophied myocardium of stroke-prone SHRS. *Clin Exp Hypertens* 1996; **18**: 595-606.

[58] Hanna MG, Nelson IP, Rahman S, Lane RJ, Land J, Heales S, Cooper MJ, Schapira AH, Morgan-Hughes JA, Wood NW. Cytochrome c oxidase deficiency associated with the first stop-codon point mutation in human mtDNA. *Am J Hum Genet* 1998; **63**: 29-36.

[59] Wanagat J, Wolff MR, Aiken JM. Age-associated changes in function, structure and mitochondrial genetic and enzymatic abnormalities in the Fischer 344 x Brown Norway F(1) hybrid rat heart. *J Mol Cell Cardiol* 2002; **34:** 17-28.

[60] Gerdts E, Omvik P, Mo R, Kjeldsen SE. [Hypertension and heart disease]. *Tidsskr Nor Laegeforen* 2004; **124**: 802-805.

[61] Yamori Y, Horie R, Handa H, Sato M, Okamoto K. Proceedings: Studies on stroke in stroke-prone spontaneously hypertensive rats (SHRSP). (I). Local factor analysis on stroke. *Jpn Heart J* 1975; **16**: 329-331.

[62] Huang CY, Hao LY, Buetow DE. Insulin-like growth factor-induced hypertrophy of cultured adult rat cardiomyocytes is L-type calcium-channel-dependent. *Mol Cell Biochem* 2002; **231**: 51-59.

[63] Huang CY, Hao LY, Buetow DE. Hypertrophy of cultured adult rat ventricular cardiomyocytes induced by antibodies against the insulin-like growth factor

(IGF)-I or the IGF-I receptor is IGF-II-dependent. *Mol Cell Biochem* 2002; **233**: 65-72.

[64] Park GH, Buetow DE. Genes for insulin-like growth factors I and II are expressed in senescent rat tissues. *Gerontology* 1991; **37**: 310-316.

[65] Crackower MA, Oudit GY, Kozieradzki I, Sarao R, Sun H, Sasaki T, Hirsch E, Suzuki A, Shioi T, Irie-Sasaki J, Sah R, Cheng HY, Rybin VO, Lembo G, Fratta L, Oliveira-dos-Santos AJ, Benovic JL, Kahn CR, Izumo S, Steinberg SF, Wymann MP, Backx PH, Penninger JM. Regulation of myocardial contractility and cell size by distinct PI3K-PTEN signaling pathways. *Cell* 2002; **110**: 737-749.

[66] Molloy CA, May FE, Westley BR. Insulin receptor substrate-1 expression is regulated by estrogen in the MCF-7 human breast cancer cell line. *J Biol Chem* 2000; **275:** 12565-12571.

[67] Shioi T, Kang PM, Douglas PS, Hampe J, Yballe CM, Lawitts J, Cantley LC, Izumo S. The conserved phosphoinositide 3-kinase pathway determines heart size in mice. *Embo J* 2000; **19**: 2537-2548.

[68] Kuemmerle JF, Bushman TL. IGF-I stimulates intestinal muscle cell growth by activating distinct PI 3-kinase and MAP kinase pathways. *Am J Physiol* 1998; **275**: G151-G158.

[69] Parrizas M, Saltiel AR, LeRoith D. Insulin-like growth factor 1 inhibits apoptosis using the phosphatidylinositol 3'-kinase and mitogen-activated protein kinase pathways. *J Biol Chem* 1997; **272:**154-161.

[70] Lembo G, Rockman HA, Hunter JJ, Steinmetz H, Koch WJ, Ma L, Prinz MP, Ross J, Jr., Chien KR, Powell-Braxton L. Elevated blood pressure and enhanced myocardial contractility in mice with severe IGF-1 deficiency. *J Clin Invest* 1996; **98**: 2648-2655.

[71] Vecchione C, Colella S, Fratta L, Gentile MT, Selvetella G, Frati G, Trimarco B, Lembo G. Impaired insulin-like growth factor I vasorelaxant effects in hypertension. *Hypertension* 2001; **37**: 1480-1485.

[72] Frey N, Olson EN. Cardiac hypertrophy: the good, the bad, and the ugly. *Annu Rev Physiol* 2003; **65**: 45-79.

[73] Haunstetter A, Izumo S. Apoptosis: basic mechanisms and implications for cardiovascular disease. *Circ Res* 1998; **82:** 1111-1129.

[74] Wang L, Ma W, Markovich R, Chen JW, Wang PH. Regulation of cardiomyocyte apoptotic signaling by insulin-like growth factor I. *Circ Res* 1998; **83**: 516-522.

[75] Pugazhenthi S, Miller E, Sable C, Young P, Heidenreich KA, Boxer LM, Reusch JE. Insulin-like growth factor-I induces bcl-2 promoter through the transcription factor cAMP-response element-binding protein. *J Biol Chem* 1999; **274**: 27529-27535.

[76] Demers C, McKelvie RS. Growth hormone therapy in heart failure: where are we now? *Congest Heart Fail* 2003; **9**: 84-90.

[77] Wu W, Lee WL, Wu YY, Chen D, Liu TJ, Jang A, Sharma PM, Wang PH. Expression of constitutively active phosphatidylinositol 3-kinase inhibits activation of caspase 3 and apoptosis of cardiac muscle cells. *J Biol Chem* 2000; **275:** 40113-40119.

[78] Cardone MH, Roy N, Stennicke HR, Salvesen GS, Franke TF, Stanbridge E, Frisch S, Reed JC. Regulation of cell death protease caspase-9 by phosphorylation. *Science* 1998; **282**: 1318-1321.

[79] Matsui T, Tao J, del Monte F, Lee KH, Li L, Picard M, Force TL, Franke TF, Hajjar RJ, Rosenzweig A. Akt activation preserves cardiac function and prevents injury after transient cardiac ischemia in vivo. *Circulation* 2001; **104**:

330-335.

[80] McKinsey TA, Olson EN. Cardiac hypertrophy: sorting out the circuitry. *Curr Opin Genet Dev* 1999; **9**: 267-274.

[81] Mizukami Y, Kobayashi S, Uberall F, Hellbert K, Kobayashi N, Yoshida K. Nuclear mitogen-activated protein kinase activation by protein kinase czeta during reoxygenation after ischemic hypoxia. *J Biol Chem* 2000; **275**: 19921-19927.

[82] Molkentin JD, Lu JR, Antos CL, Markham B, Richardson J, Robbins J, Grant SR, Olson EN. A calcineurin-dependent transcriptional pathway for cardiac hypertrophy. *Cell* 1998; **93**: 215-228.

[83] Yue TL, Ohlstein EH, Ruffolo RR, Jr. Apoptosis: a potential target for discovering novel therapies for cardiovascular diseases. *Curr Opin Chem Biol* 1999; **3**: 474-480.

[84] Ding B, Price RL, Borg TK, Weinberg EO, Halloran PF, Lorell BH. Pressure overload induces severe hypertrophy in mice treated with cyclosporine, an inhibitor of calcineurin. *Circ Res* 1999; **84**: 729-734.

[85] Zhang W, Kowal RC, Rusnak F, Sikkink RA, Olson EN, Victor RG. Failure of calcineurin inhibitors to prevent pressure-overload left ventricular hypertrophy in rats. *Circ Res* 1999; **84**: 722-728.

[86] Aoyagi T, Izumo S. Hemodynamic Overload-Induced Activation of Myocardial Mitogen-Activated Protein Kinases In Vivo: Augmented Responses in Young Spontaneously Hypertensive Rats and Diminished Responses in Aged Fischer 344 Rats. *Hypertension* 2001; **37**: 52-57.

[87] Izumi Y, Kim S, Murakami T, Yamanaka S, Iwao H. Cardiac mitogen-activated protein kinase activities are chronically increased in stroke-prone hypertensive rats. *Hypertension* 1998; **31**: 50-56.

[88] Kagiyama S, Qian K, Kagiyama T, Phillips MI. Antisense to epidermal growth factor receptor prevents the development of left ventricular hypertrophy. *Hypertension* 2003; **41**: 824-829.

附錄一 Dot blotting

The Procedures of making DIG-Probes.

1. Culture E. coli

a. strip E coli (Sure strain) which has IGFI /COX-Vb gene in Jampicilin-plates and culture plates in 37℃ O/N (12-18 hr).
b. inoculate E coli (one colony) into 6 ml LB midium O/N.

2. DNA extraction:

a. alkaline lysis of bacteria.
b. Clearing bacterial lysates using Turbofilter
c. DNA adsorption to the QIAprep membrane
d. Washing and elution of plasmid DNA

3. **Linearization of circular DNA (w/restricton enzyme digestion):**

a. measure OD
b. DNA Vol of 2 μg
   10x React 3 10 μl
   40 U/ul BamH1 3 μl
   ddH2O (total 100 μl)

   incubated at 37℃ for 5 hr
c. electrophoresis: 1.2% agarose gel, TBE buffer, 70/80 V
   to check the correct sizes of the plasmid DNA
   .

4**. Phenol- chlorophorm (1:1) extraction** for getting rid of protein

a. same volume of linearized DNA and phenol-chloroform mixture
b. inverse the mixture many times, then spin 30-60”
c. get supernatant and transfer to another tube.
d. DNA (in 200 μl ddH_2O) plus 1/10 V 3M pH5.2 sodium acetate plus 2-2.5V 100% EtOH at -70℃>1hr or -20℃ O/N.
e. centrifuge 12,000g for 15 min, remove ethanol
f. 70% ethanol wash twice.
g. air dry, then dissolve in 20 μl ddH_2O
h. measure OD

5. **Transcription Roche DIG RNA Labeling Kit)**

a.	DNA template	13 μl (2 μg)
10x	NTP labeling buffer	2 ul
10x	Tx buffer	2 μl
	RNase Inhibitor	1 μl
	T7 RNA polymerase	2 μl
	DEPC H_2O	(Total 20 μl)

Incubated at 37℃ for 5 hr

b. add EDTA (0.2 M pH 8.0) 2 μl to stop Rx

c. add DnaseI, RNase-free 2 ul, then incubate at 37℃ for 15 min.

d. add 4 M LiCl in DEPC H_2O 2-5 μl

glycogen 1 μl

100% ethanol 75 μl

and mix well, incubated at -70℃ > 30' or O/N

d. centrifuge 12,000g for 15 min, remove ethanol

e. 70% ethanol wash twice.

f. air dry, dissolve in 50 μl DEPC H_2O with putting in 37℃ water bath 15 min or at 4℃ for O/N.

g. measure OD to estimate how much probe is available for hybridization

RNA Hybridization and Detection

1. Denature diluted RNA samples (80 ng/μl) at 65℃ for 15 min.
2. Spot 3 μl sample to marked memb w/ sucking.
3. Dry memb at 80℃ for 10-15 min in oven incubator.
4. Cross linking using UV transiluminator for 5 min (RNA side down).
5. Prehybridization in 3-5 ml/sheet in bag wo/ bubble for 70 min at 68℃
6. Hybridization memb w/DIG-antisense RNA probe at 68℃ overnight (denature probe at 68℃ for 10 min before use).
7. Wash (2x7.5 min, 2x20 min), and rinse (2min) at RT.
8. Blocking w/blocking reagent (60 min, longer is acceptable)
9. Ab (anti-DIG Ab conjugated AP) binding for 60 min at RT.
10. Washing (2x20min).
11. Equilibrate for 25 min.
12. Luninescence reaction (CDP-star-substrate, 5 min).
13. Film exposure at RT.
14. Densitometer measure.

Solutions and buffers required for RNA dot blotting detection:

1. **Buffer 1 (Maleic acid buffer):**
   0.1 M Maleic acid (FW=116.1 Sigma)
   0.15 M NaCl (FW=58.54)
   adjust pH to 7.5 with solid NaOH
   autoclave
2. **DEPC water: 0.2% (v/v)**
   3 ml DEPC to 1.5 L water, need to stir for one hour
   autoclave
3. **Washing Buffer (Buffer 1 + Tween 20)**
   0.3 % (v/v)Tween 20 to Buffer 1
   Do not autoclave Buffer 1 containing Tween 20
4. **Blocking Reagent Stock Solution**
   Commercial powder is dissolved in Buffer by 10% (w/v) with stirring and heating either on a stir plate or microwave over. "avoid boiling ". It is a turbid solution.
   →Add 10 g blocking reagent to 100 ml Buffer 1 at 60 ℃ for about 1 hr, or completely in solution. If it does not go into solution, adjust the pH. It must be completely in solution before autoclaving. Autoclave only for 15'
5. **Buffer 2 (Blocking soln)**

Buffer 1	90 ml
Blocking stock soln	10 ml
	100 ml

6. **Buffer 3 (Detection Buffer)**
   15.76 g 0.1 M Tris HCL (FW=157.6)
   5.84g 0.1 M NaCl
   10.165g 50 mM $MgCl_2$ (no autoclave, otherwise omit)
   Dilute Tris and NaCl with DEPC water; adjust pH to 9.5, then autoclave
   Filter after adding $MgCl_2$

7. **20x SSC: 3M NaCl and 0.3M Sodium citrate, pH=7.0**
   10% SDS (w/v) in autoclave DEPC water, filter it
   Washing soln 2x

2x SSC	20x SSC	50 ml
0.1%SDS	10% SDS	5 ml
		500 ml

Washing soln 0.5x

2x SSC	20x SSC	12.5 ml
0.1%SDS	10% SDS	5 ml
		500 ml

Washing soln 0.1x

2x SSC	20x SSC	2.5 ml
0.1%SDS	10% SDS	5 ml
		500 ml

8. RNA denaturing buffer”

500 μl formamide

162 μl 37% formaldehyde

100 μl 10x MOPS

9. Hybridization Buffer

50% formamide (deionized)		10 ml
5x SSC	20x SSC	5 ml
2% Bolcking Reagent	10% stock	4 ml
0.1% (w/v)N-lauroyl sarcosine	10% stock	0.2 ml
0.02% (w/v) SDS	10% stock	0.04 ml
		20 ml

附錄二 已接受之期刊論文:

Journal of Biomedical Science (2005) 00:1–10
DOI 10.1007/s11373-005-7373-2

The profile of cardiac cytochrome *c* oxidase (COX) expression in an accelerated cardiac-hypertrophy model

Wei-Wen Kuo[1], Chia-Yih Chu[2], James A. Lin[3], Jer-Yuh Liu[1], Tsung-Ho Ying[4], Yi-Hsien Hsieh[1], Chu-Hsien Chu[1], Ding-Yu Lin[1], Hsi-Hsien Hsu[5] & Chih-Yang Huang[1,*]
[1]*Institute of Biochemistry, Chung-Shan Medical University, Taichung, Taiwan, ROC;* [2]*School of Applied Chemistry, Chung-Shan Medical University, Taichung, Taiwan, ROC;* [3]*Department of Veterinary Medicine, National Chung-Hsing University, Taichung, Taiwan,ROC;* [4]*Department of Obstetrics and Gynecology, Chung-Shan Medical University Hospital, Taichung, Taiwan, ROC;* [5]*Division of Colorectal Surgery, Mackay Memorial Hospital, Taipei, Taiwan, ROC*

Received 10 March 2005; accepted 17 May 2005

Key words: cytochrome *c* oxidase (COX), complete coarctation, cardiac hypertrophy, genetically hypertensive rats

Summary

The contribution of the mitochondrial components, the main source of energy for the cardiac hypertrophic growth induced by pressure overload, is not well understood. In the present study, complete coarctation of abdominal aorta was used to induce the rapid development of cardiac hypertrophy in rats. One to two days after surgery, we observed significantly higher blood pressure and cardiac hypertrophy, which remained constantly high afterwards. We found an early increased level of cytochrome *c* oxidase (COX) mRNA determined by *in-situ* hybridization and dot blotting assays in the hypertrophied hearts, and a drop to the baseline 20 days after surgery. Similarly, mitochondrial COX protein level and enzyme activity increased and, however, dropped even lower than baseline 20 days following surgery. In addition, in natural hypertension-induced hypertrophic hearts in genetically hypertensive rats, the COX protein was significantly lower than in normotensive rats. Taken together, the lower efficiency of mitochondrial activity in the enlarged hearts of long-term complete coarcted rats or genetically hypertensive rats could be, at least partially, the cause of hypertensive cardiac disease. Additionally, the rapid complete coarctation-induced cardiac hypertrophy was accompanied by a disproportionate COX activity increase, which was suggested to maintain the cardiac energy-producing capacity in overloaded hearts.

Introduction

The heart has a remarkable capacity to increase its mass in response to an increased work load, such as pressure overload, induced either pathologically or experimentally [1]. In order to be able to face the increase of cardiac muscle contraction for extra work, more energy production is required. The mitochondrial compartment is the main source of energy needed for hypertrophic growth in the myocyte. However, the reports evaluating the mitochondrial compartment behavior during the onset and progression of cardiac hypertrophy are inconsistent [2]. In addition, the investigations on the molecular events involved in mitochondrial biogenesis and function during the hypertrophy process are few. This is surprising since it is well-known that insufficient oxidative capacity often contributes to the cardiac failure

*To whom correspondence should be addressed. phone +886-4-24730022 ext. 1682; E-mail: chuang1@csmu.edu.tw

Journal : JBMS | Dispatch : 8-6-2005 | Pages : 10
CMS No. : DO00017373 | ☐ LE | ☐ TYPESET
MS Code : JBMS 59R1 | ☑ CP | ☑ DISK

observed at least in late stage hypertrophic cardiomyopathies [3,4].

Cytochrome *c* oxidase (COX) is located in the inner membrane of mitochondria and is the last component of respiration chain. This enzyme catalyzes the rate-limiting reaction of the mitochondrial oxidative phosphorylation (OXPHOS), which supplies the energy for cardiac contraction [5, 6]. Therefore, COX plays an essential role in maintaining normal cardiac function. Since the effects of this enzyme are important, the reaction rate of the mitochondrial OXPHOS can be altered by a small decrease in this oxidase activity under physiological condition. This tight control of COX suggests that the dysfunction of the enzyme may cause the mitochondrial myopathy [7, 8]. Actually, the number of known mutations of most of the genes encoding the protein subunits of COX in patients with cardiomyopathy has increased [9–11].

Aortic constriction has been used to induce cardiac hypertrophy in many studies. Our previous data showed that the heart was rapidly enlarged within 1–2 days postsurgery in this model by using a complete coarctation of the abdominal aorta in rats to induce a cardiac pressure overload [2,12,13]. In the present study, we investigated the biochemical and molecular events underlying the adaptation of the mitochondrial compartment to meet the increased energy demands of the cardiomyocyte as they underwent this rapid hypertrophic growth. We have used COX as a model protein for investigating the underlying adaptive mechanism. We measured COX activity and examined COX gene expression by determining COX-Vb mRNA, one of the nuclear-encoded subunits of COX enzyme, during cardiac hypertrophy in the model system using complete coarctation of the abdominal aorta from 1 to 20 days. The measurement of cardiac COX protein in spontaneously hypertensive rats (SHR) and stroke prone SHR (SPSHR) with naturally occurring hypertensive cardiac hypertrophy was also included in this study.

Methods

Coarctation of abdominal aorta

Male Sprague-Dawley rats weighing between 240 and 300 g were used to induce cardiac hypertrophy by complete coarctation of the abdominal aorta between the origins of the renal arteries [14]. After a rat was anesthetized with pentobarbital sodium (45.5 mg/kg), its left side was shaved and a horizontal incision 3 cm in length was made. Using curved hemostats, the superficial fascia were separated and an incision of the same size was made into the abdominal musculature. The viscera were exposed, and adipose tissue was separated from the left kidney which was moved to obtain maximal clearance to the abdominal aorta. The abdominal aorta was isolated and completely coarcted with a ligature (Coats, Dual Duty Plus, carpet thread) fixed between the origins of the renal arteries. The left kidney and adipose tissue were returned to their normal positions, the abdominal musculature was rejoined using coated vicryl sutures (Ethicon, Johnson & Johnson, FS-2 cutting), and the epidermis was rejoined using wound clips. Then, a solution of l% iodine in 70% ethanol was used to clean the wound. The rats were returned to the animal care room (one per cage) and allowed to recover. All animals were fed standard rat chow and water supplemented with tetracycline (22 mg/kg body weight) to ward off infection. Sham rats were subjected to the same procedure, but no ligature was placed. All animals were handled according to the guidelines of the Taiwan Society for Laboratory Animal Sciences for the Care and Use of Laboratory Animals.

Femoral arterial pressure measurement

The blood pressure of coarcted and sham animals was measured at l, 2, 3, 5, 7, 10 and 20 days postsurgery. The animals not subjected to the above surgery were measured as 0 day controls. After catheterization of the femoral artery of animals, blood pressure monitor (Recorder 2200S, GOULD, U.S.A.) was used to measure both the systolic and diastolic pressure by connecting the femoral artery with a sensor. The blood pressure was measured and recorded continuously [15].

Heart isolation

Once the blood pressure measurements were taken, the animals were sacrificed by cervical transaction. The thoracic cavity was opened, and the heart was removed. After removing excess adipose and connective tissue from the heart, it was drained of blood and weighed. The ratios of

Journal : JBMS | Dispatch : 8-6-2005 | Pages : 10
CMS No. : DO00017373 | ☐ LE | ☐ TYPESET
MS Code : JBMS 59R1 | ☑ CP | ☑ DISK

the total heart weight to body weight were calculated. The isolated heart was washed in cold (0–4° C) SNTE buffer (0.20 M sucrose, 0.13 NaCl, l mM Tris–HCl, pH 7.4 [5], and l mM EGTA neutralized with Tris to pH 7.4), and the entire left ventricle (LV) was excised from the heart. The LV was separated into four parts, and stored at −70° C for further analysis.

Preparation of heart mitochondria

One part of LV was minced with scissors, added with SNTE buffer (l.5 ml per g tissue) and homogenized at ice temperature with a Model PT l0/35 Polytron homogenizer for 2 cycles of l0 s each. The homogenate was centrifuged at $500 \times g$ for l0 min in a Beckman J20.l centrifuge. Then, the pellet was discarded, and the supernatant was further centrifuged at $8000 \times g$ for l5 min. The mitochondrial pellet was resuspended with SNTE buffer. The mitochondrial protein was measured [16], and prepared for COX enzyme activity assay.

Cytochrome c oxidase activity

Cytochrome *c* (horse heart, Sigma Chemical Co. no. C-7752, Type III, prepared without using TCA) was reduced with dithionite as described [17] in 50 mM phosphate (K_2HPO_4–KH_2PO_4) buffer at pH 7.0 [18]. Reduced cytochrome *c* was made fresh for each experiment and stored in an air-tight container on ice for the assays. COX activity was measured spectrophotometrically by following the oxidation of reduced cytochrome *c* at 550 nm [18] in 50 mM phosphate buffer (pH 7.0) containing 0.5% Tween 80 [19]. Rates are expressed as μmol cytochrome *c* oxidized per min per mg mitochondrial protein.

Protein extraction and Western blot analysis

The second part of LV was minced with scissors, homogenized with lysis buffer (50 mM Tris (pH 7.5), 0.5 M NaCl, 1.0 mM EDTA (pH 7.5), 10% glycerol, 1 mM BME, 1% IGEPAL-630 and proteinase inhibitor cocktail tablet (Roche)) and spun down 12,000 rpm for 30 min. Then, the supernatant was collected and stored at −70° C for further Western blotting. Proteins from animal heart extracts were quantitated by the Bradford protein assay [16] and then separated in 10% gradient sodiumdodecyl sulfate-polyacrylamide gel electrophoresis. The samples were electrophoresed at 140 V for 3.5 h and equilibrated for 15 min in 25 mM Tris–HCl, pH 8.3, containing 192 mM glycine and 20% (v/v) methanol. Electrophoresed proteins were transferred to nitrocellulose paper (Amersham, Hybond-C Extra Supported, 0.45 Micro) at 100 mA for 14 h. Nitrocellulose papers were incubated at room temperature for 2 h in blocking buffer containing 100 mM Tris–HCl, pH7.5, 0.9% (w/v) NaCl, 0.1% (v/v) fetal bovine serum. Antibody of COX-Vb (Santa Cruz Biotechnology) was diluted in antibody binding buffer containing 100 mM Tris–HCl, pH7.5, 0.9%(w/v) NaCl, 0.1% (v/v) Tween 20 and 1%(v/v) fetal bovine serum. Incubations were performed at room temperature for 3.5 h. The immunoblot was washed three times in 50 ml blotting buffer for 10 min and then immersed in the second antibody solution containing alkaline phosphatase goat anti-rabbit IgG (Promega) for 1 h and diluted 1000-fold in binding buffer. The filters were then washed in blotting buffer for 10 min three times. Color development was presented in a 20 ml mixture consisting of 7 mg nitro blue tetrazolium, 5 mg 5-bromo-4-chloro-3-indolyl-phosphate, 100 mM NaCl and 5 mM $MgCl_2$ in 100 mM Tris–HCl, pH 9.5. The immunoblot with antibody against α-tubulin which was performed with the same procedure was used as an internal control.

RNA extraction

The third part of LV was used to extract total RNA using the Ultraspec RNA Isolation System (Biotecx Laboratories, lnc.) according to directions supplied by the manufacturer. Each heart was thoroughly homogenized (1 ml Ultraspec reagent per 100 mg tissue) with a Polytron homogenizer. The RNA precipitate was washed twice by gentle vortexing with 70% ethanol, collected by centrifugation at $12{,}000 \times g$, dried under vacuum for 5–l0 min, dissolved in 50–100 μl of diethylpyrocarbonate-treated water, and incubated for l0-l5 min at 55–60° C.

Measurement of heart mRNA levels by dot blotting

RNA dot blotting was used for the hybridization and detection of mRNAs according to the method described in our previous study [20]. The

Journal : JBMS | Dispatch : 8-6-2005 | Pages : 10
CMS No. : DO00017373 | ☐ LE | ☐ TYPESET
MS Code : JBMS 59R1 | ☑ CP | ☑ DISK

corresponding digoxigenin (DIG)-labeled antisense RNA probes were prepared from pGEM-7Zf(+) containing a 500-bp cDNA encoding COX subunit Vb insert (supplied by Dr. Dennis E. Buetow, Univ. of Illinois, IL, USA, and originally form Dr. Avadhani, Univ. of Pennsylvania, PA, USA).

In-situ hybridization of COX-Vb mRNA and quantitation

The fourth part of LV was used to detect the COX-Vb mRNA in tissues, using DIG-labeled antisense RNA probes described above. The procedures of *in-situ* hybridization used in this study were described previously [13].

Statistical analysis

Statistical differences were analyzed by one-way analysis of variance (ANOVA). Fisher's Least Significant Difference test was used to determine differences. $p < 0.05$ was considered statistically significant. Data are expressed as the mean ± standard error (SE).

Results

Hypertensive cardiac hypertrophy in pressure-overloaded rats

Blood pressure measurements of rats subjected to complete coarctation clearly demonstrated the hypertensive effects of the aortic coarctation (Figure 1). On day 1, 7 and 20 postsurgery, the arterial systolic blood pressure of sham animals was 137 ± 5, 148 ± 3 and 152 ± 6 mm Hg, respectively, while that of the coarcted animals was 172 ± 6, 220 ± 10 and 200 ± 10 mm Hg, respectively. Similarly, the arterial diastolic blood pressure of sham animals was 100 ± 5, 110 ± 5 and 115 ± 5 mm Hg, while that of the coarcted animals was 128 ± 5, 154 ± 6 and 148 ± 9 mm Hg on day 1, 7 and 20 postsurgery, respectively.

The development of cardic hypertrophy after complete aortic coarctation is illustrated in Table 1. Heart weights of sham animals remained unchanged throughout the postsurgery period. In contrast, by day 2 after coarctation, hearts of coarcted rats were significantly enlarged and remained so through the rest of the observation period of 20 days. The heart weight-to-body weight ratios were increased significantly from day 2 through 20 postsurgery in the coarcted animals compared to the 0-day controls. In sham animals, these ratios remained unchanged compared to the 0-day controls during the same postsurgery period.

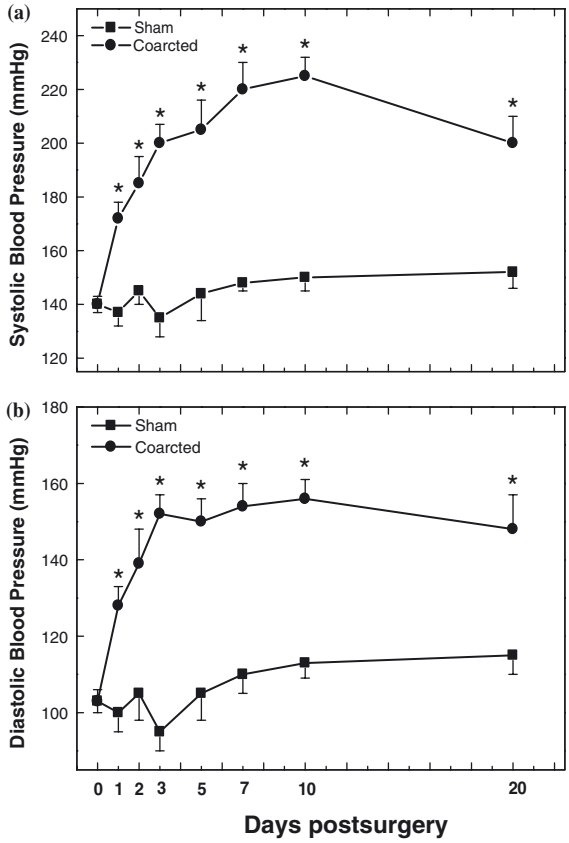

Figure 1. Arterial systolic and diastolic blood pressures of sham-operated and coarcted rats following surgery. Zero day values represent baseline data from animals sacrificed on the day of surgery. Values are mean ± SE. Numbers of animals measured at each data point are given in Table 1. $*p < 0.001$ represents the comparison to zero day sham animals.

COX-Vb gene expression

COX-Vb gene expression was measured as levels of COX-Vb mRNA using *in-situ* hybridization (Figure 2) and dot blotting (Figure 3) with an antisense COX-Vb mRNA DIG-labeled probe in hearts from rats. The level of hybridized COX-Vb mRNA in heart sections of coarcted animals significantly increased and reached a peak at day

Journal : JBMS | Dispatch : 8-6-2005 | Pages : 10
CMS No. : DO00017373 | ☐ LE | ☐ TYPESET
MS Code : JBMS 59R1 | ☑ CP | ☑ DISK

Table 1. Heart weight and heart weight to body weight ratios of sham-operated and coarcted rats.

Day postsurgery	H, g		H:B, mg:g	
	Sham	Coarcted	Sham	Coarcted
0	0.96 ± 0.02 (n = 8)	–	3.63 ± 0.08 (n = 8)	–
1	0.92 ± 0.03 (n = 7)	0.97 ± 0.02 (n = 7)	3.48 ± 0.08 (n = 7)	3.64 ± 0.14 (n = 7)
2	0.94 ± 0.02 (n = 7)	1.07 ± 0.03* (n = 6)	3.53 ± 0.07 (n = 7)	4.31 ± 0.19* (n = 6)
3	0.95 ± 0.03 (n = 7)	1.13 ± 0.03** (n = 6)	3.47 ± 0.07 (n = 7)	4.56 ± 0.13** (n = 6)
5	0.93 ± 0.01 (n = 7)	1.11 ± 0.02** (n = 6)	3.51 ± 0.08 (n = 7)	4.98 ± 0.18** (n = 6)
7	1.00 ± 0.07 (n = 7)	1.12 ± 0.04* (n = 4)	3.44 ± 0.08 (n = 7)	4.63 ± 0.30*** (n = 4)
10	1.04 ± 0.05 (n = 7)	1.16 ± 0.03* (n = 4)	3.42 ± 0.09 (n = 7)	4.83 ± 0.31*** (n = 4)
20	1.10 ± 0.04 (n = 7)	1.20 ± 0.03* (n = 37)	3.40 ± 0.12 (n = 7)	4.99 ± 0.20** (n = 3)

Data are mean ± SE. H and H:B are the heart weights (g) and heart weight to body weight ratios (mg:g), respectively, following surgery; n, number of animals. Zero day values represent baseline data from animals sacrificed on the day of surgery. *$p < 0.05$, **$p < 0.025$, ***$p < 0.001$ compared to the sham animals.

5. Then, the level declined and returned to the baseline at day 20 postsurgery (Figure 2a and 2c). In the sham animals, LV COX-Vb mRNA did not change during the 20-day postsurgery period (Figure 2c). The representative images of COX-Vb gene expression in *in-situ* hybridization at day 7 are shown in Figure 2b. No hybridization was detectable in control experiments that used a sense probe or lacked a probe. The dot blotting of hybridized COX-Vb mRNA is shown in Figure 3a. Levels of GAPDH mRNA were used as a loading control. The density of each COX mRNA dot was measured and divided by the density of the corresponding GAPDH mRNA dot. Data were quantified by densitometry, Figure 3b. Clearly, the levels of COX-Vb mRNA are significantly higher in the coarcted animals compared to the sham animals at each day postsurgery, and decreased to basal level at day 20 postsurgery.

Changes of COX-Vb protein level and enzyme activity

The levels of COX activity and subunit Vb protein were measured by enzyme kinetic assay and western blotting, respectively. The effects of the stress of the surgery were apparent in coarcted animals. A general increase in cardiac COX enzyme activity in coarcted animals after day 2 postsurgery was observed (Table 2). In all cases, COX activity per mg mitochondnal protein of coarcted hearts was significantly higher than that of sham hearts by day 10 with an exception at day 20 which was significantly lower. Cardiac COX-specific activity in coarcted animals was significantly different from that of shams. Compared with 0-day protein level, the COX-Vb protein levels at day 2, 3, 5 and 7 were significantly increased. Conversely, the COX protein level at day-20 is significantly lower than that at 0-day control (Figure 4).

Impairments of cardiac COX-Vb protein in the rat models of genetic hypertension

Relative to coarctation-induced pressure-over loaded rats, the cardiac COX-Vb protein level by Western blotting was examined in naturally hypertensive rats, spontaneously hypertensive rats (SHR) and stroke prone SHR (SPSHR), using normotensive Wistar rats (WKY) as a control group, and results were shown in Figure 5. Using β-actin as a loading control, cardiac COX-Vb protein levels of both SHR and SPSHR at age of 4-week, 6-week or 12-week-old were apparently lower than that of WKY. This indicates that the COX-Vb of hearts was impaired in genetically hypertensive rats.

Discussion

Cardiac hypertrophy resulting from chronic pressure overload was rapidly induced in the present model system in which complete coarctation of the rat abdominal aorta was done between the origins of the renal artery. In this model system, systolic blood pressure was found to increase significantly one day following surgery. It reached a peak and remained fairly constantly above 200 mm Hg after

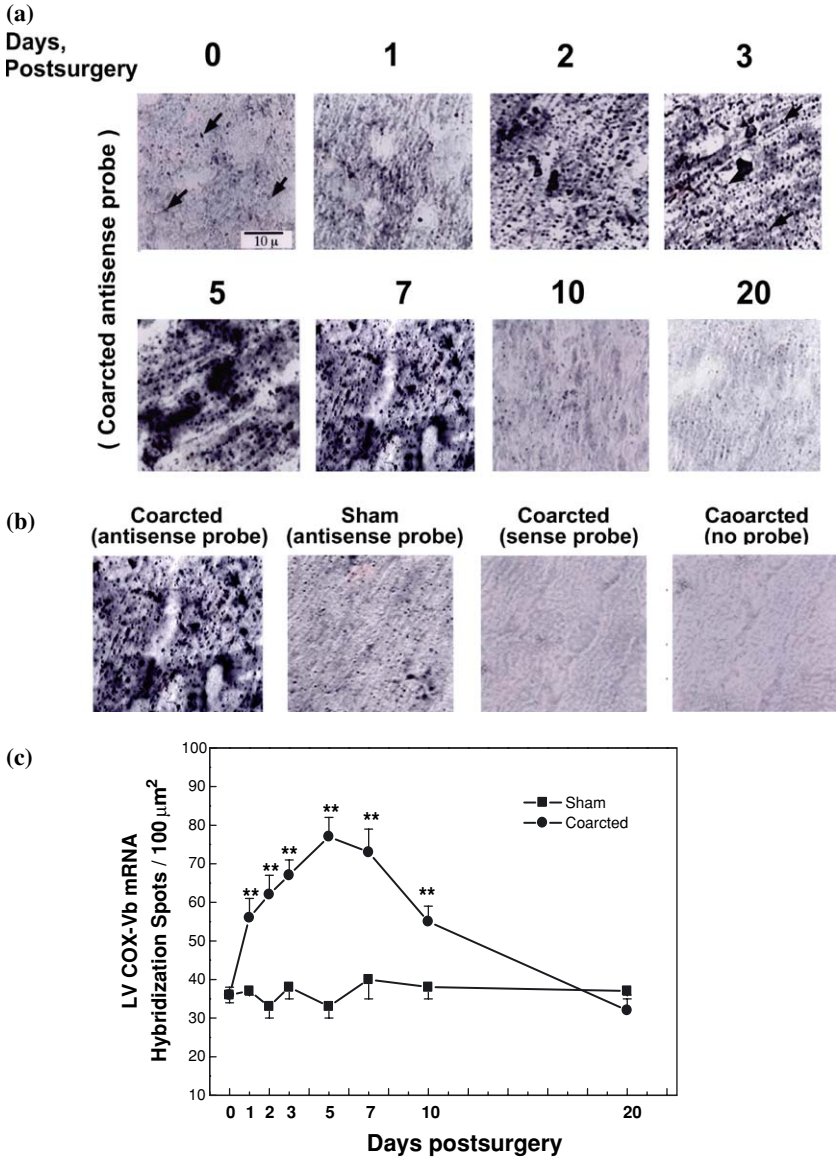

Figure 2. In-situ hybridization of LV COX-Vb mRNA. (a) Hybridization of antisense COX-Vb mRNA to LVs of sham-operated and coarcted rats at 0, 1, 2, 3, 5, 7, 10 and 20 days postsurgery. Arrows point to spots of immuno-detected hybridized antisense COX-Vb mRNA. (b) Hybridization with a digoxigenin (DIG)-labeled antisense COX-Vb mRNA probe in the LVs from sham-operated and coarcted animals at day 7 postsurgery. Control hybridizations with a sense DIG-labeled COX-Vb mRNA probe and with no probe are also shown, (essentially no hybridization is detected as expected). (c) Quantitation of *in-situ* hybridization of COX-Vb mRNA in the LVs from sham-operated and coarcted rats following surgery. The 0-day value represents baseline data from animals sacrificed on the day of surgery. Hybridized spots were counted in 100 μm^2 sections. Values are expressed as mean ± SE (3 animals per value). Data were analyzed by ANOVA and significant differences between coarcted vs. sham animals on each day postsurgery. $^{**}p < 0.01$.

3 days. Blood pressures of sham controls remained around 140 mm Hg during the same postsurgical period. In the coarcted animals, cardiac hypertrophy was observed at one and two days after the surgery. These results support the view that the model system using complete coarctation in rats was a more accelerated model of inducing cardiac hypertrophy than in the other rat models, for example, those that are partially coarcted [2,12] or treated with excess thyroid hormone [12]. To

Journal : JBMS | Dispatch : 8-6-2005 | Pages : 10
CMS No. : DO00017373 | ☐ LE | ☐ TYPESET
MS Code : JBMS 59R1 | ☑ CP | ☑ DISK

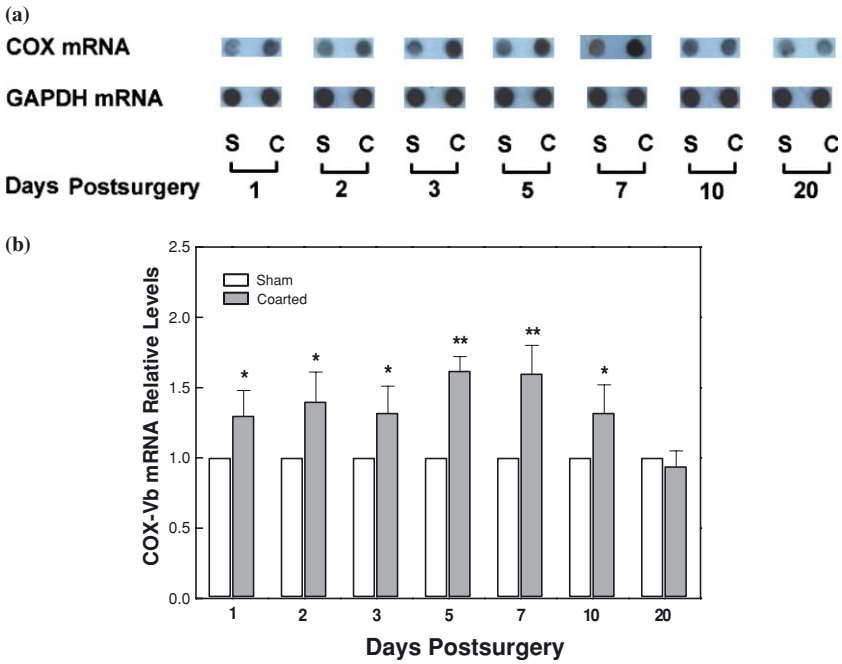

Figure 3. Gene expression for COX-Vb and GAPDH (loading control) mRNA in the hearts of sham-operated and coarcted rats at day 1, 2, 3, 5, 7, 10 and 20 postsurgery. (a) COX-Vb probe labeled with DIG on UTP was hybridized to 80 ng mRNA from sham (S) and coarcted (C) animals. COX-Vb and GAPDH mRNA levels were determined from the dot blots by densitometry. No hybridization occurred with yeast tRNA which was used as a negative control (data not shown). (b) Graph showed the level of COX-Vb mRNA relative to the GAPDH mRNA level in the hearts of sham and coarcted rats at day 1 day 1, 2, 3, 5, 7, 10 and 20 postsurgery ($n = 3$ in all cases). The level of COX-Vb mRNA in sham hearts was standardized to 1.0. *$p < 0.05$ and **$p < 0.01$ when compared to the sham rats.

maintain normal tissue function in response to extra workload during cardiac hypertrophy, the occurrence of cellular enlargement must be synchronized with proportional increases in the components of cellular organelles. In order to provide the energy needed for the hypertrophic growth and the functional maintenance of the enlarged cardiac myocytes, increases in the mitochondrial components can be expected.

Table 2. COX-Vb enzyme activity in mitochondria of coarcted (CR) and sham (S) rats on day 1 through 20 postsurgery.

Days postsurgery	Activity	
	S	CR
1	0.31 ± 0.06 ($n = 7$)	0.43 ± 0.11 ($n = 7$)
2	0.30 ± 0.05 ($n = 7$)	0.44 ± 0.06* ($n = 7$)
3	0.30 ± 0.03 ($n = 7$)	0.43 ± 0.05* ($n = 7$)
5	0.33 ± 0.02 ($n = 7$)	0.47 ± 0.02* ($n = 7$)
7	0.33 ± 0.05 ($n = 7$)	0.49 ± 0.04* ($n = 7$)
10	0.35 ± 0.03 ($n = 7$)	0.47 ± 0.03* ($n = 7$)
20	0.36 ± 0.09 ($n = 7$)	0.24 ± 0.10** ($n = 7$)

Activity values are μmoles oxidized cytochrome *c*/min/mg mitochondrial protein (mean ± SE); *n*, number of animals. *$p < 0.05$ represents significant increase when compared to the sham animals. **$p < 0.05$ represents significant decrease when compared to the sham animals.

COX is an enzyme containing thirteen different subunits. Among them, the three largest polypeptides (I, II and III subunits) are synthesized within mitochondria under the control of mitochondria DNA (mtDNA). The other ten smaller subunits (IV, Va, Vb, VIa, VIb, VIc, VIIa, VIIb, VIIc and VIII) are encoded by nuclear DNA (nDNA) and synthesized in cytosol [6].In the present study, COX-Vb mRNA detected by *in-situ* hybridization and dot blotting increased after day 1 following the surgery, reached a peak at day 5 or 7 and decreased to baseline by day 20. The results of the COX protein and activity demonstrated similar alteration patterns, and the values on the 20th day even dramatically dropped below the baseline. Indeed, by 20 days postsurgery, the mortality of completely coarcted rats at this time point was

Journal : JBMS | Dispatch : 8-6-2005 | Pages : 10
CMS No. : DO00017373 | ☐ LE | ☐ TYPESET
MS Code : JBMS 59R1 | ☑ CP | ☑ DISK

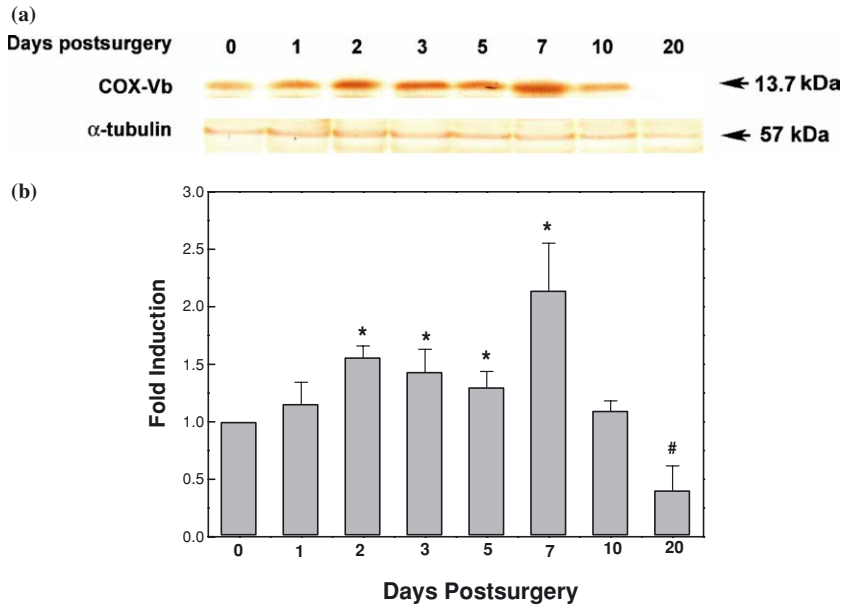

Figure 4. Activations of mitochondrial COX-Vb in cardiac tissues of rats. (a) Western blotting analysis of COX-Vb proteins in LVs of sham-operated and coarcted rats at 0, 1, 2, 3, 5, 7, 10 and 20 days postsurgery. The blotting of α-tubulin was used as a loading control. (b) Signal intensity of western blotting was quantitated using a PhosphoImager. The averaged result ± SD of three independent experiments is shown. The 0-day value represents baseline data from animals sacrificed on the day of surgery. *Represents a significant increase compared with the control group with $p < 0.05$. #Represents a significant decrease compared with the control group with $p < 0.05$.

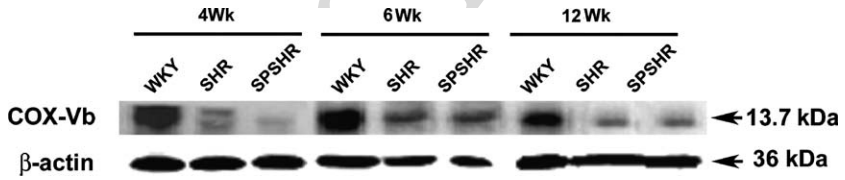

Figure 5. COX-Vb level in the left ventricle of hypertensive rats at different ages as determined by western blotting. Spontaneously hypertensive rats (SHR) and stroke prone SHR (SPSHR) were sacrificed at different ages as indicated. Lysates were prepared from hearts, and equal amounts of protein were separated by SDS/PAGE and immunoblotting with anti-COX-Vb antibody. β-actin was used as a loading control. WKY, Wistar rats as a normotensive control; Wk, week.

around 50% (data not shown). Our findings indicate that COX may be an essential adaptive factor of hypertensive cardiac hypertrophy in early onset and even prolonged pathological conditions.

A review of the relevant literature [2], however, reveals discrepancies regarding the behavior of the mitochondrial components during the onset and progression of cardiac hypertrophy even when induced by the same stimulus. Some studies of cardiac hypertrophy induced by partial aortic coarctation found an increase in mitochondrial content, i.e., mitochondrial biogenesis, but this increase has not always been found in other studies [2]. Similarly, the mitochondrial responses to renovascular hypertension-induced cardiac hypertrophy are also variable. Two reports, however, indicate changes in COX activity and the levels of mRNAs encoding COX subunits remain constant per mg total heart protein during adaptive cardiac growth induced by partial aortic coarctation [2,12]. It has been suggested that mitochondrial biogenesis is balanced with the increase of ventricular weight for 7 days [12] or even up to 28 days [2] following partial aortic coarctation. On the other hand, in the present accelerated model of cardiac hypertrophy, COX-specific activity was increased by 30–47% during the period of 1–10 days postsurgery. This result correlates with the

Journal : JBMS | Dispatch : 8-6-2005 | Pages : 10
CMS No. : DO00017373 | ☐ LE | ☐ TYPESET
MS Code : JBMS 59R1 | ☑ CP | ☑ DISK

ultrastructural study of Legato et al. [21] who showed that during cardiac hypertrophy mitochondrial DNA content in cardiac myocytes was increased and the mitochondria became smaller and more densely packed with cristae and inner membrane proteins. Similarly, in our study, since the COX activity was calculated by per gram mitochondrial protein, the increased COX activity more likely resulted from increased COX content per mitochondrion than from increased number of mitochondria. The imposition of a more severe aortic constriction in the present study than in the other studies, combined with a resulting greater pressure overload may lead to disproportionate changes in mitochondrial activity. In addition, an increased level of mRNA for the nuclear-encoded subunit Vb of COX was also observed, and this met the parallel changes of COX activity reaching a maximum as the heart hypertrophied. We suggest that the synthesis of COX is regulated at the level of transcription in the hypertrophied heart. Similar behavior of other nuclear-encoded subunits composed of the enzyme must be predictable [12]. Because there was a rapid increase of COX protein and mRNA, COX may be considered an important adaptive factor of hypertrophic hearts. The drop in cardiac COX by 20 days postsurgery in treated rats might indicate the failure of this increase of COX to balance the cardiac hypertrophy after long term coarctation, resulting in heart failure. These findings are also consistent with Lin's study [22], which demonstrated abnormal cardiac mitochondria, reduced COX enzyme activity and reduced mtDNA level in pigs with hypertrophic cardiomyopathy.

Cardiac hypertrophy found in SHR and SPSHR, other models of genetic hypertension, showed an apparent reduction of COX protein level even at ages as young as 4 weeks old. Interestingly, Tokoro et al. demonstrated a decreased antioxidant ability due to lower cardiac superoxide dismuatse (SOD) activity in SPSHR [23]. In addition, due to the lack of protection by histone, several mtDNA encoded subunits of COX genes are particularly susceptible to oxidative damage, leading to mutation occurrence [24]. Therefore, the electrophoretic band of deleted mtDNA analyzed by restriction fragment length polymorphisms (RFLP) was found in myocardiums of SPSHR [23]. These observations provide an explanation for the reduction of COX protein levels in SHR and SPSHR. Although Wanagat's study [25] demonstrated that the abnormal activity of COX was age-associated, we observed a reduction of COX protein occurring at very young age in genetically hypertensive rats. We believe genetic defects resulting in COX dysfunction at young age in SHR and SPSHR cannot be ruled out. The average life span of hypertensive rats, SHR and SPSHR, is around 8 months to one and half years, which is shorter than that of the normal rats that have an average life span of 2.5 years, and the cardiac COX protein in SHR and SPSHR was down-regulated early. Thus, the failure to have an increase of COX to balance the cardiac hypertrophy may result in heart failure and lead to a shorter life span in these genetic hypertensive rats. This is similar to the decrease in COX protein levels seen at 20 days postsurgery of complete-coarcted rats.

In summary, the rapid cardiac hypertrophy induced by complete coarctation of the abdominal aorta in rats is accompanied by a disproportionate increase in mitochondrial energy-producing activity, a result shown here for the first time. Additionally, insufficient oxidative capacity contributes to the cardiac failure frequently observed in hypertrophic cardiomyopathies induced by a variety of conditions [19]. In our study, the dysfunction of cardiac COX in SHR, SPSHR and completely coarcted rats long term (20 days) after surgery suggests that COX might be the key factor for the cardiac oxidative ability during cardiac hypertrophy. The rapid cardiac hypertrophy that develops in the present model provides a unique system to study the molecular basis underlying the adaptation of the oxidative system in cells in response to the demands of hypertrophic growth. Future work will attempt to identify the mechanism of the increment of COX, using the same complete coarctation model we used in this study.

Acknowledgements

We thank the National Science Council (grant NSC 89-2320-B-053) of Taiwan, ROC for financial support. This work could not be finished without generous gifts of COX-Vb plasmid and the guidance from Dennis E. Buetow and the help from Sam N. Pate at University of Illinois, USA.

References

1. Morgan H.E. and Baker K.M., Cardiac hypertrophy. Mechanical, neural, and endocrine dependence. Circulation 83: 13–25, 1991.
2. Nishio M.L., Ornatsky O.I., Craig E.E. and Hood D.A., Mitochondrial biogenesis during pressure overload induced cardiac hypertrophy in adult rats. Can. J. Physiol. Pharmacol. 73: 630–637, 1995.
3. Stanley W.C. and Hoppel C.L., Mitochondrial dysfunction in heart failure: potential for therapeutic interventions? Cardiovasc. Res. 45: 805–806, 2000.
4. Jarreta D., Orus J., Barrientos A., Miro O., Roig E., Heras M., Moraes C.T., Cardellach F. and Casademont J., Mitochondrial function in heart muscle from patients with idiopathic dilated cardiomyopathy. Cardiovasc. Res. 45: 860–865, 2000.
5. Tanji K. and Bonilla E., Neuropathologic aspects of cytochrome *C* oxidase deficiency. Brain Pathol. 10: 422–430, 2000.
6. Richter O.M. and Ludwig B., Cytochrome *c* oxidase – structure, function, and physiology of a redox-driven molecular machine. Rev. Physiol. Biochem. Pharmacol. 147: 47–74, 2003.
7. Kunz W.S., Kudin A., Vielhaber S., Elger C.E., Attardi G. and Villani G., Flux control of cytochrome *c* oxidase in human skeletal muscle. J. Biol. Chem. 275: 27741–27745, 2000.
8. Leary S.C., Michaud D., Lyons C.N., Hale T.M., Bushfield T.L, Adams M.A. and Moyes C.D., Bioenergetic remodeling of heart during treatment of spontaneously hypertensive rats with enalapril. Am. J. Physiol. Heart Circ. Physiol. 283: H540–H548, 2002.
9. Ruppert V., Nolte D., Aschenbrenner T., Pankuweit S., Funck R. and Maisch B., Novel point mutations in the mitochondrial DNA detected in patients with dilated cardiomyopathy by screening the whole mitochondrial genome. Biochem. Biophys. Res. Commun. 318: 535–543, 2004.
10. Moslemi A.R., Selimovic N., Bergh C.H. and Oldfors A., Fatal dilated cardiomyopathy associated with a mitochondrial DNA deletion. Cardiology 94: 68–71, 2000.
11. Minieri M., Zingarelli M., Shubeita H., Vecchini A., Binaglia L., Carotenuto F., Fantini C., Fiaccavento R., Masuelli L., Coletti A., Simonelli L., Modesti A. and Di Nardo P., Identification of a new missense mutation in the mtDNA of hereditary hypertrophic, but not dilated cardiomyopathic hamsters. Mol. Cell. Biochem. 252: 73–81, 2003.
12. Wiesner R.J., Aschenbrenner V., Ruegg J.C. and Zak R., Coordination of nuclear and mitochondrial gene expression during the development of cardiac hypertrophy in rats. Am. J. Physiol. 267: C229–C235, 1994.
13. Huang C.Y., Buchanan D.L., Gordon R.L. Jr., Sherman M.J., Razzaq J., White K. and Buetow D.E., Increased insulin-like growth factor-I gene expression precedes left ventricular cardiomyocyte hypertrophy in a rapidly-hypertrophying rat model system. Cell. Biochem. Funct. 21: 355–361, 2003.
14. White C.R. and Zehr J.E., Spontaneous rhythmic contractile behaviour of aortic ring segments isolated from pressure loaded regions of the vasculature. Cardiovasc. Res. 24: 953–958, 1990.
15. Bjorntorp P., Effects of physical training on blood pressure in hypertension. Eur. Heart J. 8(Suppl B) 71–76, 1987.
16. Bradford M.M., A rapid and sensitive method for the quantitation of microgram quantities of protein utilizing the principle of protein–dye binding. Anal Biochem 72: 248–254, 1976.
17. Storrie B. and Madden E.A., Isolation of subcellular organelles. Meth. Enzymol. 182: 203–225, 1990.
18. Smith L., Spectrophotometric assay of cytochrom c oxidase. Meth. Biochem. Anal. 2: 427–434, 1995.
19. Darley-Usmar V.M., Kennaway N.G., Buist N.R. and Capaldi R.A., Deficiency in ubiquinone cytochrome *c* reductase in a patient with mitochondrial myopathy and lactic acidosis. Proc. Natl. Acad. Sci. USA 80: 5103–5106, 1983.
20. Huang C.Y., Kasai M. and Buetow D.E., Extremely-rapid RNA detection in dot blots with digoxigenin-labeled RNA probes. Genet. Anal. 14: 109–112, 1998.
21. Legato M.J., Mulieri L.A. and Alpert N.R., The ultrastructure of myocardial hypertrophy: why does the compensated heart fail? Eur. Heart J. 5 (Suppl F) 251–269, 1984.
22. Lin C.S., Sun Y.L. and Liu C.Y., Structural and biochemical evidence of mitochondrial depletion in pigs with hypertrophic cardiomyopathy. Res. Vet. Sci. 74: 219–226, 2003.
23. Tokoro T., Ito H. and Suzuki T., Alterations in mitochondrial DNA and enzyme activities in hypertrophied myocardium of stroke-prone SHRS. Clin. Exp. Hypertens. 18: 595–606, 1996.
24. Hanna M.G., Nelson I.P., Rahman S., Lane R.J., Land J., Heales S., Cooper M.J., Schapira A.H., Morgan-Hughes J.A. and Wood N.W., Cytochrome c oxidase deficiency associated with the first stop-codon point mutation in human mtDNA. Am. J. Hum. Genet. 63: 29–36, 1998.
25. Wanagat J., Wolff M.R. and Aiken J.M., Age-associated changes in function, structure and mitochondrial genetic and enzymatic abnormalities in the Fischer 344×Brown Norway F(1) hybrid rat heart. J. Mol. Cell. Cardiol. 34: 17–28, 2002.

Journal : JBMS | Dispatch : 8-6-2005 | Pages : 10
CMS No. : DO00017373 | ☐ LE | ☐ TYPESET
MS Code : JBMS 59R1 | ☑ CP | ☑ DISK

CELL BIOCHEMISTRY AND FUNCTION
Cell Biochem Funct (in press).
Published online in Wiley InterScience (www.interscience.wiley.com). **DOI**: 10.1027/cbf.1244

Impaired IGF-I signalling of hypertrophic hearts in the developmental phase of hypertension in genetically hypertensive rats

Wei-Wen Kuo[1,9], Chia-Yih Chu[2], Chieh-Hsi Wu[9], James A. Lin[6], Jer-Yuh Liu[1], Yi-Hsien Hsieh[1], Kwo-Chang Ueng[3], Shin-Da Lee[4], Dennis Jine-Yuan Hsieh[5], His-Hsien Hsu[7], Li-Mien Chen[8] and Chih-Yang Huang[1]*

[1]*Institute of Biochemistry, Chung-Shan Medical University, Taichung, Taiwan*
[2]*School of Applied Chemistry, Chung-Shan Medical University, Taichung, Taiwan*
[3]*Department of Internal Medicine, Chung-Shan Medical University, Taichung, Taiwan*
[4]*Department of Physical Therapy, Chung-Shan Medical University, Taichung, Taiwan*
[5]*Department of Medical Technology, Chung-Shan Medical University, Taichung, Taiwan*
[6]*Department of Veterinary Medicine, National Chung-Hsing University, Taichung, Taiwan*
[7]*Division of Colorectal Surgery, Mackay Memorial Hospital, Taipei, Taiwan*
[8]*Armed Forces Taichung General Hospital, Taichung, Taiwan*
[9]*Department of Biological Science and Technology, China Medical University, Taichung, Taiwan*

Insulin-like growth factor-I (IGF-I) signalling is reported to contribute to the modulation of blood pressure and set survival and hypertrophic responses in cardiac tissue. However, whether IGF-I signalling normally acts in cardiac tissues of hypertensive rats is unknown. In this study, using spontaneously hypertensive rats (SHR) and stroke-prone spontaneously hypertensive rats (SPSHR), both with early blood pressure increases, and Wistar–Kyoto (WKY) rats as controls, we measured the hypertrophic and IGF-I signalling activity changes in rat hearts at 4, 6 and 12 weeks of age. Both SHR and SPSHR were found to have significantly increased blood pressures and ratios of heart- and left ventricle- to body weight at 12 weeks of age. However, IGF-IR and its downstream signalling, including the protein levels of PI3K and phosphorylated Akt, known to maintain physiological cardiac hypertrophy and cardiomyocyte survival, were downregulated. The results of dot blotting showed that cardiac mRNA levels of IGF-I in hypertensive rats were higher than those in controls starting from the age of 4 weeks. This difference suggests the increased ligand IGF-I mRNA levels may be a compensatory response caused by the impaired IGF-I signalling. Moreover, enhanced cardiac cytosolic cytochrome-*c*, a mitochondria-dependent apoptotic pathway component, tended to occur in both hypertensive rats, although it did not reach a significant level. These findings indicate that impaired IGF-IR signalling occurs at early stages, and it may contribute, at least partially, to the development of hypertension and pathological cardiac hypertrophy and to cardiomyocyte apoptosis at later stages in SHR and SPSHR.

KEY WORDS — insulin-like growth factor-1 signalling pathway; cardiac hypertrophy; hypertension; SHR and SPSHR

INTRODUCTION

Hypertension commonly contributes to heart diseases, such as left ventricular hypertrophy and heart failure. Particularly, ventricular hypertrophy is present in 20–50%, and up to 90% of patients with mild to moderate and with severe hypertension, respectively.[1] Animal models have been used in hypertension investigations since the early 1960s. In some of these studies, spontaneously hypertensive rats (SHR) were used to represent a model of human essential hypertension. Stroke-prone SHR (SPSHR), developed by selectively breeding SHR loaded with 1% salt in drinking water,[2] have been reported to have a more rapid increase in blood pressure and more severe cerebrovascular lesions. The

* Correspondence to: Chih-Yang Huang, Institute of Biochemistry, Chung-Shan Medical University No. 110, Section 1, Chien Kuo N. Rd., Taichung 402, Taiwan, R.O.C. Tel: 886-4-24730022 ext 11682. E-mail: chuang1@csmu.edu.tw

Received 6 December 2004
Revised 15 February 2005
Accepted 10 March 2005

average life-spans of these two genetically hypertensive animals are 1.5 years and 8 months, respectively,[2] which is much shorter than the 2.5 years reported for healthy controls. One of the pathological symptoms resulting in the short life-span of the hypertensive animals is cardiac hypertrophy which has been identified as the leading cause of sudden death. However, whether an alteration in signal transduction, contributing to irreversible damage by diminishing cardiomyocytes and organ functions, is involved in the pathogenesis of pathological hypertrophy remains unknown.

The induction of IGF-I has been associated with an increase in cellular mass in cardiac hypertrophic growth. In one of our previous studies of primary cardiac cells we found that IGF-I treatment may cause physiological hypertrophy.[3–5] Another *in vivo* experiment showed that an increase in cardiac-synthesized IGF-I of rats with pressure-overloaded constriction preceded left ventricular cardiomyocyte hypertrophy.[6] Thus far, several signal transduction pathways have been identified in cardiac hypertrophy in response to IGF-I. Through IGF-IR, IGF-I activates the PI3K-Akt/PKB pathway, which primarily maintains normal size and survival of cardiac myoctes, contributing to physiological cardiac hypertrophy.[7–9] In addition, MEK-ERK, which is one of the MAPK signalling cascades which acts downstream of IGF-I signalling, activates several hypertrophic genes through IRS-1 to modulate non-cardiomyocyte hyperplasia.[10,11] Therefore, IGF-IR signalling could possibly exert survival and hypertrophic effects on cardiac tissue in hypertensive rats. However, a previous study demonstrated that a mouse model with a mutant that has an IGF-I level that is only 30% of wild-type showed elevated blood pressure.[12] Vecchione and his colleagues[13] further identified that IGF-I vasorelaxant properties were impaired in SHR at the age of 5 and 12 to 14 weeks, suggesting that an IGF-I dysfunction could be involved in the development of genetic hypertension. However, because of the terminated differentiation of the cardiomyocytes, IGF-I action is especially important for the survival of these cells. Whether the dysfunction in IGF-I signalling similarly affects cardiac tissue is not known. Furthermore, since hypertension starts at a very young age in genetic hypertensive rats, it is not clear whether the special action of IGF-I signalling on cardiac tissue causes the development or plays a compensatory role in the development of hypertension. To understand whether changes in IGF-I signalling is involved in the cardiac transition from physiological to pathological hypertrophy during the development phase of hypertension in SHR and SPSHR, this study measured the hypertrophic and IGF-I signalling activity changes in the hearts of SHR and SPSHR, both with early blood pressure increases, and Wistar–Kyoto (WKY) rats as controls, at 4, 6 and 12 weeks of age.

MATERIALS AND METHODS

Animals

SHR and WKY rats were purchased from the National Laboratory Animal Breeding and Research Center, Taipei, Taiwan. SPSHR were generously provided by Dr Dennis E. Buetow, originating from the NIH colony. These animals, whose ages were 3, 5 and 11 weeks, were kept in a temperature-controlled environment ($24 \pm 1^{\circ}C$) illuminated for 12 h daily (05.00–17.00 hours), and were fed with commercial pellets and water *ad libitum*. All animals were handled according to the guidelines of the Taiwan Society for Laboratory Animal Sciences for the Care and Use of Laboratory Animals.

Tail pressure measurement

One week after the rats had been brought to the laboratory, tail blood pressure was measured with a sphygmomanometer (29SSP, IITC Inc./Life Science Instruments, USA), which consisted of a main board machine and a pump machine. Each rat was placed on the table and its tail was placed in the sensor area to measure blood pressure. A movement of the pointer indicated maximum blood pressure. If the rat moved during the measurement, the result was considered invalid. Blood pressure was measured five times and the five values were averaged.

Measurement of cardiac hypertrophy

The rats were weighed before they were sacrificed by decapitation. After the heart was removed, it was cleaned with double distilled H_2O and dried and weighed. Then, the left ventricle was removed and weighed. The ratio of total heart weight and left ventricle weight to the body weight was calculated.

Tissue extraction

The left ventricle was cut into three parts. One part of the left ventricle was minced with scissors, added to lysis buffer (50 mM Tris (pH 7.5), 0.5 M NaCl, 1.0 mM EDTA (pH 7.5), 10% glycerol, 1 mM BME, 1% IGEPAL-630 and proteinase inhibitor cocktail

tablet (Roche)) at a concentration of 1 mg tissue ($10\,\mu l^{-1}$) buffer and homogenized at ice temperature with a Model PT l0/35 Polytron homogenizer for 2 cycles of l0 s each. The homogenates were placed on ice for 10 min and then centrifuged at 12 000 r.p.m. for 30 min. The supernatant was collected and stored at $-70°C$ for further Western blot analysis.

Isolation of heart mitochondria

After adding PBS to another one-third of the left ventricular tissues, the tissues were minced with scissors and homogenized at 4°C with a Model PT l0/35 Polytron homogenizer (setting 11, Brinkmann lnstruments, Westburg, NY, USA) for 5 min before centrifuging at 2300 r.p.m. for 10 min in a Beckman J20.l centrifuge. The pellet was discarded, and the supernatant was then centrifuged at 9400 r.p.m. for 15 min. The mitochondrial pellet was resuspended in 200 µl PBS for Western blot analysis of cytochrome *c*. All steps were carried out at 0–4°C.

Protein contents

The protein content of the left ventricle extract and mitochondrial fraction were determined using the Bradford protein assay[14] using the protein-dye kit (Bio-Rad, Richmond, CA, USA). A commercially available bovine serum albumin (Sigma Chemical, St. Louis, MO, USA) was used as a standard. Changes in absorption were monitored at 595 nm.

Electrophoresis and Western blotting

The left ventricle extract and mitochondrial fraction samples were prepared as described above. Sodium dodecyl sulphate–polyacrylamide gel electrophoresis was carried out using 10% polyacrylamide gels. Equal amounts (20 µg) of the samples were electrophoresed at 140 V for 3.5 h and equilibrated for 15 min in transfer buffer (25 mM Tris-HCl, pH 8.3, containing 192 mM glycine and 20% (v/v) methanol). Then, the electrophoresed proteins were transferred to nitrocellulose paper (Amersham, Hybond-C Extra Supported, 0.45 Micro) using a Hoefer Scientific Instruments Transphor Unit at 100 mA with transfer buffer for 14 h. Nitrocellulose papers were incubated at room temperature for 2 h in blocking buffer containing 100 mM Tris-HCl, pH 7.5, 0.9% (w/v) NaCl, 0.1% (v/v) fetal bovine serum. Monoclonal antibodies of IGF-IR, PI3K, Akt, phosphorylated Akt and cytochrome-*c* (Santa Cruz Biotechnology) were diluted in antibody-binding buffer containing 100 mM Tris-HCl, pH 7.5, 0.9% (w/v) NaCl, 0.1% (v/v) Tween-20 and 1% (v/v) fetal bovine serum. Incubations were performed at room temperature for 3.5 h. The immunoblots were washed three times in 50 ml blotting buffer for 10 min and then immersed in the second antibody solution containing alkaline phosphatase-labelled goat anti-rabbit IgG (Promega) for 1 h and diluted 1000-fold in binding buffer. The filters were then washed three times in blotting buffer for 10 min each time. The colour was developed in a 20-ml mixture consisting of 7 mg nitro blue tetrazolium, 5 mg 5-bromo-4-chloro-3-indolyl-phosphate, 100 mM NaCl and 5 mM $MgCl_2$ in 100 mM Tris-HCl, pH 9.5. The immunoblot with antibody against β-actin, which was prepared with the same procedure, was used as an internal control.

RNA extraction

Total RNA was extracted using the Ultraspec RNA Isolation System (Biotecx Laboratories, Inc.) according to the manufacturer's instructions. The remaining one-third of the left ventricle was thoroughly homogenized in 1 ml Ultraspec reagent per 100 mg tissue using a Polytron homogenizer. The homogenates were washed twice with 70% ethanol by gentle vortexing. RNA precipitates were then collected by centrifugation at 12 000 *g* and dried under vacuum for 5–10 min before being dissolved in 50 µl diethylpyrocarbonate-treated water, and then incubated at 55–60°C for 10–15 min.

RNA dot blotting

RNA dot blotting was used for the hybridization and detection of IGF-I mRNAs according to the method described in our previous study.[15] The corresponding digoxigenin (DIG)-labelled antisense RNA probes were prepared from pGEM-1 containing a *Bam*H1-*Eco*R1 956-bp insert consisting of exon 3 and flanking intron sequences from the rat IGF-I gene (supplied by Dr Dennis E. Buetow, University of Illinois, Urbana-Champaign, IL, USA).

Statistical analysis

The data were compared between animal groups of the same age, using one-way analysis of variance (ANOVA). Fisher's Least Significant Difference test was used to determine differences. $P < 0.05$ was considered statistically significant.

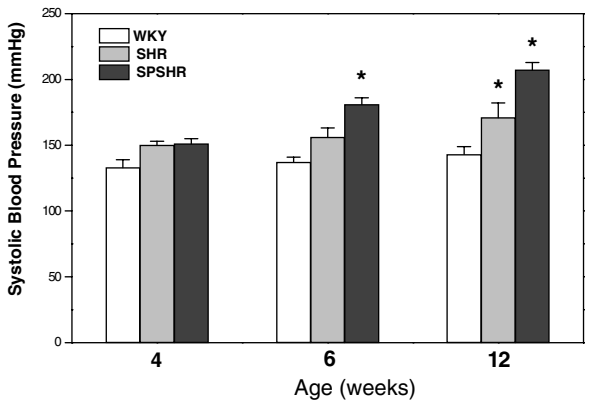

Figure 1. Systolic blood pressure of WKY rats (white), SHR (light grey) and SPSHR (dark grey) at 4, 6 and 12 weeks of age. Values are expressed as mean ± SE ($n = 8$). Significant differences from the control (WKY) were determined using the Fisher PLSD test: *$P < 0.05$

RESULTS

Development of hypertension and cardiac hypertrophy in SHR and SPSHR

Figure 1 shows an increase in systolic blood pressure in hypertensive rats over the 12-week period, indicating the progress of hypertension. Compared with controls, the SPSHR and SHR groups were found to experience significant systolic blood pressure increases starting at 6 and 12 weeks of age, respectively. Table 1 shows the development of cardiac hypertrophy over the entire period. The ratio of whole heart weight to body weight for SHR and SPSHR was not significantly different from controls until 12 weeks of age, at which time the ratio significantly increased from $2.83 \pm 0.07\,\mathrm{mg\,g^{-1}}$ in the controls to around $3.4\,\mathrm{mg\,g^{-1}}$ for the SHR or SPSHR. Similarly, compared with the controls, the left ventricular weight to body weight ratios for the SHR and SPSHR increased significantly only at 12 weeks of age.

Protein levels of IGF-IR, IGF-IR signalling components and cytochrome-c in the left ventricle of the heart using Western blotting

The left ventricle IGF-IR levels for the animals at 4, 6 and 12 weeks of age were analysed using Western blotting (Figure 2). Downregulation of IGF-IR was found in the left ventricle of SHR starting at week 6. Greater decreases were found in the SPSHR group throughout the whole period. The results for PI3K and phosphorylated Akt for IGF-I signalling were similar. Changes in cardiac PI3K levels were more significant in both hypertensive rat groups at each age (Figure 3A). A significant reduction of cardiac phosphorylated Akt only appeared in SPSHR at the age of 6 and 12 weeks (Figure 3B). The cytochrome-*c* released from the mitochondria leading to a mitochondria-dependent apoptotic pathway was also examined (Figure 3C). Although the increases became more apparent in hypertensive rats as they got older, none of the increases reached statistical significance.

Gene expression of IGF-I by dot blotting in the left ventricle of hearts

The dot blot analysis of cardiac tissue taken at ages 4, 6 and 12 weeks showed changes in IGF-I mRNA levels. While SHR IGF-I mRNA levels were found to have increased significantly each time they were measured, the levels in SPSHR were not found to have increased significantly (Figure 4).

DISCUSSION

Pathological cardiac hypertrophy is the leading cause of sudden death by heart failure, but little is understood about the molecular mechanisms behind this disease. In this study, we measured blood pressure and calculated the ratio of whole heart weight and left ventricle weight to body weight in SHR and SPSHR rats and compared the findings with a control group made up Wistar–Kyoto (WKY) rats. The hypertensive rats were

Table 1. The ratio of whole heart or left ventricle weight to the total body weight of rats

Age (weeks)	WKY	SHR	SPSHR	WKY	SHR	SPSHR
	(Whole heart per BW; $\mathrm{mg\,g^{-1}}$)			(LT ventricle per BW; $\mathrm{mg\,g^{-1}}$)		
4	4.17 ± 0.13	4.11 ± 0.19	4.15 ± 0.09	3.18 ± 0.12	3.38 ± 0.17	3.63 ± 0.08
6	3.34 ± 0.07	3.51 ± 0.13	3.53 ± 0.07	2.67 ± 0.04	2.81 ± 0.11	2.85 ± 0.07
12	2.83 ± 0.07	3.45 ± 0.06*	3.44 ± 0.04*	2.25 ± 0.06	2.86 ± 0.06*	2.86 ± 0.04*

BW, body weight; LT, left; WKY, Wistar–Kyoto rats as a control; SHR, spontaneously hypertensive rats; SPSHR, stroke-prone spontaneously hypertensive rats. All values are expressed as mean ± SE ($n = 8$).
* Significant differences from the control (WKY) were determined by the Fisher PLSD test, $P < 0.05$.

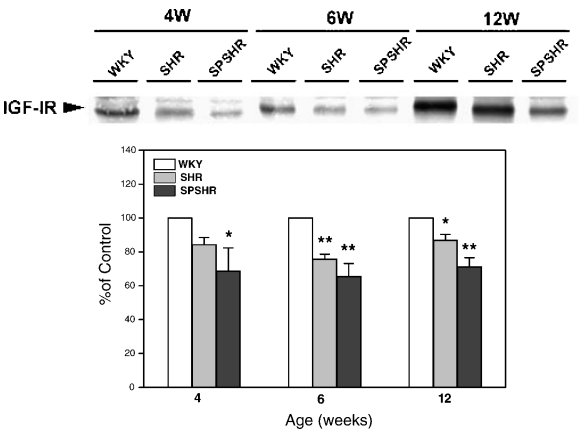

Figure 2. IGF-IR level in the left ventricle of rats at different ages as determined by Western blotting. Lysates were prepared from hearts of WKY rats (white), SHR (light grey) and SPSHR (dark grey), and equal amounts of protein (20 μg) were separated by SDS/PAGE and immunoblotting with anti-IGF-IR antibody. The blotting bands are shown at the top of the graph. Signal intensity was quantified using a phosphoImager. The average percentage ± SE for three independent experiments is related to the control (WKY) animals in each age group. Significant differences were determined using the Fisher PLSD test from the control (WKY): $*P < 0.05$; $**P < 0.01$

found to have significant increases in blood pressure by the time they were 12 weeks old. However, the cardiomyocytes of the SHR and SPSHR groups were found to have significantly lower IGF-IR and downstream PI3K protein levels. The SHR group was found to have an increased level of IGF-I mRNA starting at 4 weeks of age. We suggest that the downregulation of IGF-IR may be a result of a higher degradation rate, shorter half-life or such defects as post-translational modification at an early age. We also suggest that the increased IGF-I mRNA levels are a compensatory response to impaired IGF-I signalling.

Cardiomyocyte apoptosis has been associated with heart failure[16,17] and modulating it may be critical to the treatment of this disease. Without the presence of growth factors, Bcl_2 expression is reduced, DNA fragmentation is increased and caspase 3 activations occur. Conversely, IGF-I treatment reverses these alterations to normal levels, showing that IGF-I has an anti-apoptotic effect important to the survival of cardiomyocytes.[18] IGF-I has also been reported to be able to increase Bcl_2 promoter activity 2.3-fold in PC12 cells.[19] Clinically, IGF-I is used in the treatment of acute heart failure.[20] Moreover, cardiomyocytes are also protected by the anti-apoptotic effects of PI3K, downstream of IGF-I signalling.[9,21] Activated PI3K has been found to improve cardiac function during ischemia–reperfusion[22] by phosphorylating the pro-apoptotic regulator Bad and inactivating caspase 9.[23] Another study found that mice with cardiac-specific expression of dominant-negative PI3K had smaller hearts, indicating that P13K helps maintain normal heart size.[9] In our study, the downregulation of IGF-IR signalling may have resulted in cardiomyocyte

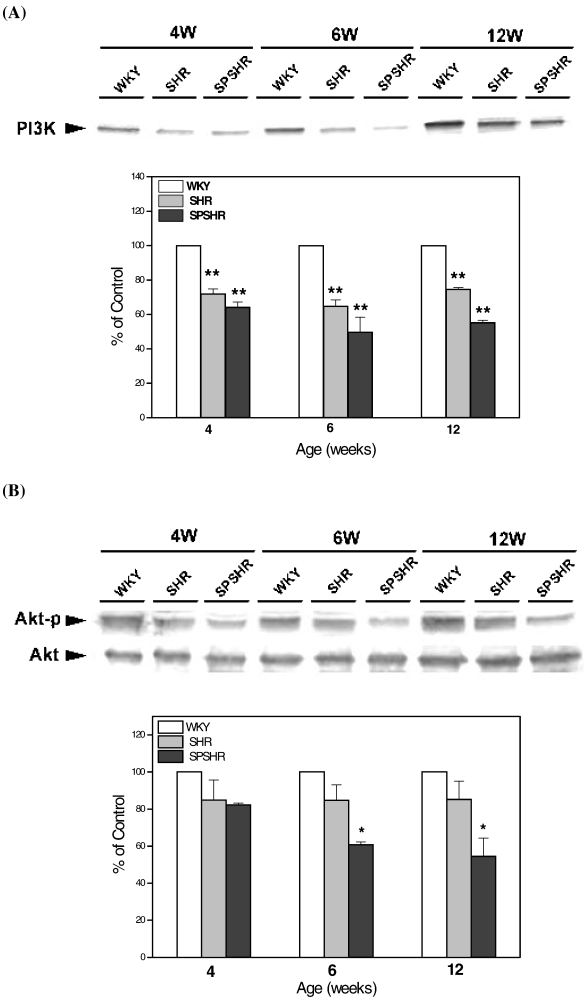

Figure 3. The alteration of IGF-IR signalling downstream components and cytochrome-*c* levels in the left ventricle of rats at different ages. Lysates were prepared from the hearts of WKY rats (white), SHR (light grey) and SPSHR (dark grey), and equal amounts of protein were separated by SDS/PAGE and immunoblotting with (A) anti-PI3K antibody, (B) anti phosphorylated Akt and Akt antibody, (C) anti-cytochrome-*c* antibody. The blotting bands are shown at the top of each graph. Signal intensity was quantified using a phosphoImager. The average percentage ± SE for three independent experiments is related to the control (WKY) animals in each group. Significant differences were determined using the Fisher PLSD test from the control (WKY): $*P < 0.05$; $**P < 0.01$

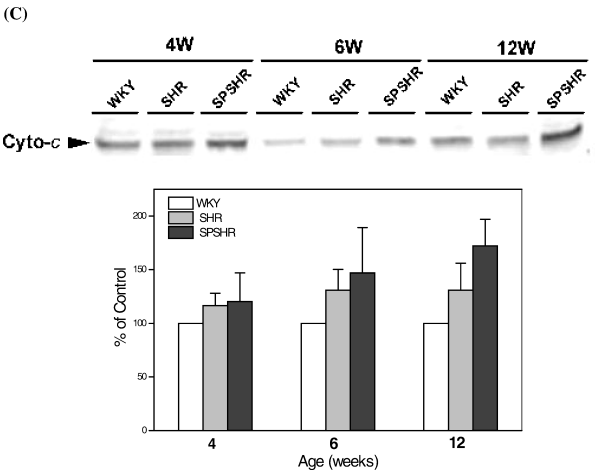

Figure 3. Continued

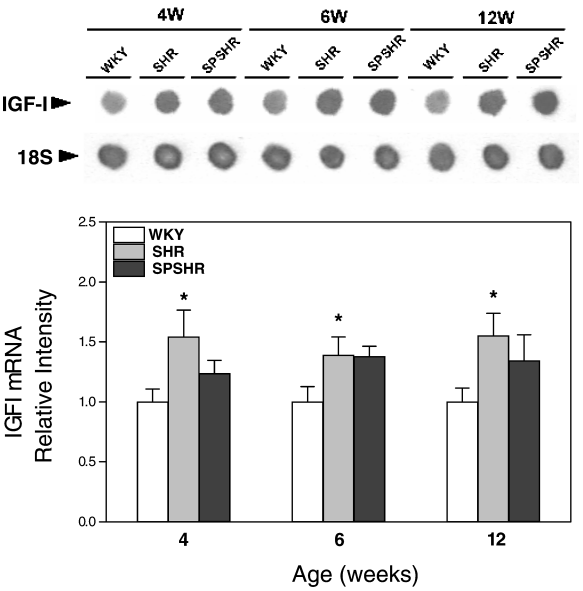

Figure 4. mRNA in the left ventricle of rats as determined by dot-blotting. Detection of mRNA was achieved with CDP-Star and the film was exposed for 10–30 s to determine the linear range of detection for these mRNAs. Total RNA was spotted at 240 ng per dot. 18S-rRNA was measured as a loading control (top of graph). Quantification of the degree of activation for the SHR (light grey) and SPSHR (dark grey) versus WKY (white) group is shown on the graph. Values are expressed as mean ± SE ($n = 8$). Significant differences from the control (WKY) were determined using the Fisher PLSD test: $^*P < 0.05$

apoptosis in SHR and SPSHR. However, possibly because the mice were young, we did not observe a significant increase in cytosolic cytochrome-*c*. Perhaps if the SHR and SPSHR had been older with more impaired IGF-I signalling, cardiomyocyte apoptosis would have been more severe. Heart failure due to apoptosis in these two strains of rats brings about their early death. The downregulation of IGF-I signalling in SHR is evidenced by a decrease in IGF-IR, PI3K and the other downstream molecule, phosphorylated Akt levels. These levels were likely further suppressed in SPSHR, which showed more rapid increases in blood pressure and more severe cardiovascular lesions.

Cardiac hypertrophy in young SHR and SPSHR may be regulated by signalling pathways other than IGF-I signalling. For example, several important studies[24–26] have demonstrated that calcium-activated calcineurin promoted the dephosphorylation of NFAT3 which then translocated into the nucleus and promoted gene expression involved in pathological cardiac hypertrophy. The activation of calcineurin signalling has also been found to promote the release of cytochrome-*c* from mitochondria, which, in turn, promotes apoptosis,[27] possibly indicating that the activation of calcineurin may lead to cardiac hypertrophy and apoptosis. However, Olson and his colleagues[28,29] found that rats treated with a calcineurin inhibitor did not experience a change in cardiac hypertrophy. Cardiac ERK signalling, the other arm of the IGF-I pathway, has also been examined in SHR and SPSHR in other studies,[30–32] demonstrating that phosphorylated ERK was reduced from the age of 5 weeks. However, our study showed that hypertrophy occurred at age 12 weeks for the two rat strains, indicating that ERK was unlikely to be involved in the hypertrophic processes. Thus, the factors causing cardiac hypertrophy in SHR and SPSHR need to be identified through further studies.

The goal of this experiment was to investigate the molecular mechanisms behind the pathogenesis of cardiac disorder in hypertensive rats during the developmental phase of hypertension. Our results showed that SHR and SPSHR experienced an increase in blood pressure and cardiac hypertrophy at the ages of 6 and 12 weeks and the early development (4 weeks old or younger) of downregulation of IGF-IR signalling. In another study, mice with severe IGF-I deficiency were found to have elevated blood pressure.[12] IGF-IR signalling deficiency is, therefore, thought to precede hypertension and cardiac disorder in SHR and SPSHR. This finding and conclusion are consistent with our interpretation that impaired cardiac IGF-I signalling initiates hypertension.

Controlling the anti-apoptotic effects of cardiac IGF-I signalling may help alleviate hypertensive cardiac disorder in its early developmental stages. These findings may provide a theoretical basis for the development of therapy for patients with hypertensive heart failure.

ACKNOWLEDGEMENTS

We are grateful to Dr Dennis E. Buetow for generously providing SPSHR.

This work was supported by a grant from the National Science Council of Taiwan, contract grant number: NSC 89-2320-B-040-053.

REFERENCES

1. Gerdts E, Omvik P, Mo R, Kjeldsen SE. Hypertension and heart disease. *Tidsskr Nor Laegeforen* 2004; **124**: 802–805.
2. Yamori Y, Horie R, Handa H, Sato M, Okamoto K. Proceedings: studies on stroke in stroke-prone spontaneously hypertensive rats (SHRSP). (I). Local factor analysis on stroke. *Jpn Heart J* 1975; **16**: 329–331.
3. Huang CY, Hao LY, Buetow DE. Insulin-like growth factor-induced hypertrophy of cultured adult rat cardiomyocytes is L-type calcium-channel-dependent. *Mol Cell Biochem* 2002; **231**: 51–59.
4. Huang CY, Hao LY, Buetow DE. Hypertrophy of cultured adult rat ventricular cardiomyocytes induced by antibodies against the insulin-like growth factor (IGF)-I or the IGF-I receptor is IGF-II-dependent. *Mol Cell Biochem* 2002; **233**: 65–72.
5. Park GH, Buetow DE. Genes for insulin-like growth factors I and II are expressed in senescent rat tissues. *Gerontology* 1991; **37**: 310–316.
6. Huang CY, Buchanan DL, Gordon RL Jr, *et al.* Increased insulin-like growth factor-I gene expression precedes left ventricular cardiomyocyte hypertrophy in a rapidly-hypertrophying rat model system. *Cell Biochem Funct* 2003; **21**: 355–361.
7. Molloy CA, May FE, Westley BR. Insulin receptor substrate-1 expression is regulated by estrogen in the MCF-7 human breast cancer cell line. *J Biol Chem* 2000; **275**: 12565–12571.
8. Crackower MA, Oudit GY, Kozieradzki I, *et al.* Regulation of myocardial contractility and cell size by distinct PI3K-PTEN signaling pathways. *Cell* 2002; **110**: 737–749.
9. Shioi T, Kang PM, Douglas PS, *et al.* The conserved phosphoinositide 3-kinase pathway determines heart size in mice. *EMBO J* 2000; **19**: 2537–2548.
10. Kuemmerle JF, Bushman TL. IGF-I stimulates intestinal muscle cell growth by activating distinct PI 3-kinase and MAP kinase pathways. *Am J Physiol* 1998; **275**: G151–G158.
11. Parrizas M, Saltiel AR, LeRoith D. Insulin-like growth factor 1 inhibits apoptosis using the phosphatidylinositol 3′-kinase and mitogen-activated protein kinase pathways. *J Biol Chem* 1997; **272**: 154–161.
12. Lembo G, Rockman HA, Hunter JJ, *et al.* Elevated blood pressure and enhanced myocardial contractility in mice with severe IGF-1 deficiency. *J Clin Invest* 1996; **98**: 2648–2655.
13. Vecchione C, Colella S, Fratta L, *et al.* Impaired insulin-like growth factor I vasorelaxant effects in hypertension. *Hypertension* 2001; **37**: 1480–1485.
14. Bradford MM. A rapid and sensitive method for the quantitation of microgram quantities of protein utilizing the principle of protein-dye binding. *Anal Biochem* 1976; **72**: 248–254.
15. Huang CY, Kasai M, Buetow DE. Extremely-rapid RNA detection in dot blots with digoxigenin-labeled RNA probes. *Genet Anal* 1998; **14**: 109–112.
16. Frey N, Olson EN. Cardiac hypertrophy: the good, the bad, and the ugly. *Annu Rev Physiol* 2003; **65**: 45–79.
17. Haunstetter A, Izumo S. Apoptosis: basic mechanisms and implications for cardiovascular disease. *Circ Res* 1998; **82**: 1111–1129.
18. Wang L, Ma W, Markovich R, Chen JW, Wang PH. Regulation of cardiomyocyte apoptotic signaling by insulin-like growth factor I. *Circ Res* 1998; **83**: 516–522.
19. Pugazhenthi S, Miller E, Sable C, *et al.* Insulin-like growth factor-I induces bcl-2 promoter through the transcription factor cAMP-response element-binding protein. *J Biol Chem* 1999; **274**: 27529–27535.
20. Demers C, McKelvie RS. Growth hormone therapy in heart failure: where are we now? *Congest Heart Fail* 2003; **9**: 84–90.
21. Wu W, Lee WL, Wu YY, *et al.* Expression of constitutively active phosphatidylinositol 3-kinase inhibits activation of caspase 3 and apoptosis of cardiac muscle cells. *J Biol Chem* 2000; **275**: 40113–40119.
22. Matsui T, Tao J, del Monte F, *et al.* Akt activation preserves cardiac function and prevents injury after transient cardiac ischemia *in vivo*. *Circulation* 2001; **104**: 330–335.
23. Cardone MH, Roy N, Stennicke HR, *et al.* Regulation of cell death protease caspase-9 by phosphorylation. *Science* 1998; **282**: 1318–1321.
24. McKinsey TA, Olson EN. Cardiac hypertrophy: sorting out the circuitry. *Curr Opin Genet Dev* 1999; **9**: 267–274.
25. Molkentin JD, Lu JR, Antos CL, *et al.* A calcineurin-dependent transcriptional pathway for cardiac hypertrophy. *Cell* 1998; **93**: 215–228.
26. Mizukami Y, Kobayashi S, Uberall F, Hellbert K, Kobayashi N, Yoshida K. Nuclear mitogen-activated protein kinase activation by protein kinase c zeta during reoxygenation after ischemic hypoxia. *J Biol Chem* 2000; **275**: 19921–19927.
27. Yue TL, Ohlstein EH, Ruffolo RR, Jr. Apoptosis: a potential target for discovering novel therapies for cardiovascular diseases. *Curr Opin Chem Biol* 1999; **3**: 474–480.
28. Ding B, Price RL, Borg TK, Weinberg EO, Halloran PF, Lorell BH. Pressure overload induces severe hypertrophy in mice treated with cyclosporine, an inhibitor of calcineurin. *Circ Res* 1999; **84**: 729–734.
29. Zhang W, Kowal RC, Rusnak F, Sikkink RA, Olson EN, Victor RG. Failure of calcineurin inhibitors to prevent pressure-overload left ventricular hypertrophy in rats. *Circ Res* 1999; **84**: 722–728.
30. Aoyagi T, Izumo S. Hemodynamic overload-induced activation of myocardial mitogen-activated protein kinases *in vivo*: augmented responses in young spontaneously hypertensive rats and diminished responses in aged Fischer 344 rats. *Hypertension* 2001; **37**: 52–57.
31. Izumi Y, Kim S, Murakami T, Yamanaka S, Iwao H. Cardiac mitogen-activated protein kinase activities are chronically increased in stroke-prone hypertensive rats. *Hypertension* 1998; **31**: 50–56.
32. Kagiyama S, Qian K, Kagiyama T, Phillips MI. Antisense to epidermal growth factor receptor prevents the development of left ventricular hypertrophy. *Hypertension* 2003; **41**: 824–829.

